| Title of thesis | **Dynamic Responses of Floating Offshore Platforms With Large Hulls** |
|---|---|

I, **NG CHENG YEE** hereby allow my thesis to be placed at the Information Resource Center (IRC) of Universiti Teknologi PETRONAS (UTP) with the following conditions:

1.  The thesis becomes the property of UTP

2.  The IRC of UTP may make copies of the thesis for academic purposes only.

3.  This thesis is classified as

    ☐ Confidential

    √ Non-confidential

If this thesis is confidential, please state the reason:
_____
_____
_____


The contents of the thesis will remain confidential for _____ years.

Remarks on disclosure:
_____
_____
_____

Endorsed by




_____          _____
Signature of Author                       Signature of Supervisor

Permanent address:                        Name of Supervisor
8, TEMIANG JAYA 3,                        PROF. DR KURIAN V. JOHN
DESA TEMIANG JAYA,
31650 IPOH, PERAK MALAYSIA



Date : _____               Date : _____

i

UNIVERSITI TEKNOLOGI PETRONAS

**DYNAMIC RESPONSES OF FLOATING OFFSHORE PLATFORMS WITH LARGE HULLS**

by

**NG CHENG YEE**

The undersigned certify that they have read, and recommend to the Postgraduate Studies Programme for acceptance this thesis for the fulfilment of the requirements for the degree stated.

Signature: _____

Main Supervisor: _____

Signature: _____

Head of Department: _____

Date: _____

# DYNAMIC RESPONSES OF FLOATING OFFSHORE PLATFORMS

# WITH LARGE HULLS

by

**NG CHENG YEE**

A Thesis

Submitted to the Postgraduate Studies Programme

As a Requirement for the Degree of

MASTER OF SCIENCE

CIVIL ENGINGEERING DEPARTMENT

UNIVERSITI TEKNOLOGI PETRONAS

BANDAR SERI ISKANDAR,

PERAK

JULY 2010

| Title of thesis | **DYNAMIC RESPONSES OF FLOATING OFFSHORE PLATFORMS WITH LARGE HULLS** |
|---|---|

I, **NG CHENG YEE** hereby declare that the thesis is based on my original work except for quotations and citations which have been duly acknowledged. I also declare that it has not been previously or concurrently submitted for any other degree at UTP or other institutions.

Witnessed by

_____ _____

Signature of Author Signature of Supervisor

Permanent address: Name of Supervisor

8, TEMIANG JAYA 3 _____
DESA TEMIANG JAYA,
31650 IPOH, PERAK, MALAYSIA

Date : _____ Date : _____

# ACKNOWLEDGEMENT

# ABSTRACT

Spar and semi-submersible are the most common types of floating offshore platforms used for deepwater operations. The spar consists of a hollow cylindrical deep-draft floating hull that provides buoyancy, with strake surrounding the hull to reduce vortex induce vibration and to held in place by mooring lines. To remain stable, it is important to maintain the centre of gravity always below the centre of buoyancy. The semi-submersible comprises of two horizontal water tight pontoons and number of column units that stand on the pontoons to provide support to the deck structure. It is held in place by mooring lines and dynamic positioning system. Both these types of platforms are made up of large-sized hull for providing buoyancy. As the ratio of the diameter of these structures to the wave length is above 0.2, the wave diffraction theory is the correct theory to be applied for the calculation of wave forces and wave damping, according to the literature. However, the application of diffraction theory, even linear one, is very much complicated and requires very costly commercial software. Hence, many research papers have reported results of dynamic analysis, using Morison equation for such cases, reasoning that for a considerable part of the frequency range, the ratio of diameter to wave length is still below 0.2. This is because of the ease of using Morison equation in programming and the possibility of incorporating the various non-linearity in the analysis. Yet, it has been established that the consultants are using only diffraction analysis for the analysis and design of such platforms.

The aim of this study was to determine and compare the responses by both Morison equation and diffraction theory to the model test responses, and to suggest nonlinear multiple regression curves to estimate the structure responses. Model tests were conducted for spar and semi-submersible platform models in the wave tank at the Offshore Engineering Laboratory of Universiti Teknologi PETRONAS and the responses were measured. The respective prototypes were analyzed using a numerical Newmark Beta time domain integration method that was developed by using Matlab program. The platforms were designed as rigid bodies and three degree of freedom; surge, heave and pitch were considered. Linear wave theory and Morison equation were used for wave force determination in time domain analysis. A commercial software was employed to determine responses of the structures by Linear Wave Diffraction module. These results proved that the diffraction theory results were much closer to the actual model test results, thereby proving that using Morison equation for such platforms is not justified. Using the results of the diffraction analysis for a large number of platforms and conducting a non-linear multiple regression analysis, this thesis also suggests formulae to obtain suitable regression curves for predicting the diffraction responses of the spar and semi-submersible for any dimension and draft within the range suggested.

# ABSTRAK

*Spar* dan *semi-submersible platform* adalah pelantaran mengambung untuk lautan dalam yang paling biasa digunakan untuk eksplorasi minyak dan gas di laut. *Spar* terdiri daripada silinder berongga yang mempunyai kedalaman yang nyata untuk memberi daya apung, *strake* mengelilingi structure untuk mengurangkan getaran dan pusaran, dan dikekalkan di lokasi dengan kabel (*mooring lines*) atau menggunakan sistem kedudukan dinamik. Untuk kestabilan, adalah penting untuk menetapkan pusat graviti di bawah pusat apung. Semi-submersible terdiri daripada dua ponton kalis air dan tiang berdiri di atas ponton untuk memberikan sokongan kepada struktur geladak. Kedua-dua jenis platform ini terdiri daripada badan berukuran besar untuk menyediakan kuasa apung. Untuk nisbah diameter struktur dengan panjang gelombang di atas 0.2, seperti yang ternyata pada literatur, teori pembelauan gelombang (*wave diffraction theory)* adalah teori yang sesuai untuk perhitungan gaya gelombang dan peredam gelombang. Namun demikian, pelaksanaan teori pembelauan adalah rumit dan memerlukan perisian komersil yang sangat mahal. Oleh kerana itu, banyak penyelidikan telah melaporkan keputusan analisis dinamik, dengan menggunakan Persamaan Morison (*Morison equation*) dengan alasan bahawa nisbah diameter dan panjang gelombang masih di bawah 0.2 untuk sebahagian besar rentang frekuensi. Ini adalah kerana penggunaan Persamaan Morison lebih senang dalam pengaturcaraan perisik dan kemungkinannya besar untuk bergabung dengan pelbagai non-linearitas dalam analisa. Namun, analisis pembelauan telah digunakan oleh perunding hanya untuk analisis dan rekabentuk platform tersebut.

Tujuan kajian ini adalah untuk membuat penilaian perbandingan kaedah-kaedah ini, dengan beberapa eksperimental percubaan untuk mevalidasikannya dan memperoleh satu kaedah yang murah dan mudah untuk mendapatkan tindakbalas dinamik untuk *spar* dan *semi-submersible platform*. *Spar* dan *semi-submersibles platform* dianalisis menggunakan kaedah Newmark Beta untuk integrasi dengan menggunakan program Matlab. Platform direka sebagai badan tegar dengan tiga darjah kebebasan iaitu *surge, heave* dan *pitch*. Teori gelombang linear dan Persamaan Morison digunakan untuk penentuan daya gelombang dalam analisis masa domain. Sebuah perisian komersil telah digunakan untuk memperoleh tindakbalas dinamik dengan modul *Linear wave diffraction*. Eksperimental untuk model *spar* dan *semi-submersible* telah diuji dalam tangki gelombang makmal teknik lepas pantai dan tindakbalas diukur. Keputusan ini membuktikan bahawa tindakbalas pembelauan teori lebih mematuhi keputusan daripada eksperimen, dan terbukti bahawa penggunaan persamaan Morison untuk platform untuk structur besar adalah tidak benar. Dengan menggunakan hasil analisis pembelauan untuk banyak platform, analisis regresi telah dilaksanakan. Dalam tesis ini juga, formula untuk menghasilkan lengkungan dari analysis regresi dicadangkan untuk memprediksi tindakbalas pembelauan untuk *spar* dan *semi-submersible platform* yang dimensi dan kedalaman dipatuhi.

In compliance with the terms of the Copyright Act 1987 and the IP Policy of the university, the copyright of this thesis has been reassigned by the author to the legal entity of the university,

**Institute of Technology PETRONAS Sdn Bhd.**

Due acknowledgement shall always be made of the use of any material contained in, or derived from, this thesis.

# TABLE OF CONTENTS

# LIST OF TABLES

# LIST OF FIGURES

## NOMENCLATURE

| | |
|---|---|
| KC number | Keulegan-Carpenter number |
| Re number | Reynolds number |
| $\Phi$ | Total velocity potential by diffraction theory |
| x, y, z | Coordinates of a point in the fluid field where the potential was calculated at time t |
| $\eta$ | Free surface elevation |
| $g$ | Gravity acceleration |
| $\Phi_0$ | Incident wave potential |
| $\Phi_s$ | Wave scattered velocity potential |
| r and $\theta$ | Polar coordinates |
| $J_m$ | Bessel function of the first kind of order m, was the |
| $H_m^{(1)}$ | Hankel function of the first kind of order m |
| $A_w$ | Body water plane area |
| K | Unit vector in z-direction |
| N | Unit vector normal to the body surface |
| $y_r$ and $x_f$ | Coordinates of the center of floatation |
| $\xi$ | Translational motion |
| $\alpha$ | Rotational motion of the structure |
| $F_I$ | Inertia force |
| $F_D$ | Drag force |
| $df_I$ | Inertia force on an incremental segment ds per unit length of the pile |
| $\rho$ | Seawater density that taken as 1.035kg/m3 |
| D | Diameter of the cylinder |
| $\partial u / \partial t$ | Local water particle acceleration |
| $C_M$ | Inertia coefficient |
| $df_D$ | Drag force on an incremental segment ds |
| $u$ | Instantaneous water particle velocity |
| $C_D$ | Drag coefficient |
| H | Wave height |
| T | Wave period |
| k | Wave number |
| s | = y+d |
| $\Theta$ | = kx-$\omega$t |
| $U_m$ | Maximum along wave water particle velocity |
| [M] | Mass matrix |
| $[M_{struc}]$ | Structural mass matrix |
| $[M_{add}]$ | Added mass matrix |
| M | Total structural mass, |
| I | Total mass moment of inertia |
| $C_m$ | Added mass coefficient |
| $\emptyset$ | Pitch angle measured from z-axis |
| Z | Distance of centre of gravity to heel plus the increment of each element with 1 m interval. |
| K | Stiffness matrix |
| $K_{hystat}$ | Stiffness of restoring hydrostatic force |
| $K_{moor}$ | Stiffness due to mooring lines |

| | |
|---|---|
| $\gamma_w$ | Weight density of sea water |
| H | Draft of the spar platform |
| $h_1$ | Distance of the center of gravity and center of buoyancy |
| $k_x$ | Constant mooring line stiffness |
| $h_2$ | Distance between center of gravity and fairlead |
| $\{X\}$ | Structural displacement vector |
| $\{\ddot{X}\}$ | Structural acceleration vector |
| $F(t)$ | Hydrodynamic forcing vector |
| $X_{t+\Delta t}$ | Displacement of the structure for each time step |
| $\widehat{K}$ | Effective stiffness matrix |
| $\ddot{X}_{t+\Delta t}$ | Acceleration of the structure for each time step |
| $\dot{X}_{t+\Delta t}$ | Velocity of the structure for each time step |
| $\widehat{F}_{t+\Delta t}$ | Effective loading matrix |
| $r_{pit}$ | Radii of gyration in pitch |
| $A_c$ | Column cross section area |
| $A_p$ | Pontoon cross-sectional area |
| $R$ | Response amplitude operator (RAO) |
| $f$ | Wave frequency |
| $a, b, c, d$ | Regression coefficient from regression analysis |

# CHAPTER ONE

# INTRODUCTION

## 1.1 Chapter overview

The demand for oil and gas has increased dramatically since last two decades. Oil and gas exploration and production began with the onshore operations and later the same were extended to the offshore region. In this chapter, a brief introduction about oil and gas industry in Malaysia, spar and semi-submersible platforms are discussed. Also, the wave force determination approaches, problem statement, objectives and the scope of study for this research are presented.

## 1.2 Oil and Gas Industry in Malaysia

Due to the decline in the tin production, petroleum and natural gas explorations and productions were encouraged and discovered in the offshore oilfields at Sabah, Sarawak and Terengganu. The first oil field of Malaysia was discovered in July 1882 at Baram, Sarawak. At that time, production from the field mainly supplied for household usage only and the commercial operations began by the year 1910. The forerunner of present Sarawak Shell, Anglo Saxon Petroleum Company discovered the first commercial oil field in Miri, Sarawak, and offshore operations became active since then.

Before 1974, Malaysia offshore was divided into two concessions areas; i.e. the concession area within Peninsular Malaysia which was awarded to Esso Production Malaysia Inc. (EPMI), and the one within East Malaysia, which was awarded to Sarawak Shell Ltd. and Sabah Shell Petroleum Co. Ltd.  This has opened up the opportunity for other oil companies to bid for the Production Share Contract (PSC) within the region.  The oil companies had to pay royalty and taxes to the State Government, which the petroleum production was controlled by the State Government at that time.  Under Petroleum Development Act 1974, Petroleum National Berhad, PETRONAS, was awarded the entire ownership and the exclusive rights, power, liberties and privileges of exploring, exploiting, winning and obtaining petroleum for both onshore and offshore region of Malaysia.  Normally, the exploration takes five years, development takes four years and production lasted for about twenty years in the PSC time frame.  At the end of the twenty-nine-year operation period, all the facilities will be re-owned by PETRONAS.  It has been estimated that, according to the current production rates Malaysia will be able to produce oil for another 15 years and gas for 35 years.

Currently, there are 175 fixed jacket platforms operated by PETRONAS in South China Sea.  These platforms are located in three main fields namely the Peninsular Malaysia Operations (PMO) at Terengganu, Sarawak Operation (SKO) and Sabah Operation (SBO).  The international operations of PETRONAS, for both upstream and downstream, are distributed over 34 countries around the world.  Table 1.1 shows the types and distribution of the fixed platform of PETRONAS domestic operations within South China Sea, and Table 1.2 shows the general overview of the domestic operations for PETRONAS [1].

Table 1. 1 Typical types and distribution of facilities of PETRONAS in South China Sea [1]

| Types of Facilities | No. of Platform | | |
|---|---|---|---|
| | PMO | SKO | SBO |
| Monopod | 3 | - | 2 |
| 3 legged | 6 | 29 | 4 |
| 4 legged | 19 | 58 | 16 |
| 6 legged | - | 12 | 1 |
| 8 legged | 10 | 6 | 7 |
| 16 legged | - | 1 | 1 |
| FSO / FPSO | 4 | - | - |
| **Total** | **42** | **106** | **31** |

Table 1. 2 General overview of the domestic operations for PETRONAS

| Domestic Operations | | No. of platform & facilities | Notes |
|---|---|---|---|
| SKO | 1. BDO (Miri) 2. Balingian (Bintulu) | 75 31 | 1. Operated based on burnt-down philosophy except for BNQ-B, TKQ-A, and D35Q-A 2. Upcoming facilities : J4, D21, PC4, Kumang Cluster Phase 1 etc. |
| SBO | 1.Semang 2.Erb West 3.Tembungo 4.Kinarut 5.Sumandak | 18 7 2 1 3 | 1. Upcoming facilities : Kinabalu Deep & East |
| PMO | 1.PM 9 2.Duyong 3.Dulang 4.Angsi 5.Marginal Field/ Floater (MASA, PNL, Abu) | OGT* KSB* 38 fixed platform* 1 FSO* 3 FPSO* | 1. Majorities of the platforms are designed with integrated concept 2. MASA & PNL are designed with burnt down concept with minimal facilities 3. Duyong is a integrated complex linked by bridge 4. Upcoming facilities : TCOT, Angsi-D, Abu kecil, Tangga Barat Cluster |

*Overall operations facilities*

In 2007, Malaysia's first deepwater field, Kikeh field was commissioned. Kikeh field is located about 120 km off the north-west coast of Sabah, Malaysia. The truss spar or Dry Tree Unit (DTU) installed in this field is 142 m long and 32 m in diameter. It was installed with a tender assisted drilling rig to drill and complete the Kikeh wells. This is also the only truss spar floating production unit installed outside the Gulf of Mexico. Besides, as a part of the Kikeh field development, a FPSO was located in 1,350 m of water. The Kikeh field is the first deepwater discovery in Malaysia with commercial potential. With only five years elapsing between discovery and production, this project achieved the world class performance. This field covers an aerial extent of about 6 km by 2.5 km with a reserve of 400 – 700m bbl of crude oil. 155,000 BPD of crude oil; 212 MMSCFD and 10,000 BWPD with 226,000 BWPD injected for pressure maintenance was expected. Table 1.3 shows the typical dimensions of Kikeh spar, and Figure 1.1 shows the main elements of the Kikeh truss spar [2].

Table 1. 3 Typical dimensions of Kikeh spar

| Description | Value |
|---|---|
| Total Hull Length, (m) | 142 |
| Draft, (m) | 131 |
| Hard tank freeboard, (m) | 11 |
| Hard tank length, (m) | 67 |
| Hard tank diameter, (m) | 32 |
| Soft tank depth, (m) | 11 |
| Total truss length, (m) | 64 |
| Truss leg spacing, (m) | 23 |
| Heave plate area ($m^2$) | 32/plate |
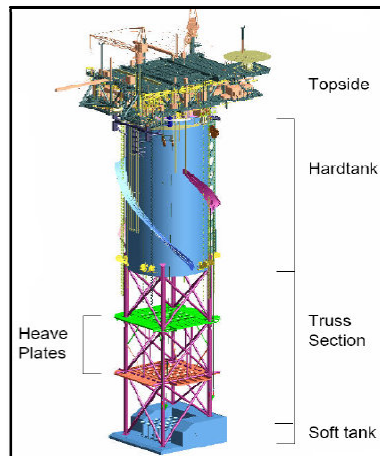
Figure 1. 1 Kikeh truss spar [2]

## 1.3    Development of offshore platform

The first offshore platform, i.e. a fixed type of jacket structure was installed in the Gulf of Mexico in 1947.  After this, the discovery and development of offshore platforms with efficient solutions for the oil and gas operations became a challenge for the industry and for researchers.

The offshore water depth was classified into three categories i.e. the shallow water, deep water and ultra deep water.  The water depth range below 350 m is classified as shallow water, the deep water region ranges from 350 m to 1500 m, and the ultra deep water depth region is deeper than 1500 m.  Due to the depletion of shallow water resources, the development of exploration and production are mostly deep and ultra deep water regions now.

The major function of the offshore platform is to support the exploration and production operation of oil and gas.  It is important to provide a stable workstation by minimizing the movement of the supporting structure.  Typical offshore structures are built with steel, concrete or a combination of steel and concrete (hybrid).  Offshore platforms may be classified as fixed and compliant structures.  Fixed structures are preferable for operations, where the deformation due to wave loading is small.  Fixed

5

structures may be economically viable for the shallow water region; compliant structures are preferable beyond this region. There are mainly two types of compliant structures i.e. the rigid floating structure that is connected to the sea floor e.g. tension leg platform, and structures that allow large deformation when subjected to environmental load e.g. spar and semi-submersible platforms [3].

## 1.4    Spar Platform

Spar platforms are used for exploration, production and oil storage purposes. The structure weight is balanced by buoyancy provided by the closed and water tight circular deep draft hull. The center of gravity for it always remains below the center of buoyancy and that stabilizes the spar against overturning. Furthermore, it is held in place by station-keeping mooring line system. Spar concept has gone through evolution stages from classic spars through truss spar to cell spar. There are even some new concepts, cell truss spar and geometric spar, which will be discussed in chapter 2. Table 1.4 shows the spar structures that are sanctioned, installed or operating.

## 1.5    Semi-submersible Platform

Semi-submersible platform is a multi-legged floating structure which is kept stationing by a combination of mooring line system and dynamic positioning system. The concept of this floater consists of pontoons, columns and station keeping system. The semi-submersible pontoons are water tight horizontal rectangular members and the vertical columns are interconnected by pontoons at the bottom to support the upper deck. This type of structure is suitable for ultra deep water exploration and production. Table 1.5 illustrates the details of the existing semi-submersible platforms.

6

Table 1. 4 Spars structure which are sanctioned, installed or operating [4]

| No | Spar Name | Location | Water Depth (m) | Year | Types / Notes |
|----|-----------|----------|-----------------|------|---------------|
| 1 | Neptune | US GOM | 588 | 1997 | Classic Spar |
| 2 | Genesis | US GOM | 792 | 1999 | Classic Spar |
| 3 | Hoover/Diana | US GOM | 1463 | 2000 | Classic Spar |
| 4 | Boomvang | US GOM | 1052 | 2002 | Truss Spar |
| 5 | Nansen | US GOM | 1121 | 2002 | Truss Spar |
| 6 | Horn Mountain | US GOM | 1653 | 2002 | Truss Spar |
| 7 | Medusa | US GOM | 678 | 2003 | Truss Spar |
| 8 | Gunnison | US GOM | 960 | 2003 | Truss Spar |
| 9 | Front Runner | US GOM | 1015 | 2004 | Truss Spar |
| 10 | Holstein | US GOM | 1324 | 2004 | Truss Spar |
| 11 | Red Hawk | US GOM | 1615 | 2004 | First Cell spar |
| 12 | Devils Tower | US GOM | 1710 | 2004 | Truss Spar |
| 13 | Mad Dog | US GOM | 1347 | 2005 | Truss Spar |
| 14 | Constitution | US GOM | 1515 | 2006 | Truss Spar |
| 15 | Kikeh | Malaysia | 1330 | 2007 | First Spar installed out of GOM |
| 16 | Tahiti | US GOM | 1250 | 2008 | Truss Spar |
| 17 | Mirage | US GOM | 1219 | 2009 | MinDoc 3 |
| 18 | Perdido | US GOM | 2383 | 2009 | Truss Spar |
| 19 | Telemark | US GOM | 1356 | N/A | MinDoc 3 |

*Note :US GOM: the Gulf of Mexico in United State*

Table 1. 5 Existing semi submersible (semis) units [5]

| No. | Semi-submersible | Location | Water Depth (m) | Year |
|---|---|---|---|---|
| 1 | BUCHAN A | UK | 118 | 1981 |
| 2 | P-09 | Brazil | 230 | 1983 |
| 3 | P-15 | Brazil | 243 | 1983 |
| 4 | P-12 | Brazil | 103 | 1984 |
| 5 | P-21 | Brazil | 112 | 1984 |
| 6 | BALMORAL | UK | 143 | 1986 |
| 7 | P-22 | Brazil | 114 | 1986 |
| 8 | P-07 | Brazil | 209 | 1988 |
| 9 | AH001 | UK | 140 | 1989 |
| 10 | VESLEFRIKK B | Norway | 175 | 1989 |
| 11 | P-20 | Brazil | 625 | 1992 |
| 12 | P-08 | Brazil | 423 | 1993 |
| 13 | P-13 | Brazil | 625 | 1993 |
| 14 | P-14 | Brazil | 195 | 1993 |
| 15 | P-18 | Brazil | 910 | 1994 |
| 16 | NAN HAI TIAO ZHAN | China | 332 | 1995 |
| 17 | TROLL-B | Norway | 320 | 1995 |
| 18 | P-25 | Brazil | 252 | 1996 |
| 19 | P-27 | Brazil | 530 | 1996 |
| 20 | P-19 | Brazil | 770 | 1997 |
| 21 | NJORD A | Norway | 330 | 1997 |
| 22 | TROLL-C | Norway | 340 | 1999 |
| 23 | VISUND | Norway | 335 | 1999 |
| 24 | ASGARD B | Norway | 300 | 2000 |
| 25 | P-26 | Brazil | 515 | 2000 |
| 26 | NA KIKA | US GOM | 936 | 2003 |
| 27 | SS-11 | Brazil | 126 | 2003 |
| 28 | P-40 | Brazil | 1080 | 2004 |
| 29 | KRISTIN | Norway | 320 | 2005 |
| 30 | ATLANTIS | US GOM | 327 | 2007 |
| 31 | P-51 | Brazil | 374 | 2007 |
| 32 | P-52 | Brazil | 1795 | 2007 |
| 33 | SNORRE B | Norway | 351 | 2007 |
| 34 | BLIND FAITH | US GOM | 1980 | 2008 |
| 35 | THUNDER HORSE | US GOM | 1849 | 2008 |
| 36 | GJOA | Norway | 360 | 2010 |
| 37 | P-56 | Brazil | 1700 | 2010 |
| 38 | GUMUSUT | Malaysia | 1006 | 2011 |
| 39 | CALAUIT | By Fridstad Offshore | N/A | N/A |
| 40 | DAI HUNG I | By Petrovietnam | N/A | N/A |
| 41 | EXMAR OPTI EX | By Exmar Opti Ltd | N/A | N/A |
| 42 | MOLLY BROWN | By Compass Energy | N/A | N/A |

## 1.6    Wave force determination approaches

Wave force constitutes about 70% of the environmental load exerted on an offshore structure.   For the design of these structures, wave force calculation is a very important aspect.  Wave force can be determined by three different approaches, i.e. Morison Equation, Froude-Krylov theory and diffraction theory.  The applicability of these theories is based upon the relationship of structure's size and wave length.  If the structure is small in comparison to the wave length, Morison equation is applicable.  Froude-Krylov theory is appropriate if the drag force is insignificant and inertia force predominates, while the ratio of the diameter to wave length is still relatively small.  When the structure is large enough comparative to the wave length, diffraction theory is applicable [6].  However, the application of diffraction theory, even linear one, is very much complicated and requires very costly commercial software.  Hence, many research papers have reported results of dynamic analysis, using Morison equation for such cases, reasoning that for a considerable part of the frequency range, the ratio of diameter to wave length is still below 0.2.  This is because of the ease of using Morison equation in programming and the possibility of incorporating the various non-linearity in the analysis.  Yet, it has been established that the consultants are using only diffraction analysis for the analysis and design of such platforms.

### 1.6.1    Morison equation

Morison et al [7] developed the equation describing the horizontal wave forces acting on a vertical pile that extended from the bottom through the free surface. They proposed that the force cause by unbroken surface waves on a circular pile was composed two components, the inertia and drag.

A water particle moving in a wave carries a momentum with it.  As the water particle passes around the circular cylinder, it accelerates and then decelerates.  This requires work be done through the application of a force on the cylinder to increase

this momentum. The increment of inertia force on a small segment of the cylinder needed to accomplish this is proportional to the water particle acceleration at the center of the cylinder.

On the other hand, the drag force component is mainly caused by the existence of a wake region on the downstream side of the cylinder. The low pressure zone, i.e. the wake, has lower pressure in comparison to the upstream pressure. Therefore, the pressure variation is created by the wake between the upstream and downstream of the cylinder at a given instant of time. The force exerted in the direction of the instantaneous water particle velocity is mainly caused by the pressure differential. In a steady flow, downstream side is fixed and the drag force is proportional to the square of the water particle velocity. The absolute value of the water particle velocity is inserted to insure that the drag force is in the same direction as the velocity for an oscillatory flow [6].

### 1.6.2   Diffraction theory

In most of the papers [6], [8], [9], it was concluded that if the structure is large enough comparative to the wave length, Morison equation was no longer applicable. In such case, the incident waves experience significant diffraction as it approaches the structure. Diffraction of waves from the surface of the structure should be taken into account in the wave-force calculation.

Unlike Morison equation, diffraction theory involves mathematical function such as the Bessel function and Hankel function which are complicated and not easy for programming. A commercial structural analysis computer software is needed to determine the responses due to wave diffraction.

### 1.7   Problem Statement

Wave forces exerted on the offshore structure can be calculated by three different approaches namely, the Morison equation, Froude-Krylov theory and diffraction

theory. The application of Morison equation is simple and easy as it only involves the determination of the water particle kinematics and substitution into the equation. On the other hand, the application of diffraction method involves very cumbersome solutions, such as Bessel and Hankel Functions. Nonlinearities can be easily incorporated into Morison equation while nonlinear diffraction method is extremely complicated. Morison equation can be applied using normal computer programming while diffraction method needs very costly software e.g. WAMIT and SACS. Hence, it can be observed that majority of the research papers that deal with such studies resort to the use of Morison equation even for large cylinders, where diffraction method is the only correct method. Naturally, the wave forces and the resulting responses are erroneous. There are studies comparing on these two theories, but papers that provide a solution to determine wave forces with consideration of diffraction effects are rare. The aim of this study is to determine and compare the responses by both Morison equation and diffraction theory to the model test responses. It is also proposed to suggest nonlinear multiple regression curves for the estimation of responses on large offshore structures, which would serve as very useful guidelines for researches on the deepwater platforms.

## 1.8    Objectives

As mentioned previously, the aim of this study is to determine and compare the responses by both Morison equation and diffraction theory to the model test responses, and to suggest nonlinear multiple regression curves to estimate the structure responses. Following is the objectives that were set to achieve the aim for this study.

i.   To determine the dynamic responses of typical models of spar and semi-submersible in the wave basin subjected to regular waves.

ii.  To determine the dynamic responses of the corresponding prototype of the spar and semi-submersible platforms by using a time domain integration method, where the wave force was determined using Morison equation.

iii. To determine the dynamic responses of the above prototype using linear diffraction analysis software.

iv. To compare the model responses using the results of time domain analysis and diffraction analysis in order to determine the appropriate and accurate method for the analysis of the platforms with large-sized hull.

v. To obtain the design curves using regression analysis that determines the response of spars and semi-submersible for the practical range of dimensions.

## 1.9   Scope of Study

i. The studies are limited to Spar and Semi-submersible platform.

ii. The mooring line system was taken as station keeping method for both of the platforms.  Four mooring lines were considered for spar structure i.e. each of it located at every quarter of the cylindrical hull.  For the semi-submersible platforms, a total of eight mooring lines were assumed.

iii. Unidirectional waves in the surge direction of the platforms were considered.

## 1.10  Chapter Summary

Introduction of this study was presented.  The introduction of the oil and gas industry and the development of the spar and semi-submersible platforms were given.  Morison equation and diffraction theory were briefly explained.  Finally, the problem statement, objectives and scope of study were presented.

# CHAPTER TWO

# LITERATURE REVIEW

## 2.1    Chapter overview

The research findings regarding the wave load determination reported in the literature for the dynamic analysis of spar and semi-submersible platforms are discussed in this chapter.  Special attention is given to the discussion related to the Morison equation and diffraction theory.

## 2.2    Spar platform

Spar platform is a floating platform deployed for oil and gas operations in the deep and ultra deep water region.  The configuration of the spar platform consists of a hollow cylindrical deep-draft floating hull with its major part submerged to provide enough buoyancy, and held in place by mooring lines.  Spar was initially used for oceanography and oil storage before it was deployed as offshore platform.  Since the installation of first spar in 1996, the spar concept has undergone evolution from classic spar through truss spar, to cell spar and even some newly introduced spar concepts such as the geometric spar and cell-truss spar.

### 2.2.1 Classic spar

Classic spar is the first spar concept introduced at the Kerr-McGee-operated Neptune field in 1996. The configuration of classic spar consists of a watertight circular deep draft floating hull that makes the structure buoyant. It is surrounded by strakes to reduce the vortex induced vibration and held in place by mooring lines, which are connected from the fairlead on the hull to the seabed. Figure 2.1 shows the illustration of a typical classic spar structure.
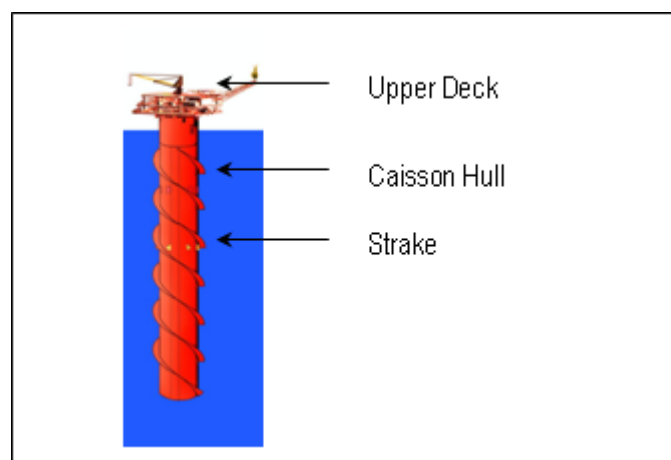


Figure 2. 1 Illustration of a typical classic spar structure [10]

### 2.2.2 Truss spar

Even though the classic spar provides excellent motion characteristics, the ambient deep current becomes the main problem. To solve this problem, the truss spar concept was introduced. The upper portion of the truss spar remains the cylindrical deep draft of the classic spar, connected by the truss system at the intermediate part of the structure, which separated by heave plates, and the bottom soft tank acts as fixed ballast for it. It is worth highlighting that, in the year 2007 the Kikeh truss spar, the only truss spar outside the Gulf of Mexico, was installed in Malaysia. Figure 2.2

shows the configuration of the truss spar structure.
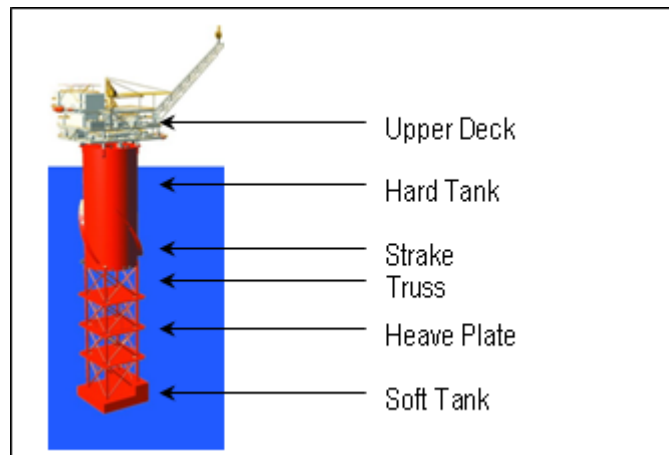


Figure 2. 2 Configuration of truss spar structure [10]

### 2.2.3 Cell spar

The third generation of the spar namely cell spar was introduced with the installation of Red Hawk cell spar. Cell spar is a combination of smaller sized hulls surrounding the center cell that provides buoyancy. It is connected together by horizontal and vertical structure elements located at the intermediate space between cells. Cell spar is more cost effective and less difficult in fabrication in comparison to the earlier generations of spars. Figure 2.3 shows the concept of cell spar and its main component.
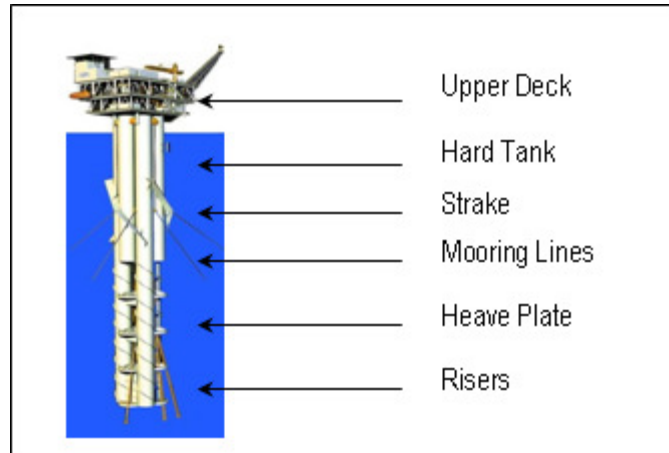
Figure 2. 3 Concept of cell spar and its main component [10]

## 2.2.4   Cell-truss spar

The cell-truss spar is a new concept spar which combines the special features of cell spar and truss spar.  This spar provides a better solution by undertaking the advantage of truss spar's heave plate damping feature and cell spar's fabrication ease.  The hard tank consists of a bundle of cylinders having same size and length.  The bottom portion is fitted with a truss system and soft tank for the position adjustment of center of gravity.  Strakes are designed surrounding the hard tank to reduce the vortex induced vibration affecting the structure.  The structure is held in place by mooring lines as for the other type of spar [11], [12].  Figure 2.4 shows the illustration of cell-truss spar concept.
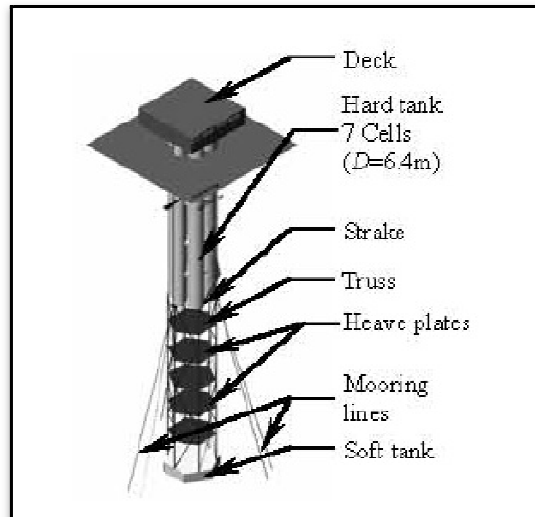
Figure 2. 4 Illustration of Cell-Truss Spar Concept [11]

## 2.2.5 Geometric spar

Geometric spar is different in terms of hull geometry and the Integrated Buoyancy Can (IBC) in comparison to the other types of spar platforms. The caisson hull of geometric spar is modified as an octagonal shaped cross section with a square moon-pool instead of cylindrical cross section of the conventional spar caisson hull. The heave plates are distributed at every edge of the octagon to form a square. The buoyancy can is modified by implementing the IBC to replace the traditional buoyancy can [13]. Figure 2.5 shows the geometric spar concept.

17
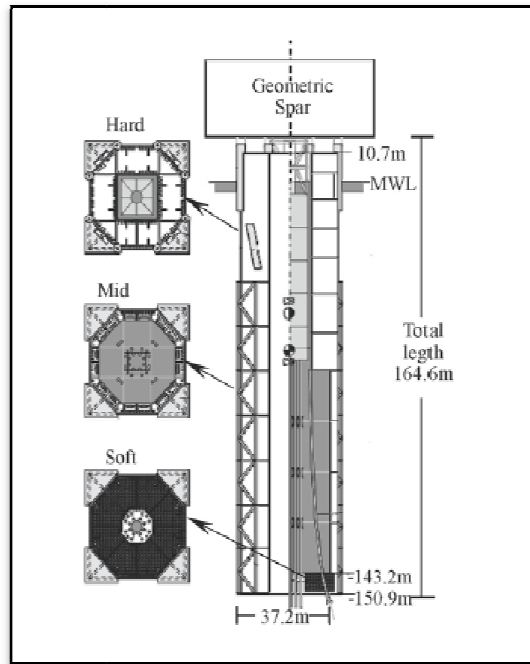
Figure 2. 5 Illustration of Geometric Spar Concept [13]

## 2.3    Semi-submersible platform

The semi-submersible platform is another mobile type of floating structure that is popular for drilling operation.   This floater comprises of horizontal watertight pontoons and columns that are interconnected by these pontoons at the bottom to support the upper deck.   The pontoons are fully submerged in the water, and combined with the small water plane areas of the columns provide a natural period beyond the region of significant wave energy [14].   For maintaining the location of the structure, fixed mooring system or dynamic positioning system is normally employed.

The semi-submersible platforms have reached the sixth generation now.   The classification is distinguished by age, environmental rating, deck load and water depth capacity [15].   The evolution of the semi-submersible could be observed in the new riser types, hull forms, construction methods and increasing production rate. [14]. The first semi-submersible platform (Bluewater I) was installed in the late 1950s. This unit was converted from an existing four-column submersible unit to a semi-

submersible drilling platform and operated at the Gulf of Mexico in a water depth of 180 m. For second generation semi-submersible platforms, the water depth reached up to 300 m. Conventionally moored semi-submersible rigs that operated in water depth ranging from 366 m to 1035 m was classified as the third generation of semi-submersible platforms. The water depths ranged up to 1750 m and 2440 m for the fourth and fifth generations. In the year 2007, the latest, the sixth generation of the semi-submersible platform was installed. It was designed to serve in a water depth of 3000 m in the harsh environment. The configuration of this latest generation of the semi-submersible platform comprises of a dual derrick system and advanced dynamic positioning system [16].

Most of the early semi-submersibles are out of service, and 160 units are still in operation [17]. Figure 2.6 shows the sixth generation of semi-submersible platform namely The Eastern Drilling 1.



Figure 2. 6 The sixth generation semi-submersible platform [17]

## 2.4    Wave load determination

The estimation of environmental loads, particularly the wave load, is significant for the analysis and design of an offshore structure. The geometry of the structure i.e. the ratio of size to the wave length, the hydrodynamic parameters and the rigidity of the structure, would affect the wave load experienced by the structure [18]. Depending

on the type and size of the structure, different approaches might be applied i.e. the Morison equation, Froude-Krylov theory and diffraction theory. In this study, the applications of Morison equation and diffraction theory for the large-sized members are investigated.

### 2.4.1 Morison equation

Morison equation has been used for wave force calculation in many studies, even for large structures. Morison equation is applicable when the drag force is significant, which usually happens when the structure is small in comparison to the water wave length.

From an experimental study, Morison et al [7] recommended that forces exert by unbroken surface waves on a vertical pile that extended from the bottom through the free surface consisted of two main components i.e. the inertia and drag, which given as

$$F = F_I + F_D \tag{2.1}$$

Inertia force, $F_I$ could be found when a water particle moving along the circular. The inertia force exerted on a small segment of the cylinder, is proportional to the water particle acceleration at the centre of the cylinder, which given as.

$$df_I = C_M \rho \frac{\pi}{4} D^2 \frac{\partial u}{\partial t} ds \tag{2.2}$$

Where $df_I$ was the inertia force on an incremental segment $ds$ per unit length of the pile, $\rho$ was the seawater density that taken as 1.035kg/m$^3$, D was the diameter of the cylinder, $\frac{\partial u}{\partial t}$ was the local water particle acceleration and $C_M$ was the inertia coefficient.

Morison wave force was predominated by drag force component, $F_D$. The drag force was found due to pressure difference at the wake region surrounded the cylinder. It was proportional to the square of water particle velocity as.

$$df_D = \frac{1}{2}C_D\rho D|u|u\,ds \tag{2.3}$$

Where $df_D$ was the drag force on an incremental segment $ds$, $u$ was the instantaneous water particle velocity and $C_D$ was the drag coefficient.

Water particle velocity and acceleration were calculated according to linear wave theory which was given respectively by

$$u = \frac{\pi H}{T}\frac{\cosh ks}{\sinh kd}\cos\Theta \tag{2.4}$$

and

$$\frac{\partial u}{\partial t} = \frac{2\pi^2 H}{T^2}\frac{\cosh ks}{\sinh kd}\sin\Theta \tag{2.5}$$

where $H$ was wave height, $T$ was wave period, $k$ was the wave number, $s = y+d$, and $\Theta = kx-\omega t$.

Chitrapu and Ertekin [19] implemented the modified Morison equation to obtain the hydrodynamic forces for floating platforms. In the modification, they incorporated the Froude-Krylov force, the hydrostatic pressure force, acceleration force and the relative velocity drag force. Low and Langley [20] employed the modified Morison equation to run the analysis of deepwater floating production systems. In the case, inertia and drag forces were computed separately with the hydrodynamic coefficient in direction normal and tangential to the model.

Rainey [21] also proposed a new equation for calculating wave loads on offshore structure by modifying the Morison equation to incorporate the axial divergence term to the drag and inertia term of original Morison equation. For numerical purposes, Han and Benaroya [22] conducted a study on a TLP model, which the fluid force on the platform was due to random waves, and the random waves are modeled using the Pierson – Moskowitz spectrum and the modified Morison equation. The modified Morison equation incorporated the added mass term to the Morison equation, which the added mass effects results from some of the fluid particles being permanently displaced by the motion of the cylinder.

The hydrodynamic coefficients were considered as a function of the KC number, Re number, roughness parameter and interaction parameters [6]. The drag and inertia coefficients of Morison equation were derived experimentally according to Teng and Li [23]. Isaacson and Balwin [24] used the numerical simulations of random wave force to study the accuracy of the alternative methods of estimating Morison coefficient. Isaacson et al [25] also gave a summary of the alternative methods of estimating the drag and inertia coefficients from irregular waves and wave force data. Chakrabarti [26] analyzed the in-line forces on a small section of a fixed vertical cylinder for the purpose of determining the effects of hydrodynamic coefficients on the water depth parameter and the orbital shape parameter.

Lake et al [27] estimated the hydrodynamic coefficients of a cylinder and a disk. Burrows et al [28] studied the use of rigid and flexible member form of Morison equation for the estimation of the drag and inertia coefficients under random wave excitation. The hydrodynamic coefficients of a semi-submersible undergoing slow-drift oscillation were determined through the model test conducted by Chakrabarti and Cotter [29].

Due to the simplicity in implementation and programming, Morison equation has been used in many papers and has been established as the primary basis of wave load determination for offshore structures, made up of small sized members.

## 2.4.2   Diffraction theory

When the size of structure relative to the wave length is greater than 0.2, Morison equation is no longer applicable. The existence of the structure will affect the surrounded wave field. In such case, the diffraction effects of the wave from the surface of the structure should be taken into account for the wave force computation [6].

The linear diffraction problem for a fixed vertical circular that cylinder extended from the seabed to above the free surface was solved analytically. It was assumed that the fluid was frictionless and the flow was irrotational; and linear wave theory might

be used if the incident waves are of small steepness in comparison to their lengths in a finite water depth. The force in surge direction i.e. the direction of wave propagation was found to be a function of integration of pressure around the cylinder. The force undergoes a phase shift due to the diffraction of waves from the surface of the cylinder. Anam [30] and Anam and Roesset [31] claimed that the hydrodynamic forces by diffraction-radiation theory were a sum of radiation force, wave exciting force, wave drift damping force, and hydrostatic restoring force.

According to Chakrabarti [32], the total velocity potential, $\Phi$ by diffraction theory under potential theory that satisfied the Laplace equation was given as

$$\nabla^2\Phi = \frac{\partial^2\Phi}{\partial x^2} + \frac{\partial^2\Phi}{\partial y^2} + \frac{\partial^2\Phi}{\partial z^2} = 0 \tag{2.6}$$

Where potential, $\Phi = \Phi(x, y, z, t)$ and x, y, z were the coordinates of a point in the fluid field where the potential was calculated at time t.

The boundary condition could be defined as

i.      Dynamic boundary condition

$$\frac{\partial\Phi}{\partial t} + g\eta + \frac{1}{2}\left[\left(\frac{\partial\Phi}{\partial x}\right)^2 + \left(\frac{\partial\Phi}{\partial y}\right)^2 + \left(\frac{\partial\Phi}{\partial z}\right)^2\right] = 0 \quad \text{on } y = \eta \tag{2.7}$$

$\eta$ was the free surface elevation and $g$ was the gravity acceleration

ii.     Kinematic boundary condition

$$\frac{\partial\eta}{\partial t} + u\frac{\partial\eta}{\partial x} + w\frac{\partial\eta}{\partial z} - v = 0 \quad \text{on } y = \eta \tag{2.8}$$

Where $u = \frac{\partial\Phi}{\partial x}, v = \frac{\partial\Phi}{\partial y}, w = \frac{\partial\Phi}{\partial z}$

iii.    Bottom boundary condition

$$\frac{\partial\Phi}{\partial y} = 0 \quad \text{at } y = -d \tag{2.9}$$

iv.    Body surface boundary condition

23

$$\frac{\partial \Phi}{\partial n} = 0 \qquad -d \le y \le \eta \tag{2.10}$$

The velocity potential, $\Phi$ was taken as the summation of incident wave potential, $\Phi_0$ and wave scattered velocity potential, $\Phi_s$.

$$\Phi = \Phi_0 + \Phi_s \tag{2.11}$$

$$\Phi_0 = \frac{igH}{2\omega} \frac{\cosh ks}{\cosh kd} e^{i(kx - \omega t)} \tag{2.12}$$

$$e^{i(kx - \omega t)} = [J_0(kr) + \sum_{m=1}^{\infty} 2i^m J_m(kr) \cos m\theta] e^{-i\omega t} \tag{2.13}$$

The Sommerfeld radiation condition gave the scattered potential, $\Phi_s$

$$\lim_{R \to \infty} \sqrt{R} \left( \frac{\partial}{\partial R} \pm i\lambda \right) \Phi_s = 0 \tag{2.14}$$

The total potential satisfied the radiation-boundary condition given by,

$$\Phi = \frac{H\omega}{2k} \frac{\cosh ks}{\sinh kd} \sum_{m=0}^{\infty} \delta_m i^{m+1} \left[ J_m(kr) - \frac{J_m'(ka)}{H^{(1)'}(ka)} H_m^{(1)}(kr) \right] \cos m\theta e^{-i\omega t} \tag{2.15}$$

Then, wave profile, $\eta$ was given as

$$\eta = \frac{H}{2} \sum_{m=0}^{\infty} \delta_m i^{m+1} \left[ J_m(kr) - \frac{J_m'(ka)}{H^{(1)'}(ka)} H_m^{(1)}(kr) \right] \cos m\theta e^{-i\omega t} \tag{2.16}$$

$$\omega^2 = gk \tanh kd \tag{2.17}$$

Where $i = \sqrt{-1}$, r and $\theta$ was the polar coordinates, $J_m$ was the Bessel function of the first kind of order m, $H_m^{(1)}$ was the Hankel function of the first kind of order m.

Dynamic pressure due to waves at the surface of the cylinder was given by,

$$
\begin{aligned}
p = \frac{\rho g H}{\pi k a} \frac{\cosh ks}{\cosh kd} \sum_{m=0}^{\infty} \delta_m (-1)^m & \left[ \frac{Y_{2m}' \sin \omega t - J_{2m}' \cos \omega t}{J_{2m}'^2 + Y_{2m}'^2} \cos 2m\theta \right. \\
& \left. - \frac{Y_{2m+1}' \cos \omega t - J_{2m+1}' \sin \omega t}{J_{2m+1}'^2 + Y_{2m+1}'^2} \cos(2m+1)\theta \right]
\end{aligned}
$$

$$\tag{2.18}$$

24

Net force in surge (x) direction was found to be a integration function of the pressure around the cylinder, which given as

$$f_x = \frac{2\rho gH}{k} \frac{\cosh ks}{\cosh kd} \frac{1}{\sqrt{A_1(ka)}} \cos(\omega t - \alpha) \qquad (2.19)$$

where

$$A_1(ka) = J_1^{'2}(ka) + Y_1^{'2}(ka) \qquad (2.20)$$

$$\alpha = tan^{-1}\left(\frac{J_1^{'}(ka)}{Y_1^{'}(ka)}\right) \qquad (2.21)$$

Anam [26] computed the first order hydrodynamic force by integrating the dynamic pressure over the body surface and the hydrodynamic force vectors given as

$$F = F_{I,D,R} + F_{HS} \qquad (2.22)$$

$$F_{I,D,R} = -\rho \iint \frac{\partial \Phi}{\partial t} n \, dS \qquad (2.23)$$

$$F_{HS} = -\rho A_w\left(\xi_3 + y_r\alpha_1 - x_f\alpha_2\right)k \qquad (2.24)$$

where $A_w$ was the body water plane area, $k$ was the unit vector in z-direction, $n$ was the unit vector normal to the body surface, $y_r$ and $x_f$ were the coordinates of the center of floatation, $\xi$ denoted the translational motion and $\alpha$ term was the rotational motion of the structure.

## 2.5 Review of Literature

In this study, dynamic responses of spar and semi-submersible platform, using both Morison equation and diffraction theory are compared. Reviews of papers on the related studies are discussed here.

### 2.5.1  Behavior of Spar Platform

A study on nonlinear responses of spar was carried out by Mekha et al [33]. In that study, a spar model was subjected to regular and random waves. Coupled analysis was conducted with different mooring line model using the Morison equation incorporating linear diffraction aspects. The second order effect that caused slow varying drift forces was included in the random wave analysis. Mekha et al [34] studied the hydrodynamic forces on the global responses of a spar, w

hich they incorporated the second order diffraction force into the Morison equation. The different nonlinear modifications to Morison equation were included to obtain the diffraction effects. The particular of the JIP spar they used are given in Table 2.1. These values were taken as the reference values for locating the position of center of gravity and fairlead, for the spars used in this study.

Table 2. 1 Particular of the JIP spar

| Description | Value |
|---|---|
| Diameter (m) | 40.5 |
| Draft (m) | 198.2 |
| Mass (with entrapped water) (kg) | $2.6 \times 10^8$ |
| Keel to center of gravity (m) | 92.4 |
| Keel to fairlead  (m) | 92.6 |
| Mass radius of gyration (m) | 62.33 |

Prislin and Halkyard [35] conducted a full scale measurement of the Oryx Neptune production spar platform performance. They discussed the measured and predicted heave and pitch motions from two storms i.e. the Earle and Georges. A time domain program (TDSIM) based on modified Morison equation incorporated with the hydrodynamic coefficients related to potential flow e.g. the radiation damping and slow varying drift forces was used for validation. Interesting effects on heave motion were found by the nonlinear coupling between spar and risers. The full scale data did not show a significant heave response at the spar natural period. However, heave responses at the wave peak period seemed to be more noticeable than the one predicted analytically. Two model tests were conducted for spar with and without risers. The results for the spar without risers did not show remarkable heave response at wave frequencies. The heave free-decay model test with riser showed noticeable

responses around natural heave frequency. While the pitch response seemed to be less sensitive to both cases with and without risers, some pitch damping and restoring moments seemed to be beneficial in the analytical prediction.

Ma and Patel [36] studied the nonlinear forces acting on a floating spar platform in ocean waves that focused on the nonlinear interaction components of spar. The formulation of the nonlinearities i.e. the axial divergence force and the centrifugal force, which was neglected in the previous studies, were investigated. The wave load calculation based on a method in the literature that incorporated drag force calculation were modified for Morison equation for validation. It was found that the effects of the nonlinearities may be significant in comparison to those caused by wave acceleration. The magnitude of these two components strongly depended on the wave conditions and might be small in some conditions but could not be neglected in general. This was important for the nonlinear difference frequency forces which have an inconsistent effect on spar horizontal motions and mooring loads because they were always in a long period range capable of exciting mooring system resonance.

Agarwal and Jain [37] conducted a numerical analysis on the dynamic behavior of offshore spar platforms under regular sea waves. The analysis was performed by using time domain analysis incorporating iterative incremental Newmark Beta approach. A unidirectional regular wave model was used for computing the incident wave kinematics by Airy's wave theory and wave load by Morison's equation, which they made an assumptions that the wave field is virtually undisturbed by the structure due to the ratio of structure dimension to spectrum peak wave length is small. The heave response was affected mostly with the consideration of coupled stiffness matrix. With lower initial horizontal force, the structure showed higher flexibility and gave lower dynamic responses, even though the static contribution of responses were more due to lower stiffness of the structure. Variation in initial horizontal force affected surge and heave response significantly. The change in structural damping ratio mainly affected the heave response and insignificant effect was found in surge and pitch responses. The surge, heave and pitch responses proportionally varied with the value of inertia coefficient, while the drag coefficient affected the surge response only.

27

Spanos et al [38] discussed the spar response due to the effects of riser stiffness exerted by wave and current loads. The response obtained by Monte Carlo simulation was used to validate the applicability of the statistical linearization technique for the preliminary design processes for coupled analysis. Morison equation was used for the estimation of drag force. The linear and nonlinear surge response for the peak wave region agreed with each other. The surge response derived by the statistical linearization procedure was conservative in comparison to the surge response based on the Monte Carlo analysis in the low frequency region. On the other hand, the heave response determined by Monte Carlo simulation exceeded the equivalent linear response in the low frequency region. The pitch response obtained by both Monte Carlo analysis and the statistical linearization procedure agreed well at the low frequency region and also the peak wave frequency region.

John et al [39] conducted a frequency domain analysis of truss spar platform, to gain general understanding on truss spar responses exerted by random waves using simpler dynamic analysis approach. In that study, frequency domain analysis, where Morison equation was used to determine the wave force, was carried out by choosing a suitable wave spectrum model to represent an appropriate density distribution of sea water at the site under consideration. The wave spectrum for each of the motions and the motion response profiles were evaluated from the spectra to obtain the motion response spectra. The results showed similar trend but lower amplitudes in comparison to the responses obtained by time domain dynamic analysis.

Montasir et al [40] conducted a dynamic analysis of classic spar and truss spar, and the motion responses in surge, heave and pitch were evaluated. In this analysis, unidirectional regular waves and random waves by PM spectrum were used. The incident wave kinematics was determined by Chakrabarti's stretching formula and wave loads were obtained Morison equation. Time domain analyses were performed to solve the dynamic behavior of the moored spar platform as an integrated system using the iterative Newmark Beta method. The comparisons showed that truss spar had a better response characteristic when subjected to waves and ambient deep current.

Steen et al [41] conducted an assessment of spar motion experimentally and analytically. Model tests were conducted in the deepwater test basin for a classic spar model. The analytical approach was performed by frequency domain and time domain analysis. WAMIT program was used for obtaining diffraction parameters and Morison equation was used to determine the drag force and hydrodynamic loads. In this study, semi-coupled and full coupled models were analyzed. It was found that the responses obtained by both methods gave a close agreement.

Sadeghi et al [42] developed a simplified technique to calculate the responses of a truss spar due to wave load. A new approach was developed that used the tensor properties of the added-mass coefficients, which was generally applicable to bodies with an arbitrary shape. It was found that the approach was more effective and computationally more efficient than the usual implemented methods. The total surge force and pitch moment acting on the hull was approximated by linear diffraction theory. The force decomposition of the Morison equation was used to add viscous effects to linear equation of motion. The nonlinear equation of motion for the heave of the truss spar was solved without any iteration in the frequency domain. It was shown that the method gave results that closely agreed with the experimental heave motions in the literatures. However, the method underestimated the pitch motions and overestimated the surge motions. They also found that heave plates effectively reduced the amplitude and natural frequency of the heave motion. The heave response was found to be sensitive to the value of the drag coefficient of the heave plates.

Wang et al [13] performed a hydrodynamic analysis by frequency and time domain for the coupling effects of the geometric spar platform. In the frequency domain analysis, the inertia force and diffraction force on the hull were obtained by linear diffraction theory. Morison equation was applied to solve the wave drag force on mooring lines and risers. 3-D panel model of the spar and the related free water surface model were established by boundary element method. The first and second order different frequency wave loads and other hydrodynamic coefficients were obtained. The results were validated experimentally. It was found that, the numerical and experimental motion responses agreed well within the wave frequency range.

Anam and Roesset [31] conducted a study on the slender body approximations of hydrodynamic force for spar platform. The paper presented the effects of different nonlinear forces on the dynamic response of spars and illustrated the basic difference. The second order frequency forces on the spar were evaluated analytically and numerically using various nonlinear hydrodynamic models i.e. the full time domain Morison equation, second order Morison equation, the second order diffraction-radiation theory and the second order diffraction-radiation theory assuming very slender structure dimensions. The different nonlinear force on the dynamic responses of spar was determined and illustrated. The use of Morison equation was found inappropriate for the approximation of hydrodynamic forces on the spar.

A new spar concept, the Cell-Truss Spar was introduced by Zhang et al [11]. This concept was introduced to remedy the weakness, i.e. the fabrication difficulties and the cost efficiency, of earlier generation spar. This paper focused on global performance and mooring line system analysis of the cell-truss spar. Hydrodynamic forces were modeled by Morison equation. The mooring line tension and motion responses were found governed by the wave height and wave period. Zhang et al [12] conducted another analysis on cell-truss spar coupling effects of the mooring lines and risers. The analysis was conducted by using numerical simulation and model tests, and the results were compared. The hydrodynamic coefficients in the numerical simulation were calculated based on wave diffraction-radiation theory. From the analysis, it was found that the model test needed to be improved for simulating the dynamic performance of slender structure. The calculation for numerical simulation at the low frequency region and mooring line tension were affected by the nonlinear effects.

Jha et al [43] made a comparative study, experimentally and analytically, on the predicted motions of a floating spar buoy platform subjected to the extreme conditions in Gulf of Mexico and North Sea. The responses were compared for three frequencies range i.e. the relatively high-frequency contribution due to first order wave energy, a low frequency contribution due to pitch and a still lower frequency contribution due to surge. The basic model combined the nonlinear diffraction loads and a linear multiple-degree-of-freedom model of the spar stiffness and damping characteristics.

The refined model incorporated the effect of wave-drift damping and of viscous force. The models were found to provide good agreement with model test results. The analytical prediction showed the ability to capture another notable feature of the spar model tests i.e. the apparent "mode-swapping" between the spar responses in pitch and surge motions, during the hour-long tests. The results indicated the need of the numerical model for nonlinear forces, i.e. the diffraction, drag or both, to explain the mean offset and the amplitude of slow drift oscillation of the spar.

Kim et al [44] investigated the diffraction of wave on two bottom mounted vertical cylinder. The investigation was conducted by Boundary Element Method (BEM) based on Green's theorem, which incorporated linear potential theory. Linear diffraction theory was used for the wave force analysis of the vertical circular cylinder. Also, they introduced an integral equation for the fluid velocity potential. The numerical results by BEM were compared with the results in literature. The comparison showed close agreement between the numerical analysis value and the published results. Similar study was carried out by Kim et al [45], where they compared the numerical results of BEM with the results of previous studies computed by multiple scattering methods. The development of numerical analysis method with boundary element method was verified.

### 2.5.2 Behavior of semi-submersible platform

Yilmaz and Incecik [46] conducted an investigation on the motion response of a moored semi-submersible platform by using frequency and time domain analysis. Two time domain models were developed to estimate the dynamic response of the semi-submersibles and the effects of the thruster and mooring line damping were incorporated into the time domain models. Morison equation was applied to evaluate the first order wave force; current effect was taken into account by modifying the drag term of the equation. Total extreme motions and mooring forces were obtained. The effects of mooring line damping on the motions and the mooring forces were found when slowly varying wave forces were dominant.

Soylemez and Incecik [47] conducted an investigation on the nonlinearities that

affected the motion responses of the semi-submersible platforms by numerical simulation using the time domain analysis. The analysis also incorporated the nonlinear physical effects such as the wave excitation force, rigid-body induced motion force and restoring force. Morison equation was used to obtain these force components. The nonlinear coupled large-amplitude motion of the semi-submersible platform was found to give higher responses than the linear uncoupled motion responses.

An analysis on the semi submersible of type GVA 4000 was conducted to investigate the response of the structure on extreme condition towards the motion and force. Clauss et al [48] investigated the sea keeping behavior of a semisubmersible in a reported rough wave, i.e. the Draupner New Year Wave in random sea state. A numerical time domain analysis by panel method and potential theory was conducted and were compared with the frequency domain results. The commercial code, TiMIT was employed for time domain analysis to provide motions and forces on the wetted body by Morison equation, and RAO were obtained by diffraction based analysis software, WAMIT, which served as a control for the TiMIT program. A physical wave tank test was conducted for validation. The results by TiMIT show good agreement with the model tests. Another investigation was carried out by Clauss et al (2003) to study the motion behavior and resultant splitting force of the same type of semi-submersible platform using time domain analysis. Good agreement was found on the results of WAMIT and TiMIT.

Low and Langley [20] developed a more efficient linearized frequency domain approach for coupled floating production system which incorporated the first and second order motions. In this paper, time domain and frequency domain coupled analysis for deepwater floating production systems were compared. The time domain approach of the study implemented the Wilson-theta integration method, which was more stable than many other methods when relatively large time steps were employed. The formulation of lumped mass approach was employed to approximate frequency domain analysis. Diffraction analysis was implemented to obtain the wave force for the vessel. The Morison equation's drag component was incorporated with current for the mooring liner and risers. The numerical simulations showed that a consistently

formulated frequency domain analysis could provide good estimation of vessel motions and mooring line tensions comparable to the time domain analysis. The geometric nonlinearity of the lines was insignificant for the deepwater floating system where the motions were small compared to the line dimensions.

Truss pontoon semi-submersible was introduced by Chakrabarti et al [49] as the floating concept combining the advantages of conventional semi-submersible and truss spar platforms. Truss pontoon semi-submersible concept remedied the ineffectiveness of the separated flow of conventional semi-submersible by introducing heave plates at the bottom of the truss columns, which was analyzed by both Morison equation and linear diffraction theory. The motion characteristic of this new concept was found enhanced in comparison to the conventional semi-submersible platforms.

Zhang and Li [50] studied the effects of volumetric allocation on heave response of semi-submersible in the deep sea. The objective of this study was to provide a theoretical approach to estimate the effects of volumetric allocation on natural period and response amplitude operator (RAO) in heave motion. Two theoretical formulae were derived, which showed that the natural period and heave response were dependent on the volumetric ratio of pontoon to total structure rather than specific geometric configuration. It was validated by the published diffraction analysis results. It also showed that the semi-submersible with the same volumetric ratio, in fact, have the same natural period and behavior RAO. The evident difference in the response amplitude of heave motion around the natural period was attributed to the difference of damping in the resonance period region.

## 2.6    Chapter summary

In this chapter, methods of dynamic analysis of spar and semi-submersible platforms reported in the literature were discussed. They used Morison equation, diffraction theory and combinations of both methods in the frequency and time domain analysis. Furthermore, comparisons with model test were discussed for validation.

i.  In the majority of the papers that focused on the behavior of the spar, the Morison equation was employed for the determination of the hydrodynamic responses, especially for the drag term.  Also, the applications combining both approaches were found.  In this case, the hydrodynamic components were obtained by using diffraction theory for the hull structures, and Morison equation was applied for the mooring lines or risers.  Few papers used the application of the diffraction theory for wave calculation.

ii.  For semi-submersible platforms, most of the paper used methods combining Morison equation and diffraction theory for wave force estimation.  One paper used diffraction theory only for estimation of responses.

iii.  Morison equation is easier to program and gave correct estimation of wave force for small sized members.  However, as the spar and semi-submersible platforms have large-sized members, Morison equation resulted in errors and this was compensated in some papers by modifying the hydrodynamic coefficients and damping values.

iv.  The very cumbersome procedure for applying the diffraction theory necessitated costly software programs to be used and most of the researchers resorted to methods employing a combination of Morison equation incorporating a correction of wave force estimation using simple diffraction methods.

# CHAPTER THREE

# RESEARCH METHODOLOGY

## 3.1    Chapter overview

In this chapter, research methodologies employed for this study are discussed.  The dynamic responses of the spar and semi-submersible platforms were investigated experimentally and numerically in this study.  First, the platform models were tested in the wave tank, and the responses were measured.  Next, the dynamic analyses for the corresponding prototypes were carried out by two approach i.e. time domain analysis, and linear wave diffraction analysis.  The dynamic analysis was performed using time domain analysis incorporating Newmark Beta integration method executed by Matlab program.  The platforms were designed as rigid bodies and three degree of freedom; surge, heave and pitch were considered.  Linear wave theory and Morison equation were used for wave force determination in time domain analysis and responses were obtained as response amplitude operators (RAO).  The linear wave diffraction analysis was conducted using a commercial software and the dynamic responses in terms of RAO were obtained.  As reported in the literature, the diffraction results gave better comparisons with the model test responses.  A large number of diffraction analyses for various sizes of the platform were conducted using these results.  A non-linear multiple regression analysis was conducted and regression curves were developed for predicting the dynamic responses of spar and semi-submersible platform for any dimension and draft.  Typical progress flow chart of this study was shown in Figure 3.1.
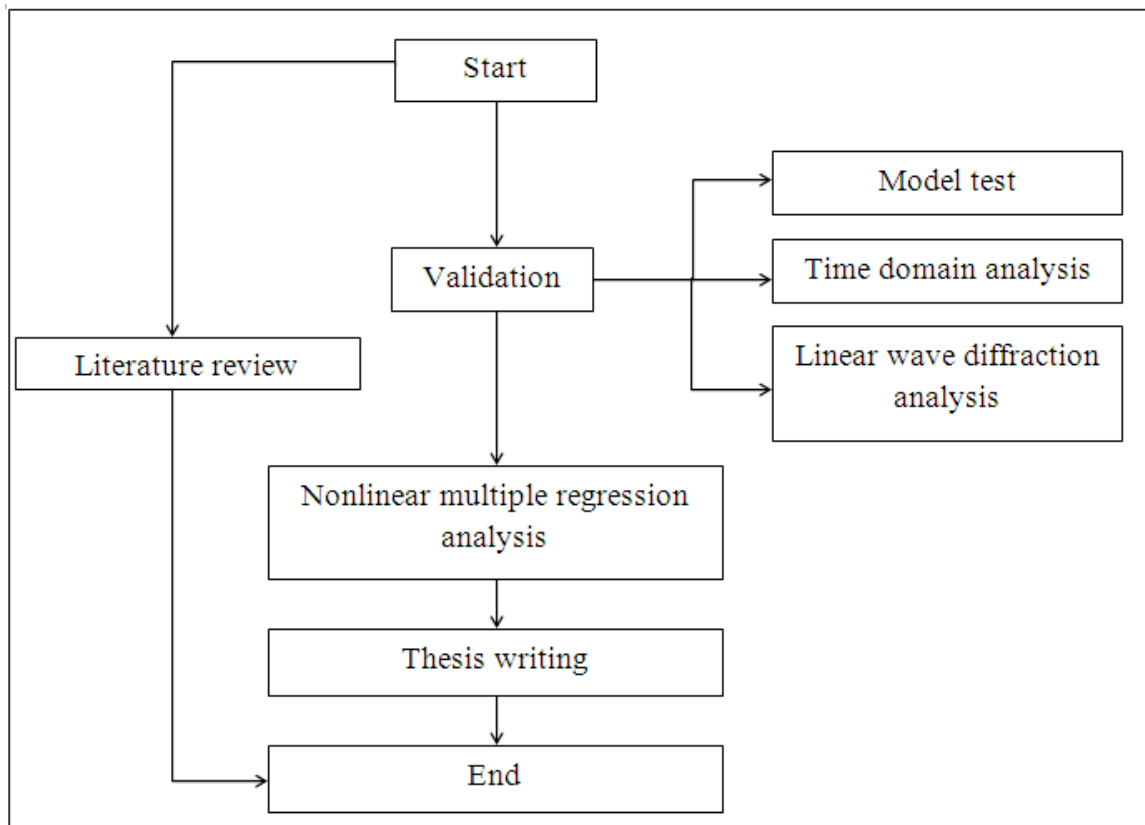
Figure 3. 2 Typical progress flow chart of this study

## 3.2 Model test in the wave tank

Wave tank tests were conducted on spar and semi-submersible platform models to investigate the dynamic responses. The tests were conducted in the wave tank in the Offshore Engineering Laboratory of Universiti Teknologi PETRONAS.

### 3.2.1 Wave tank details

The tests were conducted using regular wave in the wave tank 22 m long, 10 m wide and 1.0 m deep. The waves were generated by the multi-element wave generation system of the wave maker. This wave maker consisted of sixteen individual paddles that moved independently to each other. By the backward and forward movement of

these paddles waves were generated. Also, the wave maker could generate waves at an angle instead of uni-directional waves. However, in this study, the uni-directional waves in surge direction only were considered.

### 3.2.2 Wave data

Due to the limitation on the performance of the wave makers, regular wave with 60mm wave height was implemented to avoid wave reflection, and wave breakage before the maximum wave height is achieved. The wave frequencies varying from 0.4 Hz to 2.0 Hz at an increment of 0.2 Hz were implemented for testing both models based upon the capability of the wave makers.

### 3.2.3 Experimental models

Spar and semi-submersible models with the dimensions given in Table 3.1 were fabricated. As the water depth of the wave tank was only 1 m, the model dimensions were chosen to simulate the behavior of the floaters fairly well.

Table 3. 1 Dimensions of experimental models

| Model | Description | Value (mm) |
|-------|-------------|------------|
| Spar | Diameter (D) | 80 |
| | Hull length (L) | 700 |
| | Draft (d) | 630 |
| Semi submersible | Pontoon | |
| | Length | 1100 |
| | Breath | 150 |
| | Depth | 80 |
| | Column | |
| | Diameters | 80 & 100 |
| | Draft | 200 |
| | Spacing (longitudinal) | 240 |
| | Spacing (transverse) | 600 |
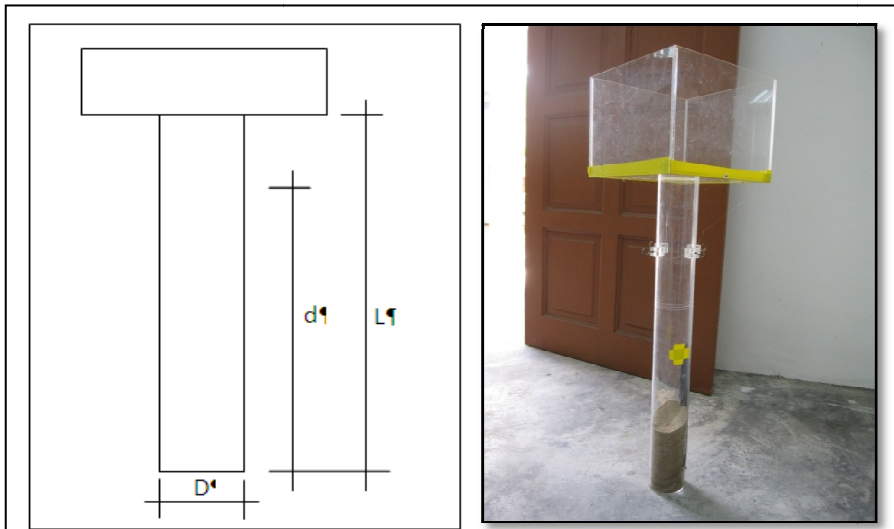
Figure 3. 3 Typical spar model
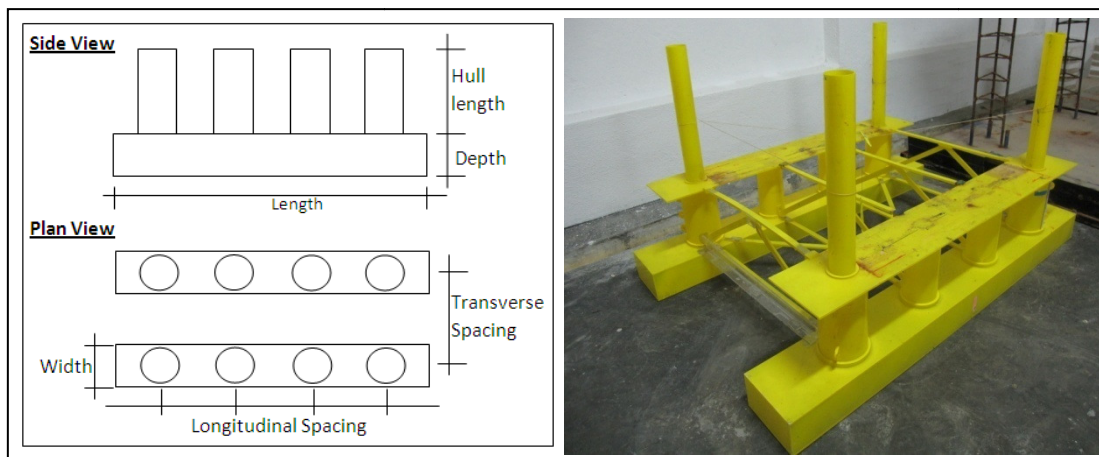


Figure 3. 4 Typical semi-submersible model

### 3.2.4   Mooring line set up

Four taut mooring lines were used for both the models.  Wires of 1.55 mm diameter and modulus of elasticity 3600 MPa were used as the mooring lines.   The arrangements are shown in Figure 3.4 and Figure 3.5 for spar and semi-submersible respectively.  The mooring lines were made of aluminum alloy wire that connected from the fairlead of the hull to the anchors placed at the bottom of the tank.
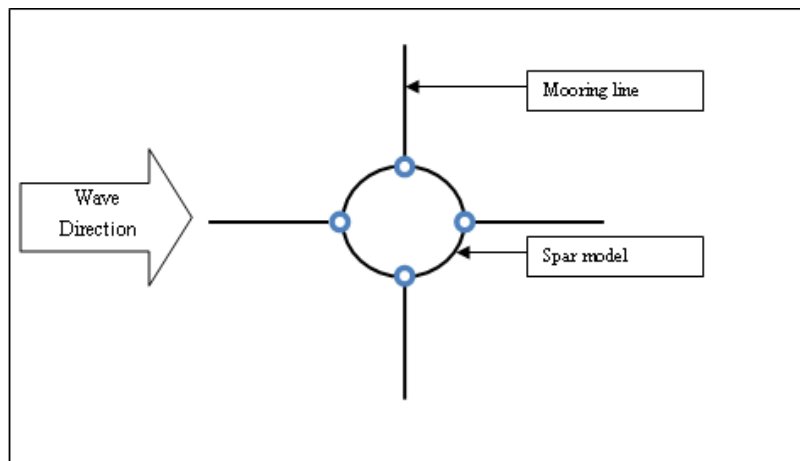
Figure 3. 5 Spar model in position (Plan view)
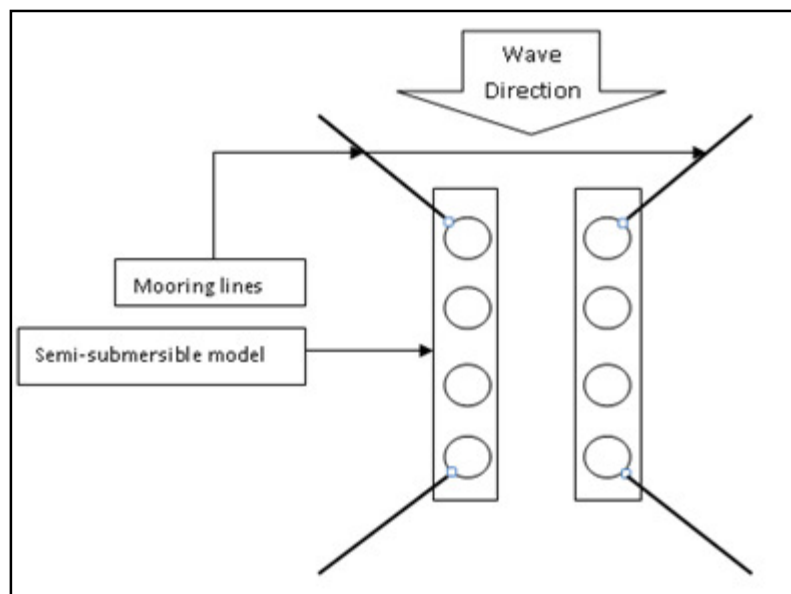


Figure 3. 6 Semi-submersible model in position (Plan view)

### 3.2.5 Experimental set up

The procedure for model testing was as follows.

    i.      Preparations

        a.  The model was positioned in the wave tank with moorings connected from the fairlead on the hull to the anchors at wave tank bed. Figure 3.6 and Figure 3.7 show the experimental models of spar and semi-submersible after setting up and ready for test.

        b.  The wave tank, as shown in Figure 3.8, was then filled with water to a depth of 1m.

    ii.     Test method

        a.  Regular waves as specified in 3.1.2 were programmed and generated using the generation software.

        b.  The wave heights near the model were measured using two wave probes.

        c.  The responses of the models in surge, heave and pitch motions were measured from video recording by a recorder.

    iii.    Processing of the video recorded

        a.  The video recorded were reviewed with software that has the capability to capture motion on every millisecond.

        b.  The motion responses were measured for every 0.5 sec by referring to the scale attached on the wave tank. The relationship of the responses to the time series were plotted, and RAO were obtained for each wave frequency as discussed in 3.1.2. The relationship between the RAOs and frequencies were plotted.
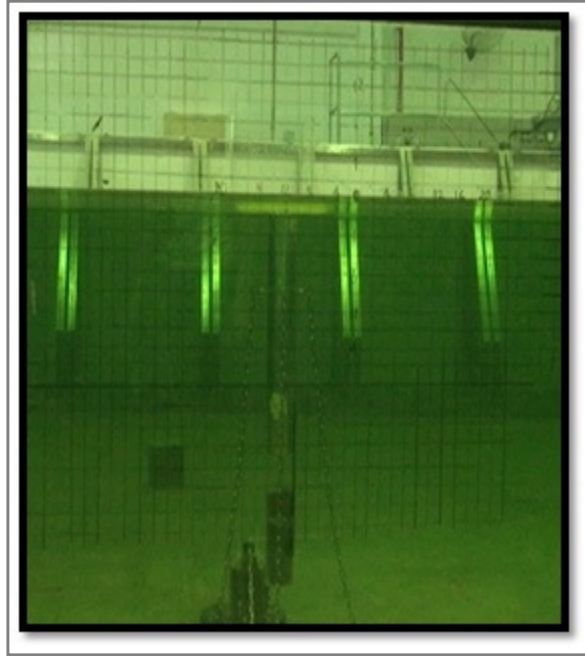
Figure 3. 7 Spar platform model set up
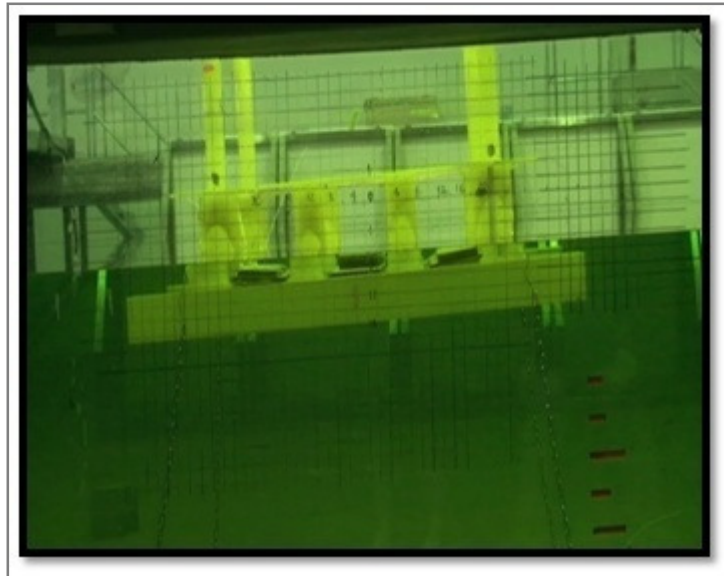


Figure 3. 8 Semi-submersible model set up

Figure 3. 9 Wave tank filled with water

## 3.3    Dynamic analysis in time domain

A dynamic analysis was carried out by using a numerical Newmark Beta time domain integration method executed by MATLAB program.  In the program, linear wave theory and Morison equation were used for wave kinematics and wave force determination, respectively in the time domain.  The responses were obtained as Response Amplitude Operators (RAO).  The procedure for time domain analysis is discussed as follows.

### 3.3.1    Morison equation

Morison equation, as discussed in 2.3.1, considered the wave force as summation of drag and inertia component.  In this study, the drag and inertia coefficient were obtained from the mean curves developed from test data conducted by Chakrabarti [6], reasoning that the curves obtained from wave tank tests subjected to regular wave is similar to the condition of this study.   The mean curves were developed corresponding to the Keulegen-Carpenter (KC) number which was given as.

$$KC = \frac{U_m T}{D} \qquad\qquad (3.1)$$

Where $U_m$ was the maximum along wave water particle velocity, $T$ was the wave period and $D$ was the diameter of the vertical cylinder. Figure 3.9 and Figure 3.10 show the mean curves developed by Chakrabarti on the drag and inertia coefficient with the response to the KC number for smooth circular cylinder in waves.
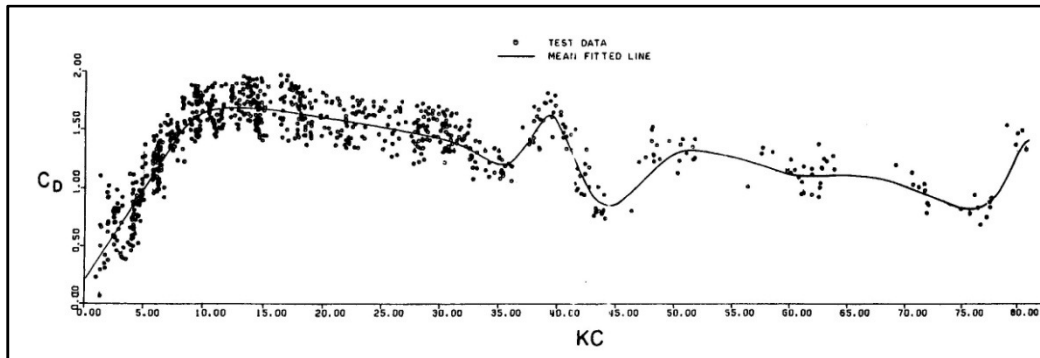


Figure 3. 10 Drag coefficients vs. KC for smooth circular cylinder in waves [6]
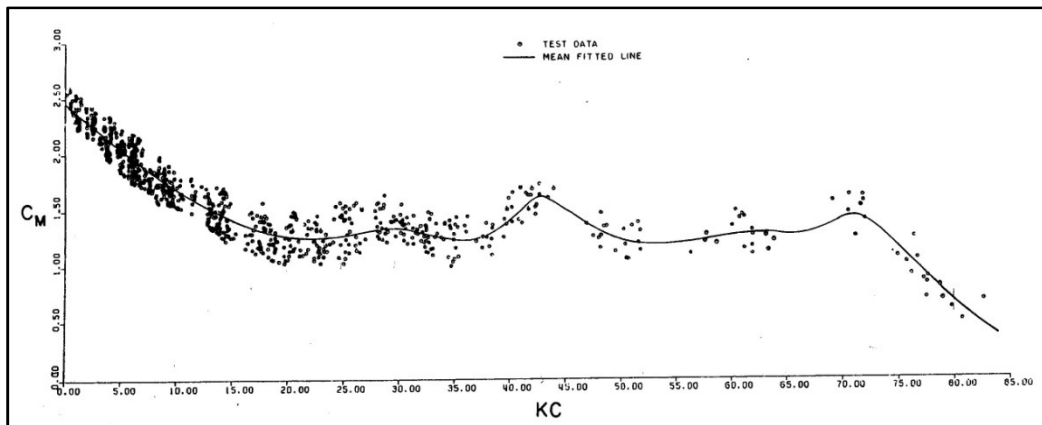


Figure 3. 11 Inertia coefficients vs. KC for smooth circular cylinder in waves [6]

### 3.3.2   Spar prototype

The frequency of sea waves varies from 0.063 Hz to 0.316 Hz. In the offshore laboratory, the wave generator could generate waves of frequencies 0.4 Hz to 2 Hz.

43

That made the model scale to be about 1/6.3. Using Froude Law, the linear scale worked out $(1/6.3)^2 = 1/40$ of the prototype for time domain were selected. The prototype particular are as given in Table 3.2, by multiplied the model dimensions by 40. The modulus of elasticity for mooring line, E was calculated as 40 times of the model test mooring line, which worked out as $1.44 \times 10^8$ kN/m$^2$. The area of cross-section of mooring lines was taken as $1.887 \times 40^2 = 3020$ mm$^2$.

Table 3. 2 Particular of spar prototype and wave data

| Description | Value |
|---|---|
| Diameter, D (m) | 3.200 |
| Total hull length, l (m) | 28.000 |
| Draft length, H (m) | 25.200 |
| Center of gravity from MSL(CG), (m) | -14.332 |
| Center of buoyancy from MSL(CB), (m) | -14.000 |
| Distance of CG and CB, h1, (m) | 0.332 |
| Distance from CG to fairlead, h2 , (m) | 0.168 |
| Mooring lines EA (kN) | 434800 |
| Total structural mass, M (Tonne) | 229.200 |
| Total mass moment of inertia, I (kg-m$^2$) | $15.141 \times 10^6$ |
| Added mass coefficient, $C_m$ | 2.45 |
| Wave height, m | 2.40 |
| Wave frequency, Hz | 0.063 – 0.316 |

### 3.3.2.1  Mass matrix

The mass matrix of spar platform mainly consisted of by two parts, the structural mass matrix and added mass matrix. The mass matrix was given as

$$[M] = [M_{struc}] + [M_{add}] \tag{3.2}$$

$$[M_{struc}] = \begin{bmatrix} M & 0 & 0 \\ 0 & M & 0 \\ 0 & 0 & I \end{bmatrix} \tag{3.3}$$

$$[M_{add}] = \begin{bmatrix} M_{11} & M_{12} & M_{13} \\ M_{21} & M_{22} & M_{23} \\ M_{31} & M_{32} & M_{33} \end{bmatrix} \tag{3.4}$$

44

The elements of added mass matrix were given as

$$M_{11} = \rho \frac{\pi D^2}{4} (C_m - 1) \cos^2 \emptyset \; dz \qquad (3.5)$$

$$M_{12} = M_{21} = -\rho \frac{\pi D^2}{4} (C_m - 1) \sin \emptyset \cos \emptyset \; dz \qquad (3.6)$$

$$M_{13} = M_{31} = -\rho \frac{\pi D^2}{4} (C_m - 1) \; Z \cos \emptyset \; dz \qquad (3.7)$$

$$M_{22} = \rho \frac{\pi D^2}{4} (C_m - 1) \sin^2 \emptyset \; dz \qquad (3.8)$$

$$M_{23} = M_{32} = \rho \frac{\pi D^2}{4} (C_m - 1) \; Z \cos \emptyset \; dz \qquad (3.9)$$

$$M_{33} = \rho \frac{\pi D^2}{4} (C_m - 1) \; (Z^2) \qquad (3.10)$$

Where $M_{add}$ was the added mass matrix, $M_{struc}$ was the structural mass matrix, M was the total structural mass, I was the total mass moment of inertia, D was the diameter, $\rho$ was the seawater density, $C_m$ was the added mass coefficient, $\emptyset$ was the pitch angle measured from z-axis and Z was the distance of center of gravity to heel plus the increment of each element with 1 m interval.

The structural mass matrix was given by the total mass of the spar platform which comprises the deck, hard tank, ballast and entrapped water. The added mass matrix was obtained using to the added mass term of Morison equation. The added mass matrix was integrated along the submerged draft of the hard tank of the spar structure.

*3.3.2.2 Stiffness matrix*

Same as mass matrix, stiffness matrix consisted of two parts, the stiffness of restoring hydrostatic force and stiffness due to mooring lines which was given as

$$[K] = [K_{hystat}] + [K_{moor}] \qquad (3.11)$$

$$[K_{hystat}] = \begin{bmatrix} 0 & 0 & 0 \\ 0 & K_{22_h} & 0 \\ 0 & 0 & K_{33_h} \end{bmatrix} \tag{3.12}$$

where

$$K_{22_h} = \pi \frac{\pi D^2}{4} \gamma_w \tag{3.13}$$

$$K_{33_h} = K_{22_h} Hh_1 - \frac{\pi}{64} \gamma_w D^4 \tag{3.14}$$

H denoted the draft of the spar platform, $\gamma_w$ was the weight density of sea water, and $h_1$ was the distance of the center of gravity and center of buoyancy.

The mooring line stiffness was given as,

$$[K_{moor}] = \begin{bmatrix} K_{11_m} & 0 & K_{13_m} \\ 0 & 0 & 0 \\ K_{31_m} & 0 & K_{33_m} \end{bmatrix} \tag{3.15}$$

$$K_{11_m} = k_x \tag{3.16}$$

$$K_{13_m} = K_{31_m} = -k_x h_2 \tag{3.17}$$

$$K_{33_m} = k_x h_2^2 \tag{3.18}$$

where $k_x$ was taken as constant mooring line stiffness, $h_2$ was taken as the distance between center of gravity and fairlead, as referred in Table 3.2.

### 3.3.2.3   Equations of motion

Using mass matrix and stiffness matrix as discussed, the equation of motion of the spar platform under regular wave was given as

$$[M]\{\ddot{X}\} + [K]\{X\} = \{F(t)\} \tag{3.19}$$

Where $\{X\}$ was the structural displacement vector, $\{\ddot{X}\}$ was the structural acceleration vector, [M] was the mass matrix, [K] was the stiffness matrix, F(t) was the

46

hydrodynamic forcing vector.

### 3.3.2.4 Newmark Beta method

To solve the equation of motion for spar platform, Newmark beta integration was implemented. The displacement of the structure calculated at each time step was given as

$$X_{t+\Delta t} = \widehat{K}^{-1}\widehat{F}_{t+\Delta t} \tag{3.20}$$

When the effective stiffness matrix, $\widehat{K}$ was given as

$$\widehat{K} = K + a_0 M \tag{3.21}$$

Then the acceleration, $\ddot{X}_{t+\Delta t}$, and the velocity, $\dot{X}_{t+\Delta t}$ of the structure were calculated as

$$\ddot{X}_{t+\Delta t} = a_0(X_{t+\Delta t} - X_t) - a_2\dot{X}_t - a_3\ddot{X}_t \tag{3.22}$$

$$\dot{X}_{t+\Delta t} = \dot{X}_t + a_6\ddot{X}_t + a_7\ddot{X}_{t+\Delta t} \tag{3.23}$$

The effective loading matrix, $\widehat{F}_{t+\Delta t}$ was formulated as

$$\widehat{F}_{t+\Delta t} = F_{t+\Delta t} + M(a_0X_t + a_2\dot{X}_t + a_3\ddot{X}_t) \tag{3.24}$$

To solve the above formulations, the integration constants of Newmark beta method were taken as

$$a_0 = 1/(\alpha\Delta t^2) \tag{3.25}$$

$$a_1 = \delta/\alpha\Delta t \tag{3.26}$$

$$a_2 = 1/\alpha\Delta t \tag{3.27}$$

$$a_3 = \left(\frac{1}{2\alpha}\right) - 1 \tag{3.28}$$

$$a_4 = \left(\frac{\delta}{\alpha}\right) - 1 \tag{3.29}$$

47

$$a_5 = \left(\frac{\Delta t}{2}\right)[(\delta/\alpha) - 2] \qquad (3.30)$$

$$a_6 = \Delta t(1 - \delta) \qquad (3.31)$$

$$a_7 = \delta \Delta t \qquad (3.32)$$

Where δ=0.5, α=0.25*(0.5+δ) 2, and Δt was take as time step.

### 3.3.2.5 Solution procedure

The following steps were adopted in the program, for the determination of the spar platform.

1. Calculation of wave properties ( wave length, L; wave frequency, ω and wave number, k)

2. Initialize displacement, X0; velocity, R0 and acceleration, A0 for the first time step

3. Formulate stiffness matrix and mass matrix

4. Evaluate wave force acting

5. Solution of equation of motion by Newmark beta method; and displacement, velocity and acceleration for second time step

6. Repetition of step 3 to 5 until the accuracy of 0.01% achieved

7. Plot of responses in time series

According to the procedure mentioned, the algorithm of the MATLAB program developed is shown in Figure 3.11.



```
                            ┌──────────────┐
                            │    Start     │
                            └──────┬───────┘
                                   ▼
                            ┌──────────────┐
                            │  Data input  │
                            └──────┬───────┘
                                   ▼
                    ┌──────────────────────────────────┐
                    │  Calculation of stiffness matrix  │
                    │(Hydrostatic stiffness and mooring │
                    │            stiffness)             │
                    └──────────────┬───────────────────┘
                                   ▼
                    ┌──────────────────────────────────┐
                    │   Calculation of mass matrix      │
                    │  (Physical mass and added mass)   │
                    └──────────────┬───────────────────┘
                                   ▼
                    ┌──────────────────────────────────┐
                    │ Calculation of Drag and Inertia   │
                    │           component               │
                    └──────────────┬───────────────────┘
                                   ▼
                    ┌──────────────────────────────────┐
                    │ Calculation of hydrodynamic       │
                    │           pressure                │
                    └──────────────┬───────────────────┘
                                   ▼
                    ┌──────────────────────────────────┐
                    │  Solution of equation of motion   │
                    │     by Newmark Beta Method        │
                    └──────────────┬───────────────────┘
                                   ▼
  ┌──────────────┐        ┌──────────────────────────────────┐
  │ If no, Repeat│        │        Time step over?            │
  └──────────────┘        └──────────────┬───────────────────┘
                                   ▼
                          ┌──────────────────────────────────┐
                          │     If yes, Plot of responses     │
                          └──────────────┬───────────────────┘
                                   ▼
                            ┌──────────────┐
                            │     End      │
                            └──────────────┘
```
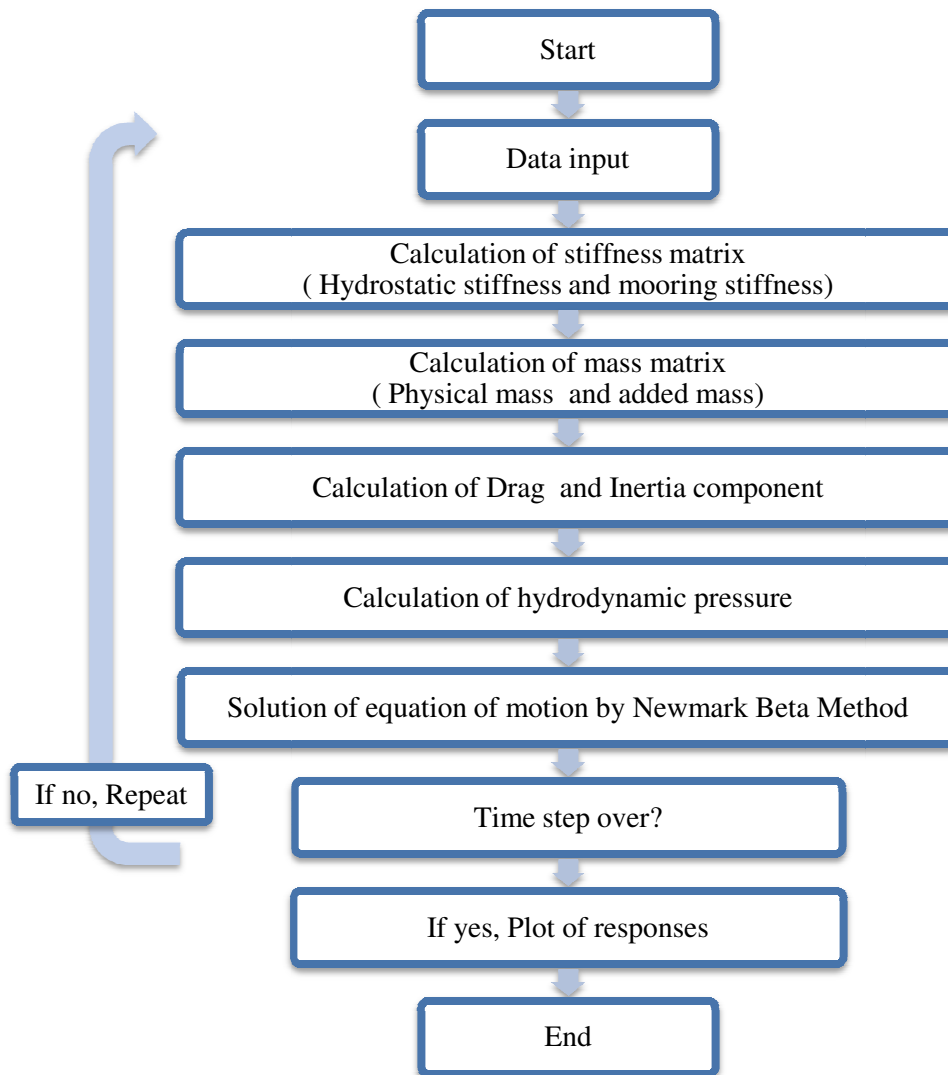
Figure 3. 12 Algorithm of MATLAB program for spar platform

### 3.3.3    Semi-submersible prototype

The wave force calculation was done by Morison equation for semi-submersible prototype. The dimensions of it are given in Table 3. 3. Matrices used are explained as follows.

Table 3. 3 Dimensions of semi-submersible prototype and wave data

| Description | | Value (m) |
|---|---|---|
| Column | Diameter, (m) | 3.2 & 4.0 |
| | Draft, (m) | 8.000 |
| | x-direction spacing, $x_c$, (m) | 9.600 |
| | y-direction spacing, $y_c$, (m) | 24.000 |
| Pontoon | Length, (m) | 44.000 |
| | Width, (m) | 6.000 |
| | Depth, (m) | 3.200 |
| Center of gravity (From MSL) , (m) | | -7.742 |
| Center of buoyancy (From MSL) , (m) | | -6.440 |
| Total structural mass, M, (Tonne) | | 530.250 |
| Radii of gyration in pitch motion, $r_{pit}$, , (m) | | 12.774 |
| Metacentric height for pitch, $GM_p$, (m) | | 1.046 |
| Column added mass coefficient, $C_{mc}$ | | 2.00 |
| Pontoon added mass coefficient, $C_{mp}$ | | 2.00 |
| Mooring lines EA (kN) | | 434800 |
| Wave height, m | | 2.40 |
| Wave frequency, Hz | | 0.063 – 0.316 |

#### 3.3.3.1   Mass matrix

Mass matrix of the semi-submersible platform consisted of structural mass matrix and added mass matrix, was given as

$$[M] = [M_{struc}] + \ [M_{add}] \tag{3.33}$$

Structural mass matrix was taken as

$$[M_{struc}] = \begin{bmatrix} M & 0 & 0 \\ 0 & M & 0 \\ 0 & 0 & Mr_{pit}^2 \end{bmatrix} \tag{3.34}$$

50

where M was the total structural mass; $r_{pit}$ was the radii of gyration in pitch.

Added mass matrix of the semi-submersible platform comprised of added mass matrices of all the columns and pontoons. The summations of added mass matrix for each column were evaluated as the column added mass matrix. Column was divided into elements for the estimation of wave force evaluation by numerical integration.

$$[M_{add_c}] = \begin{bmatrix} M_{11_c} & M_{12_c} & M_{13_c} \\ M_{21_c} & M_{22_c} & M_{23_c} \\ M_{31_c} & M_{32_c} & M_{33_c} \end{bmatrix} \tag{3.35}$$

The elements of the added mass matrix were obtained as

$$M_{11_c} = \rho\, A_c(C_{m_c} - 1)\cos^2\emptyset\ dz \tag{3.36}$$

$$M_{12_c} = -\rho\, A_c(C_{m_c} - 1)\cos\emptyset \sin\emptyset\ dz \tag{3.37}$$

$$M_{13_c} = M_{31,c} = -\rho\, A_c(C_{m_c} - 1)(Z)\cos\emptyset\ dz \tag{3.38}$$

$$M_{22_c} = \rho\, A_c(C_{m_c} - 1)\sin^2\emptyset\ dz \tag{3.39}$$

$$M_{23_c} = M_{32,c} = \rho\, A_c(C_{m_c} - 1)(Z)\cos\emptyset\ dz \tag{3.40}$$

$$M_{33_c} = \rho\, A_c(C_{m_c} - 1)(Z)^2\ dz \tag{3.41}$$

where $A_c$ was the column cross section area, $C_{m_c}$ was the added mass coefficient, $\emptyset$ was the pitch angle response, Z was the inclined element distance to the CG.

The pontoon added mass matrix was given as

$$[M_{add_p}] = \begin{bmatrix} M_{11_p} & M_{12_p} & M_{13_p} \\ M_{21_p} & M_{22_p} & M_{23_p} \\ M_{31_p} & M_{32_p} & M_{33_p} \end{bmatrix} \tag{3.42}$$

The elements of the pontoon added mass matrix were given as

$$M_{11_p} = \rho\, A_p\left(C_{m_p} - 1\right)\sin^2\emptyset\ dz \tag{3.43}$$

51

$$M_{12_p} = \rho\, A_p \left(C_{m_p} - 1\right) \cos\emptyset \sin\emptyset \; dz \tag{3.44}$$

$$M_{13_p} = M_{31_p} = \rho\, A_c \left(C_{m_p} - 1\right)(Z)\sin\emptyset \; dz \tag{3.45}$$

$$M_{22_p} = \rho\, A_p \left(C_{m_p} - 1\right)\cos^2\emptyset \; dz \tag{3.46}$$

$$M_{23_p} = M_{32,c} = \rho\, A_p \left(C_{m_p} - 1\right)(Z)\sin\emptyset \; dz \tag{3.47}$$

$$M_{33_p} = \rho\, A_p \left(C_{m_p} - 1\right)(Z)^2 \; dz \tag{3.48}$$

where $A_p$ was the pontoon cross-sectional area, $C_{mp}$ was the added mass coefficient.

### 3.3.3.2   Stiffness matrix

Total stiffness matrix consisted of hydrostatic stiffness and mooring lines stiffness. The hydrostatic stiffness, $K_{hystat}$, was contributed by the degree of freedom in heave and pitch motion due to buoyancy force in the water plane cutting members of the hull. The hydrostatic stiffness was given as.

$$\left[K_{hystat}\right] = \begin{bmatrix} 0 & 0 & 0 \\ 0 & K_{22_h} & K_{23_h} \\ 0 & 0 & 0 \end{bmatrix} \tag{3.49}$$

The elements of hydrostatic stiffness matrix were given as

$$K_{22_h} = \rho g A_{wn} \tag{3.50}$$

$$K_{23_h} = \rho g \Delta GM_p \tag{3.51}$$

Where $A_{wn}$ denoted the water plane area, $GM_p$ was the metacentric height for pitch and $\Delta$ was the vessel displacement by volume.

The mooring line stiffness was given as

$$K_{moor}=\begin{bmatrix} K_{11_m} & 0 & K_{13_m} \\ 0 & 0 & 0 \\ K_{31_m} & 0 & K_{33_m} \end{bmatrix}$$

(3.52)

The elements of mooring stiffness were denoted as

$$K_{11_m} = k_x$$ (3.53)

$$K_{13_m} = K_{31_m} = -k_x h$$ (3.54)

$$K_{33_m} = k_x h^2$$ (3.55)

Where $k_x$ was the constant mooring line stiffness, h was the fairlead distance measured vertically from the vessels center of gravity.

Next, the equations of motion were solved and the force was obtained as discussed in 3.2.2.3 and 3.2.2.4.

### 3.3.3.3   Solution procedure

The procedures implemented on semi-submersible platform for the determination of response was similar to spar platform, and discussed as follow,

1. Calculation of wave properties ( wave length, L; wave frequency, ω and wave number, k)

2. Initialize displacement, X0; velocity, R0 and acceleration, A0 for the first time step

3. Formulate stiffness matrix and mass matrix

4. Evaluate wave force acting

5. Solution of equation of motion by Newmark beta method; and displacement, velocity and acceleration for second time step

6. Repetition of step 3 to 5 until the accuracy of 0.01% achieved

7. Plot of responses in time series

According to the procedure mentioned, algorithm of the MATLAB program developed is similar to Figure 3.11 with modification made for the geometry, which the semi-submersible prototype needs to consider the columns and pontoons instead of only cylindrical hull for spar prototype.

## 3.4 Diffraction analysis for the prototypes

For structures which are large comparative to the wave length, Morison equation will lead to inaccurate results due to drastic change of velocity and acceleration fields and significant diffraction experienced by incident wave [1], [2], [3].

The diffraction analysis was carried out by a commercial code (Structural Analysis Computer System, SACS) for both spar and semi-submersible platforms. The SACS to WAMIT (Wave Analysis developed at MIT) analysis program was used, which the program created WAMIT diffraction models and map the WAMIT results in the SACS model. The program is capable to calculate the transfer function by linear wave diffraction; mooring line stiffness contribution, also the draft and trim for center of gravity and center of buoyancy balance. Furthermore, the program could also determine the wave heights from the wave periods and specified steepness; water plane properties e.g. the area, moment of inertia, metacentric heights and so on which were necessary in this study.

Figure 3. 14 Typical model of classic spar prototype
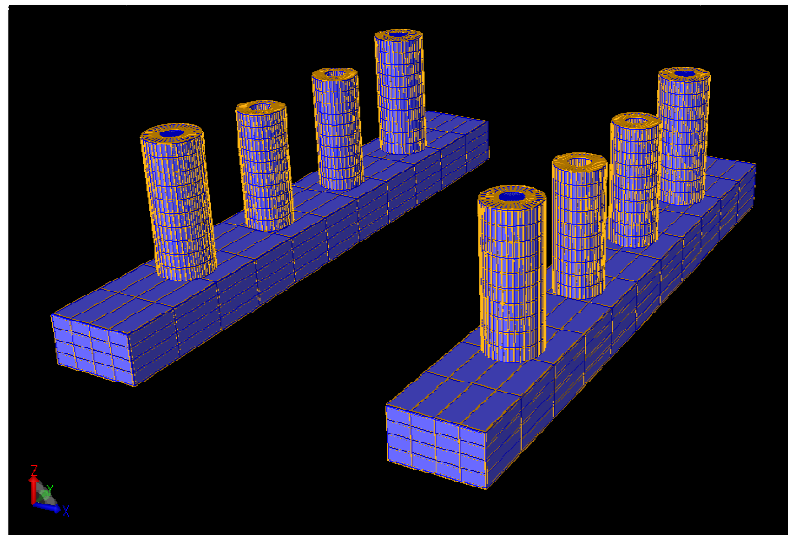


Figure 3. 13 Typical model of semi-submersible prototype

To simulate the prototype, columns of the semi-submersible platforms and cylindrical hull of spar were modeled in the form of cylindrical meshes. The pontoons of semi-submersible platforms were modeled in the form rectangular meshes. Figure 3.12 and Figure 3.13 show the simulated model of the spar and semi-submersible prototype respectively.

Linear wave diffraction analysis was conducted for selected waves. Table 3.4 shows the typical input data for linear wave diffraction module.

Table 3. 4 Typical input information for linear wave diffraction module

| Description | | Value |
|---|---|---|
| Water Depth (m) | | 40 |
| Wave height (m) | | 1 |
| Sea water Density (MT/m3) | | 1.030 |
| Origin Orientation (vertical axis) | | +z |
| Frequency range (Hz) | | 0.05 – 0.20 |
| Mooring line | Cross section area (cm$^2$) | 30.20 |
| | Elastic Modulus (1000kN/cm$^2$) | 14.400 |

## 3.5    Nonlinear multiple regression curves

By using the results of the diffraction analysis for a large number of spars and semi-submersible platforms, which referred to the practical dimension ranges, a nonlinear multiple regression analysis was conducted.  From the analysis, suitable regression curves for predicting the diffraction responses of the spar and semi-submersible standard types of platforms for any dimension and draft within the practical range were suggested.  Table 3.5 and Table 3.6 illustrate the dimensions of the spar and semi-submersible platform analyzed.

Table 3. 5 Dimensions for classic spar platform for linear diffraction analysis

| | | Diameter (m) | | | | |
|---|---|---|---|---|---|---|
| | | 30 | 32.5 | 35 | 37.5 | 40 |
| Draft (m) | 150 | CS 1 | CS 12 | CS 23 | CS 34 | CS 45 |
| | 155 | CS 2 | CS 13 | CS 24 | CS 35 | CS 46 |
| | 160 | CS 3 | CS 14 | CS 25 | CS 36 | CS 47 |
| | 165 | CS 4 | CS 15 | CS 26 | CS 37 | CS 48 |
| | 170 | CS 5 | CS 16 | CS 27 | CS 38 | CS 49 |
| | 175 | CS 6 | CS 17 | CS 28 | CS 39 | CS 50 |
| | 180 | CS 7 | CS 18 | CS 29 | CS 40 | CS 51 |
| | 185 | CS 8 | CS 19 | CS 30 | CS 41 | CS 52 |
| | 190 | CS 9 | CS 20 | CS 31 | CS 42 | CS 53 |
| | 195 | CS 10 | CS 21 | CS 32 | CS 43 | CS 54 |
| | 200 | CS 11 | CS 22 | CS 33 | CS 44 | CS 55 |

Table 3. 6 Dimensions for semi-submersible platform for linear diffraction analysis

| Semis | Pontoon dimension (m) | | | Column dimension (m) | | Spacing (m) | |
|---|---|---|---|---|---|---|---|
| | Width | Depth | Length | Diameter | Draft | x | y |
| 1 | 15 | 8 | 110 | 8 | 20 | 60 | 22 |
| 2 | 15 | 8 | 110 | 10 | 20 | 60 | 22 |
| 3 | 16 | 10 | 110 | 12 | 20 | 60 | 22 |
| 4 | 16 | 10 | 110 | 14 | 20 | 60 | 22 |
| 5 | 15 | 8 | 110 | 8 | 22.5 | 60 | 22 |
| 6 | 15 | 8 | 110 | 10 | 22.5 | 60 | 22 |
| 7 | 16 | 10 | 110 | 12 | 22.5 | 60 | 22 |
| 8 | 16 | 10 | 110 | 14 | 22.5 | 60 | 22 |
| 9 | 15 | 8 | 110 | 8 | 25 | 60 | 22 |
| 10 | 15 | 8 | 110 | 10 | 25 | 60 | 22 |
| 11 | 16 | 10 | 110 | 12 | 25 | 60 | 22 |
| 12 | 16 | 10 | 110 | 14 | 25 | 60 | 22 |

Following are the procedures carried out for the nonlinear multiple regression analysis.

i. Diffraction RAOs for spar and semi-submersible platforms

The diffraction RAOs in surge, heave and pitch motion for each of the platform stated in Table 3.5 and Table 3.6 were obtained and tabulated. From the tabulated data, maximum and minimum RAOs were identified for the purpose of frequency range decision.

ii. Dimension range

Due to large number of platforms were in consideration and to provide formulae with higher accuracy, the nonlinear multiple regression formulae for spar were given as five sets draft range as follows,

*Set 1* –150 m – 160 m

*Set 2* –160 m – 170 m

*Set 3* –170 m – 180 m

*Set 4* –180 m – 190 m

*Set 5* –190 m – 200 m

The formulae for semi-submersible platforms were given as three sets of diameter range as follows,

*Set 1* –8 m – 10 m

*Set 2* –10 m – 12 m

*Set 3* –12 m – 14 m

iii.  Frequency range determination

For each of the above sets, the frequencies for the maximum and minimum response obtained from the diffraction analysis were considered. Based upon these frequencies, about four to seven ranges of frequency were selected based on the number of maximum and minimum responses available for each platform.

iv.  Input data

The diffraction RAO, wave frequency, member draft, and member diameter from diffraction analysis were taken as the input data. The relation of these data was given as

$$R = af^b D^c h^d \qquad (3.56)$$

where *R* was the diffraction RAO, *f* was the wave frequency, *D* was the member diameter and *h* was the member draft, and *a, b, c, d* were the regression coefficient obtained from regression analysis.

v.  Regression analysis

The analyses were carried out on the logarithm term of the input data discussed.

$$\log R = \log a \cdot b \log f \cdot c \log D \cdot d \log h \qquad (3.57)$$

Diffraction RAO was taken as the Y input, while the wave frequency, structural diameter and structural draft were taken as the X input for the regression analysis. As an output of the analysis, four regression

coefficients were determined. Coefficient $a$ was obtained as intercept; $b,c,d$ were obtained as x variables. By inputting these regression coefficients to Equation 3.56, one formula was prepared and suggested.

Similar procedures were carried out for each of the frequency ranges and diameter or draft ranges as discussed to suggest the series formulae for surge, heave and pitch RAOs of spar and semi-submersible platforms.

The nonlinear multiple regression curves obtained from the series of formulae suggested were then compared with the results of diffraction analysis for each platforms.

## 3.6    Chapter summary

In this chapter, the research methodology for this study was discussed. The methodology was carried out mainly to verify the wave force estimation approaches for large offshore structures and to provide a simpler approach for researchers for the research purposes. First, model test validations were conducted in the wave tank for spar and semi-submersible platforms. The responses found were then compared with the dynamic responses obtained by Morison equation and diffraction theory. Then, a simpler approach for wave force estimation based upon diffraction theory, using nonlinear multiple regression curves obtained from regression analysis was recommended.

# CHAPTER FOUR

# RESULT AND DISCUSSION

## 4.1 Chapter Overview

This chapter discusses the results of the dynamic responses by the methods elaborated in Chapter 3 and presents the nonlinear multiple regression curves recommend for the response determination of spar and semi-submersible platforms. Wave tank tests were conducted to investigate the dynamic responses for spar and semi-submersible platform models. For accuracy, two tests were performed and the average values are presented. The RAOs in surge, heave and pitch were measured for regular wave runs at different frequencies. The RAOs of the time domain analysis using Morison equation for wave force calculation, and the diffraction responses by linear wave diffraction analysis are presented. The experimental model results are compared with the prototype analysis results using time domain analysis and diffraction analysis. The diffraction analysis results were in good agreement with the model test results for these two types of platform with large-sized members. A series of diffraction analysis were conducted for spar and semi-submersibles varying the dimensions and drafts. From these results, formulae for obtaining the diffraction RAOs are suggested by using nonlinear multiple regression analysis.

## 4.2 Wave tank test results

Wave tank tests were performed on spar and semi-submersible platform models. The following discussions present and explain the results obtained. For accuracy, the wave runs were repeated once. The values were nearly same and the average values are presented.

### 4.2.1 Spar model results

The surge, heave and pitch values were measured for regular wave runs at different frequencies as mentioned in Chapter 3. Typical responses during frequency 1 Hz and 60 mm wave height are shown in Figure 4.1 to Figure 4.3. The surge, heave and pitch responses were found followed the trend of input wave with a frequency of 1 Hz.



Figure 4. 1 Spar model surge response by wave tank test

61

Figure 4. 2 Spar model heave response by wave tank test



Figure 4. 3 Spar model pitch response by wave tank test

From the responses for the regular wave of different frequencies, the RAOs were obtained as shown in Figure 4.4 to Figure 4.6. The maximum surge RAO was observed to be 4 m/m at 0.4 Hz, the maximum heave RAO was 1 m/m at 1 Hz and the maximum pitch RAO was 13 deg/m at 1 Hz.
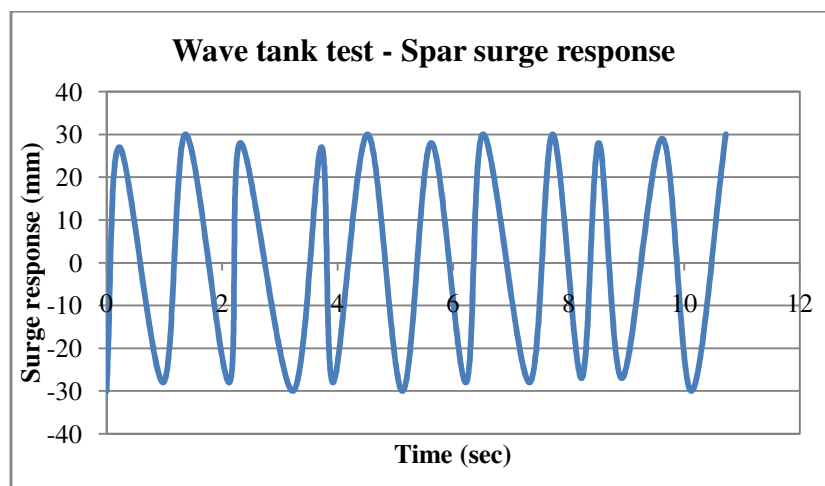
Figure 4. 4 Spar model surge RAO by wave tank test
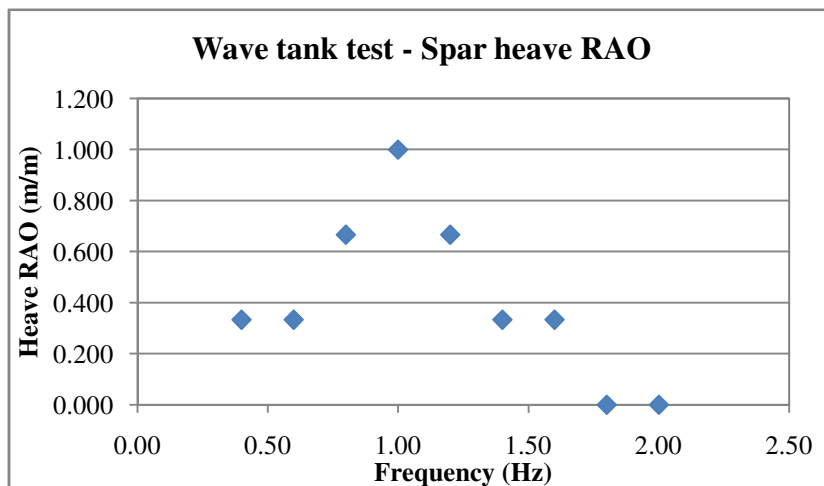


Figure 4. 5 Spar model heave RAO by wave tank test
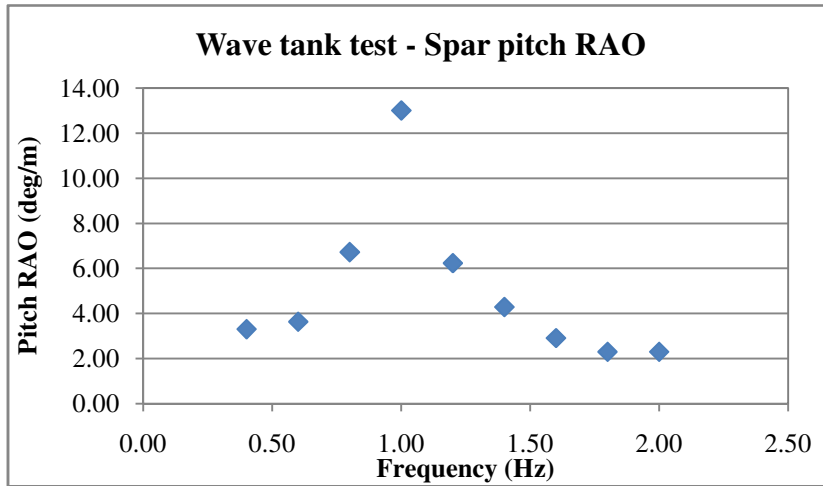
Figure 4. 6 Spar model pitch RAO by wave tank test

### 4.2.2 Semi-submersible model results

Typical responses of semi-submersible model test in surge; heave and pitch motion for 1 Hz wave frequency and 60 mm wave height of regular wave runs are presented in Figure 4.7 to Figure 4.9. The surge, heave and pitch responses for semi-submersible model were found same with the trend of input wave frequency of 1 Hz.
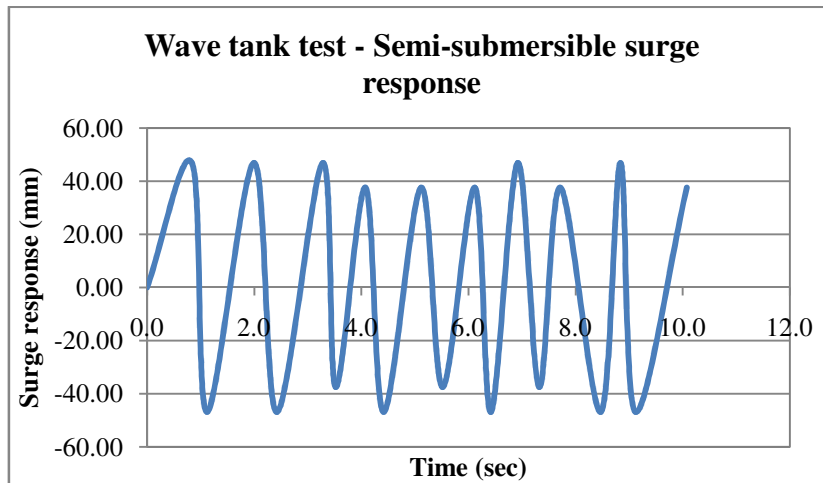


Figure 4. 7 Semi-submersible model surge response by wave tank test
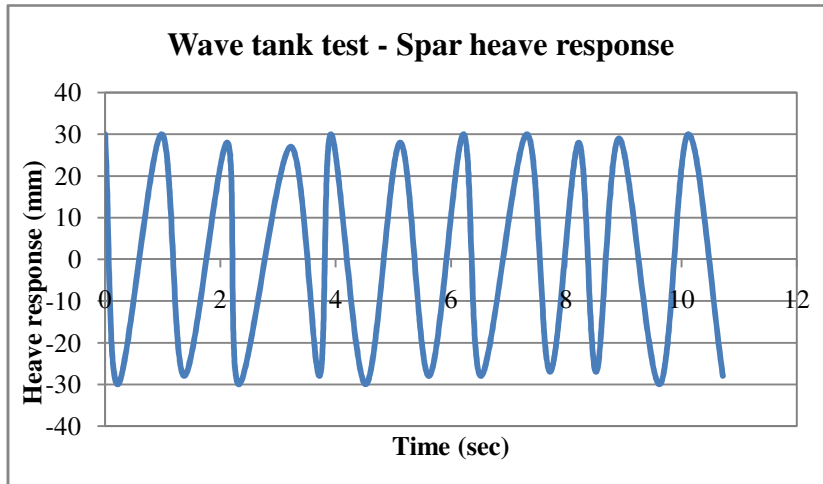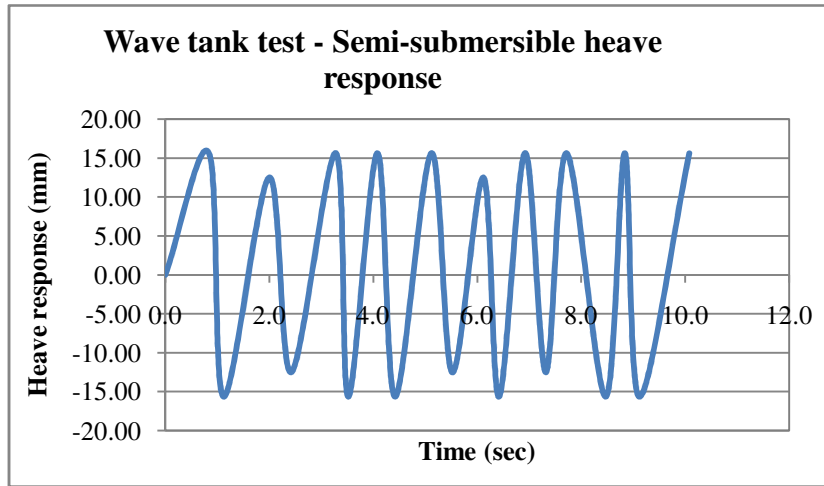
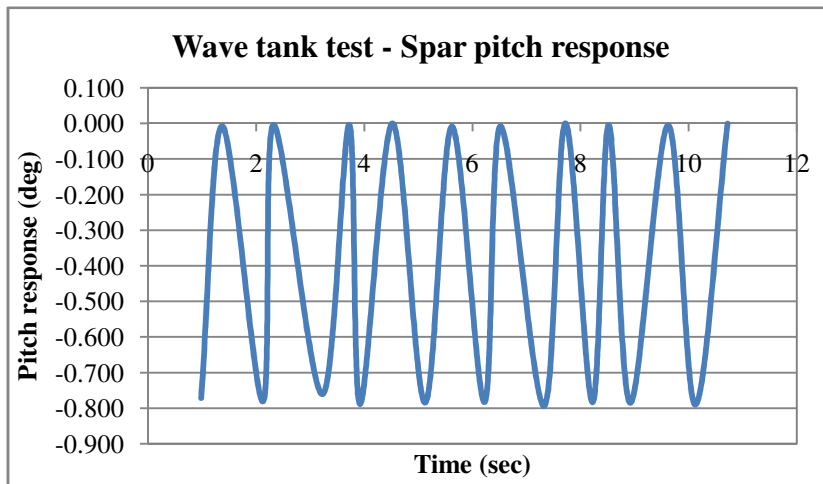Figure 4. 8 Semi-submersible model heave response by wave tank test
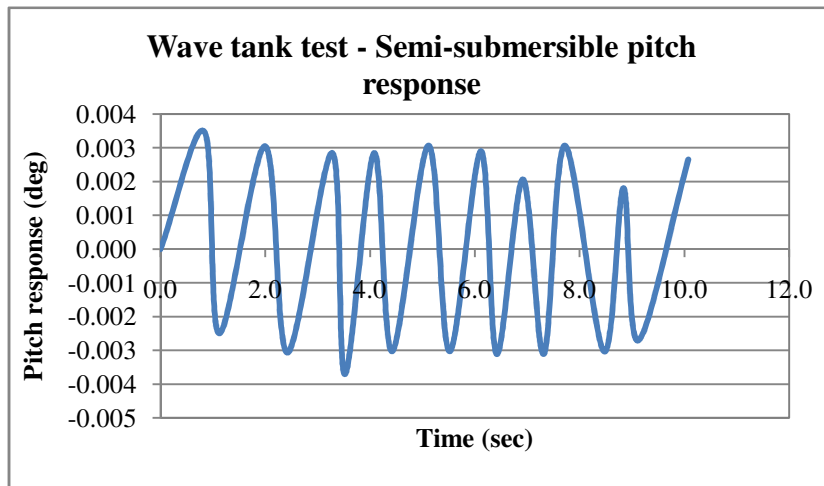


Figure 4. 9 Semi-submersible model pitch response by wave tank test

From the responses of the regular wave for different frequencies, the RAO for semi-submersible model are shown in Figure 4.10 to Figure 4.12. The maximum surge RAO was found to be 2.4 m/m at 0.6 Hz, the maximum heave RAO was 1.78 m/m at 0.4 Hz and the maximum pitch RAO was 0.53 deg/m at 0.4 Hz.
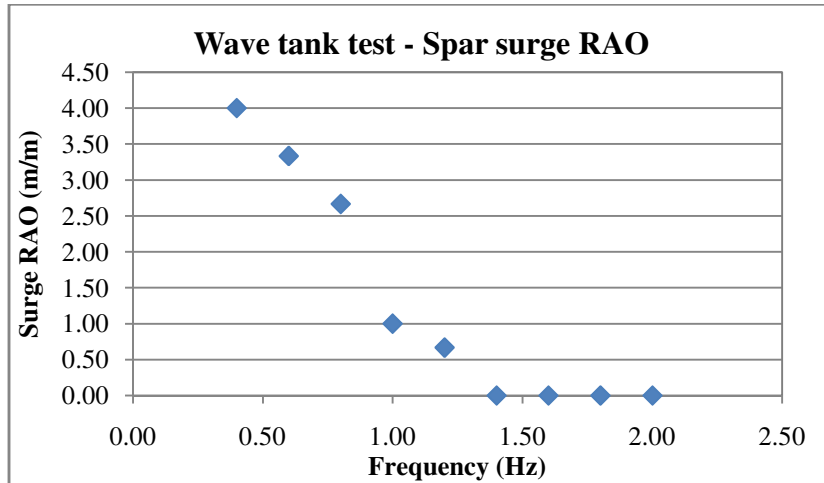
Figure 4. 10 Semi-submersible model surge RAO by wave tank test
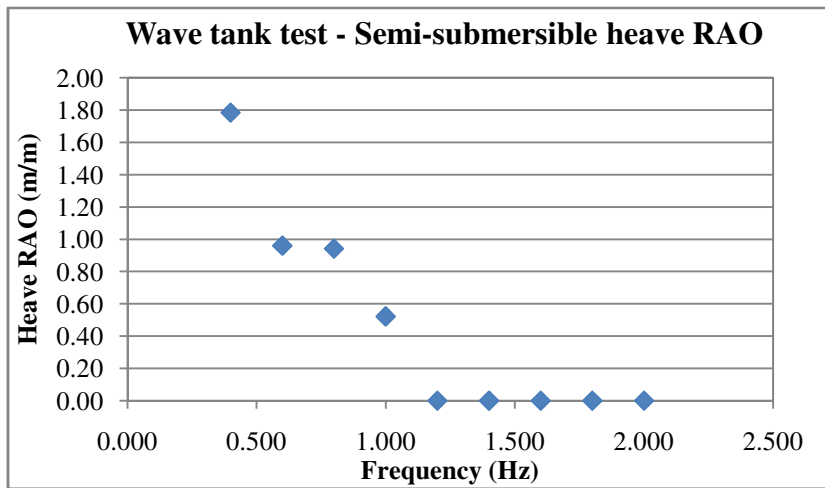


Figure 4. 11 Semi-submersible model heave RAO by wave tank test
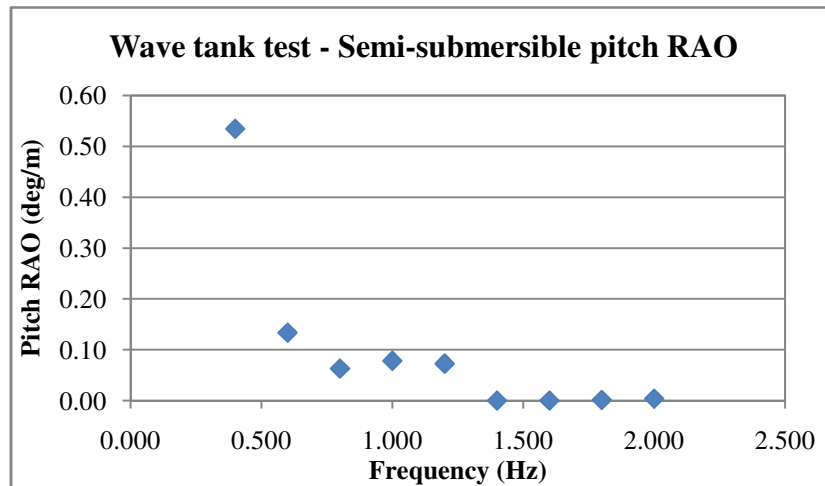
Figure 4. 12 Semi-submersible model pitch RAO by wave tank test

## 4.3    Time domain analysis results for prototypes

Time domain analysis for spar and semi-submersible prototype were carried out by using Morison equation to determine the wave force.  The results are presented and elaborated as discussed below.

### 4.3.1    Drag and Inertia coefficient

The hydrodynamic coefficients were determined correlating with the KC number. From Equation 3.1, the value of KC number was found to be about 1 for both spar and semi-submersible platform.  The value of the drag and inertia coefficients obtained from Figure 3.1 and Figure 3.2 are given in Table 4.1.

Table 4.1 Drag and inertia coefficient of spar and semi-submersible platform

| Platform | | Drag coefficient | Inertia coefficient |
|---|---|---|---|
| Spar | | 0.25 | 2.45 |
| Semi-submersible | Columns | 1.20 | 2.00 |
| | Pontoons | 0.55 | 2.00 |

67

### 4.3.2   Spar prototype

A time domain analysis was performed for the spar prototype. The program was validated at first. The motion responses for spar prototype subjected to regular waves were obtained.

#### 4.3.2.1   *Time domain analysis program validation*

Chitrapu et al [51] performed a time-domain simulation of classic spar platform response. The surge and pitch response by regular waves was adopted to validate the time domain analysis program used in this study. The comparison was performed for 6 m wave height and 14 s wave period.

The surge obtained by Chitrapu's program and the time domain analysis program were observed to be 1.35 m and 1.33 m respectively. The pitch response obtained was found to be 1.6 deg and 1.92 deg by Chitrapu's program and time domain analysis program. In Table 4.2 shows the comparison of the surge and pitch RAO by both approaches. The RAOs obtained by time domain analysis agreed well with the results found in the literature.

Table 4. 2 Program validations: Comparison of RAOs

|  | Chitrapu's Program | Time Domain Program |
|---|---|---|
| Surge RAO (m/m) | 0.225 | 0.222 |
| Pitch RAO (deg/m) | 0.267 | 0.320 |

#### 4.3.2.2   *Results of time domain analysis*

Figure 4.13 to Figure 4.15 illustrate the surge, heave and pitch RAOs for spar prototype. The maximum surge RAO was found to be 0.042 m/m at 0.155 Hz, the maximum heave RAO was 0.10 m/m at 0.042 Hz and the maximum pitch RAO was 0.052 deg/m at 0.158 Hz by time domain analysis for spar prototype.
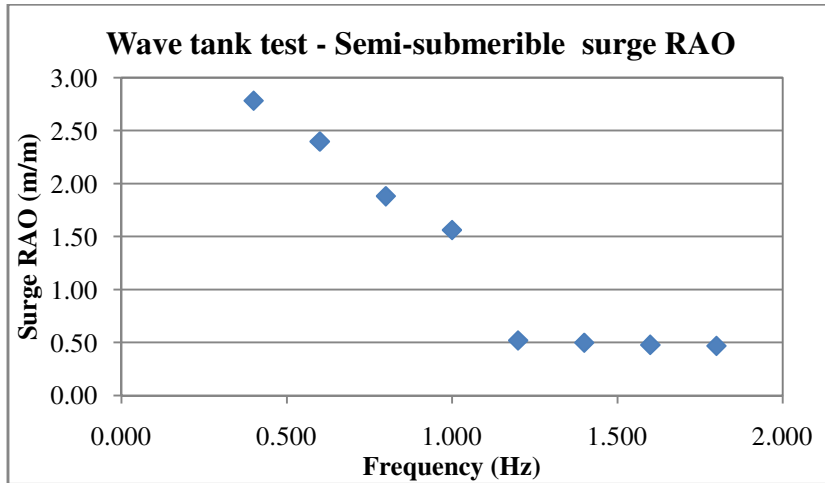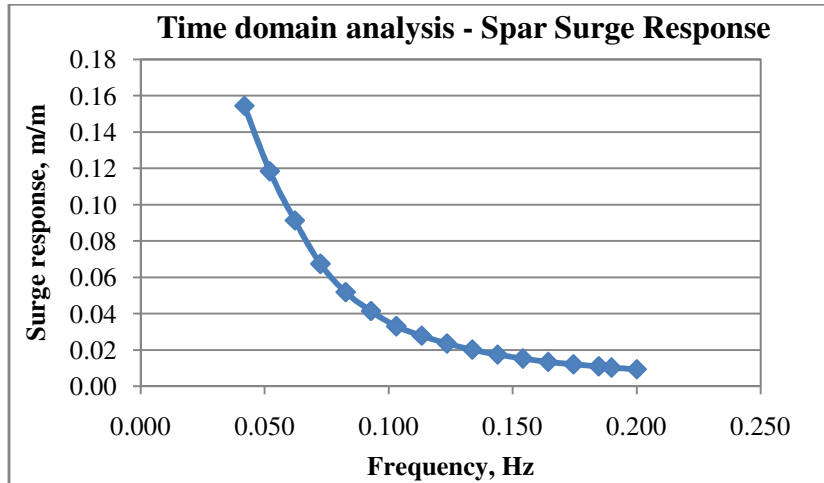
Figure 4. 13 Spar prototype surge RAO by time domain analysis
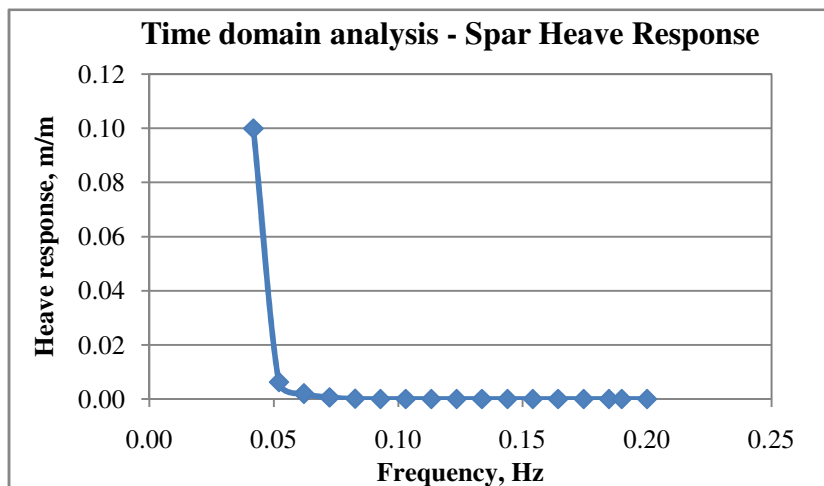


Figure 4. 14 Spar prototype heave RAO by time domain analysis
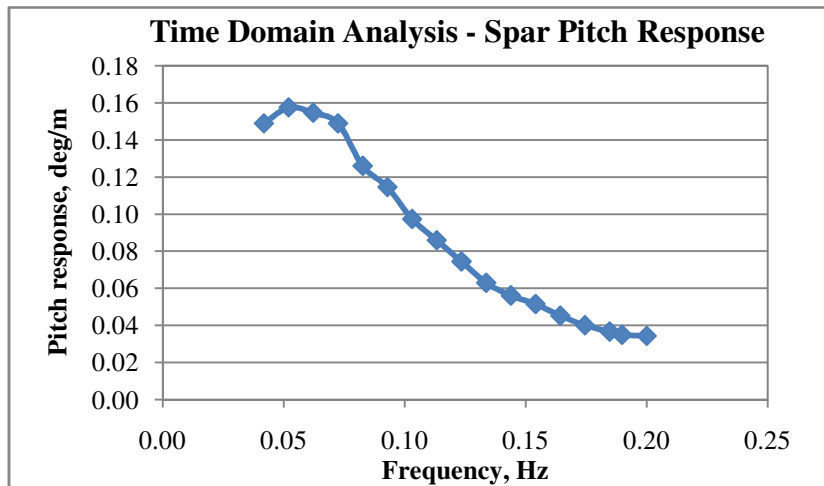
Figure 4. 15 Spar prototype pitch RAO by time domain analysis

### 4.3.3 Semi-submersible prototype

The time domain analysis program for semi-submersible platform was validated, and then the RAOs in surge, heave and pitch were obtained. The following discussion present and explain the result determined.

#### 4.3.3.1 *Time domain analysis program validation*

Tankagi conducted a series of tests on the 1:64 scale model of an eight column semi-submersible in a wave tank of 3 m (192 m. full scale) [52]. Following discussion presents and explains the surge, heave and pitch motions comparison between the time domain analysis results for semi-submersible and the experimental data obtained by Tankagi.
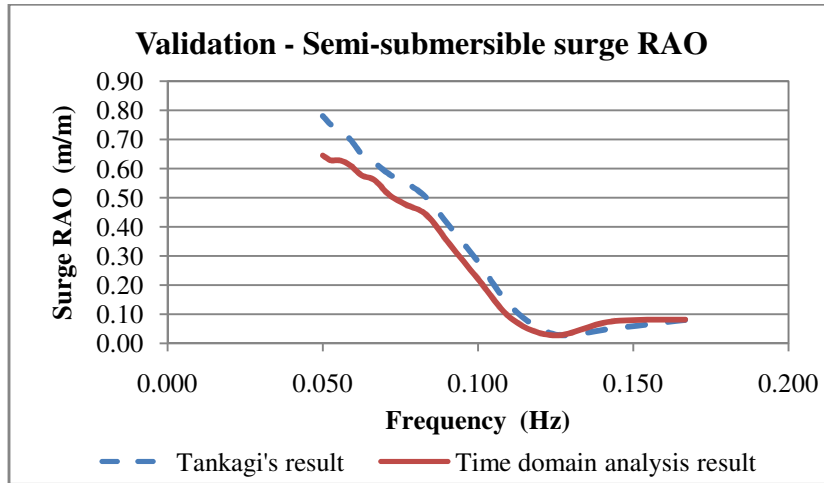
Figure 4. 16 Semi-submersible surge RAO by time domain analysis validation
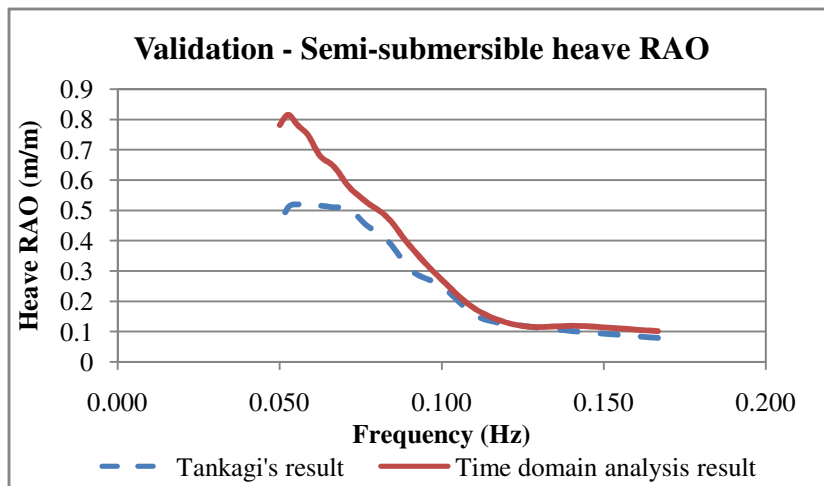


Figure 4. 17 Semi-submersible heave RAO by time domain analysis validation
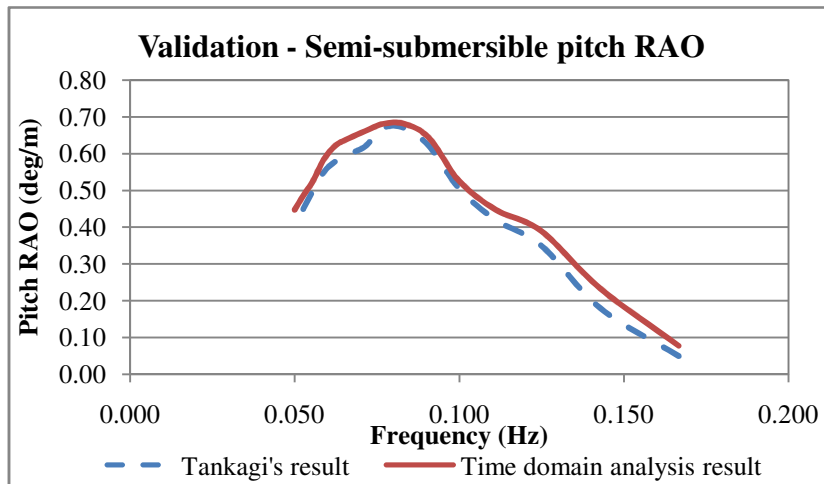
Figure 4. 18 Semi-submersible pitch RAO by time domain analysis validation

Figure 4.16 shows the comparison in surge motion. Above the frequency 0.10 Hz, good agreement was observed. However, different about 11% was found below this frequency.

Figure 4.17 shows the comparison in heave motion. Above the frequency 0.10 Hz, the time domain results closely agreed with the Tankagi's results. However, variation was found below this frequency up to a maximum different about 35% was achieved on 0.05Hz.

Figure 4.18 presents the comparison in pitch motion. Good agreement was generally found for the comparison, whereby maximum variation about 5% was found.

### 4.3.3.2 Results of time domain analysis

The results of time domain analysis for semi-submersible platforms are presented in Figure 4.19 to Figure 4.21.

The surge RAO for semi-submersible prototype is shown in Figure 4.19. The response comes down up to 0.19 Hz from maximum RAO that found to be 1 m/m at frequency 0.06 Hz and then takes a turn upwards, reaching a maximum value 0.25 m/m at a frequency 0.225 Hz and then reduces.

Figure 4.20 shows the heave RAO for semi-submersible prototype. The maximum RAO was observed to be 0.185 m/m at the frequency 0.06 Hz. Then, it was found decreased after frequency 0.13 Hz, and almost nil at frequency 0.3 Hz.

The pitch RAO is shown in Figure 4.21. The maximum RAO was observed to be 0.7 deg/m at frequency 0.06 Hz.

The wave frequency was taken above the frequency 0.05 Hz to avoid the instability of the programming, which would affect the quality of the results determined for the time domain analysis.
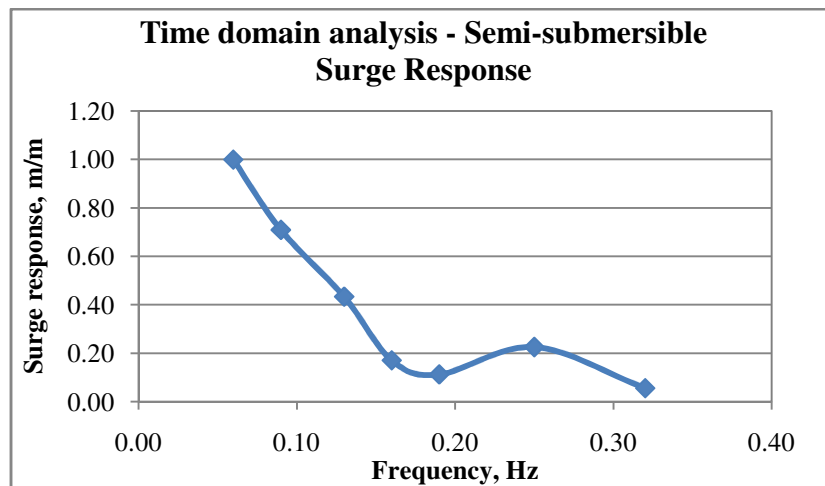


Figure 4. 19 Semi-submersible prototype surge RAO by time domain analysis

73
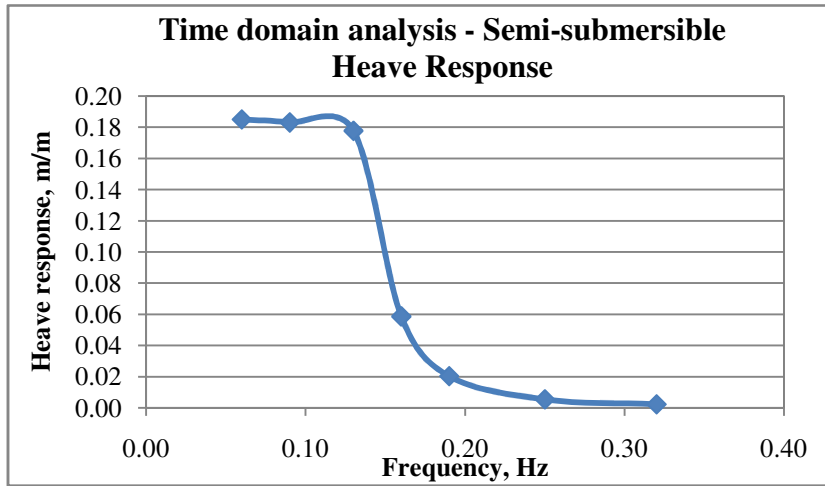
Figure 4. 20 Semi-submersible prototype heave RAO by time domain analysis
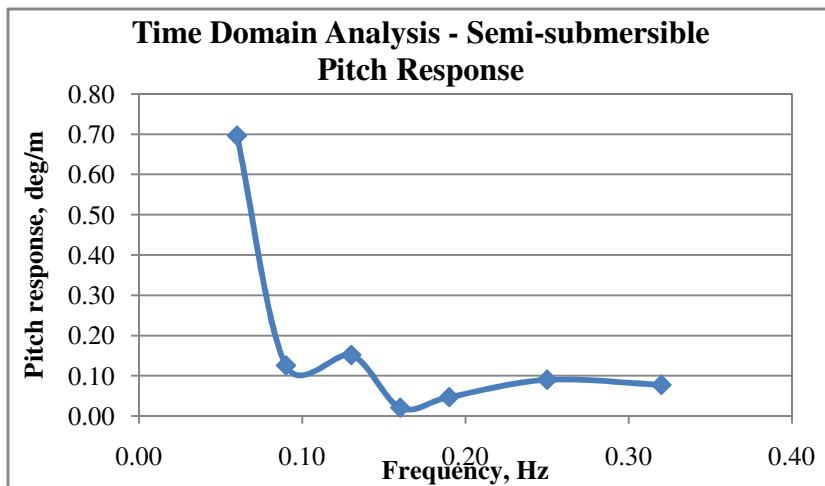


Figure 4. 21 Semi-submersible prototype pitch RAO by time domain analysis

## 4.4 Linear wave diffraction analysis results for prototypes

Linear wave diffraction analyses were performed for spar and semi-submersible prototypes for diffraction theory. Typical responses for spar and semi-submersible prototypes are as illustrated in Figure 4.22 to Figure 4.24; and Figure 4.25 to Figure 4.27 respectively.

74

### 4.4.1 Spar prototype

The dynamic response for spar prototype by using linear wave diffraction analysis was performed as discussed in Chapter 3. Figure 4.22 to Figure 4.24 illustrate the RAOs in surge, heave and pitch motions for spar. The maximum by linear wave diffraction analysis for surge RAO was observed to be 7.1 m/m at 0.03 Hz, the maximum heave RAO was 0.81 m/m at 0.05 Hz and the maximum pitch RAO was 2.02 deg/m at 0.5 Hz.
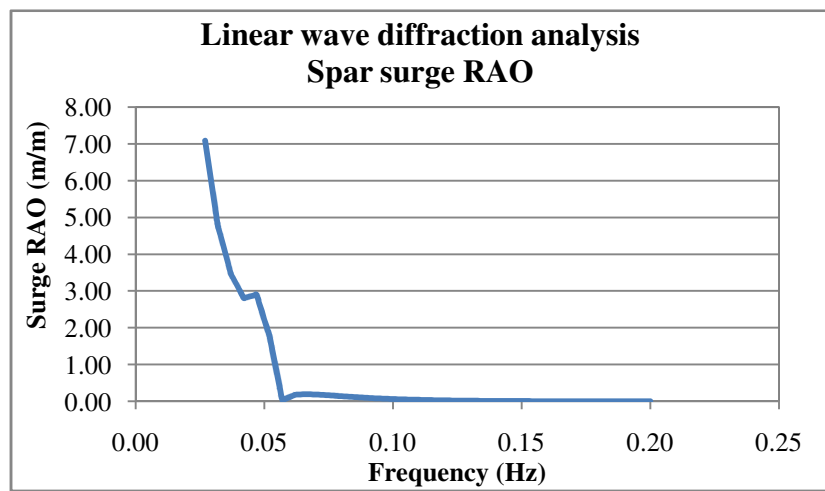


Figure 4. 22 Spar prototype surge RAO by linear wave diffraction analysis
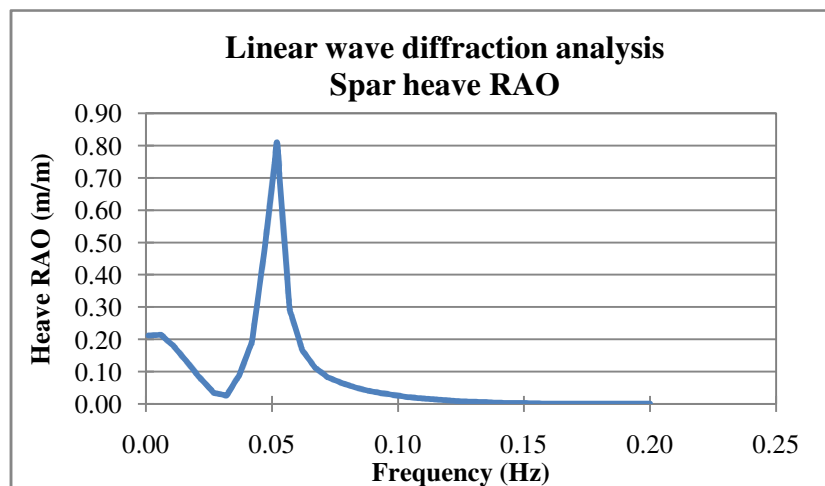


Figure 4. 23 Spar prototype heave RAO by linear wave diffraction analysis

75
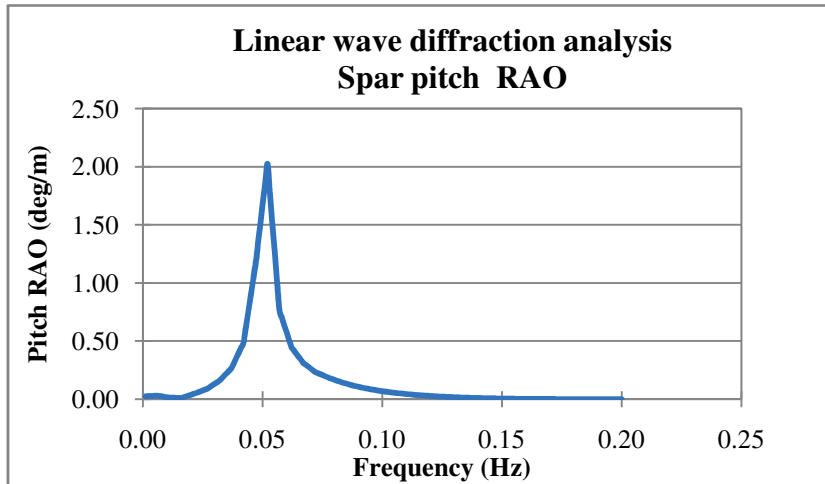
Figure 4. 24 Spar prototype pitch RAO by linear wave diffraction analysis

### 4.4.2 Semi-submersible prototype

The surge, heave and pitch RAOs were determined at frequency 0.027 Hz to 0.2 Hz for the semi-submersible prototype. Typical responses are as shown in Figure 4.25 to Figure 4.27. The maximum RAO by linear wave diffraction analysis for surge, heave and pitch was observed to be 29.23 m/m, 1.704 m/m and 0.127 deg/m respectively at frequency 0.3 Hz.
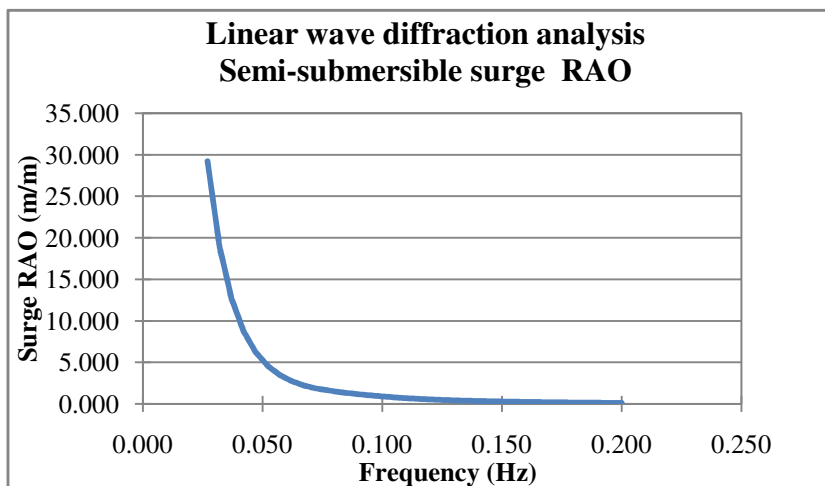


Figure 4. 25 Semi-submersible prototype surge RAO by linear wave diffraction analysis

76
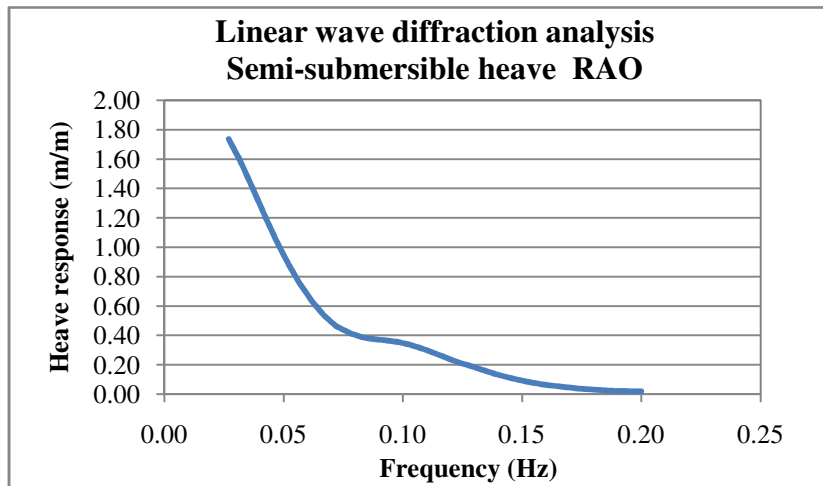
Figure 4. 26 Semi-submersible prototype heave RAO by linear wave diffraction analysis
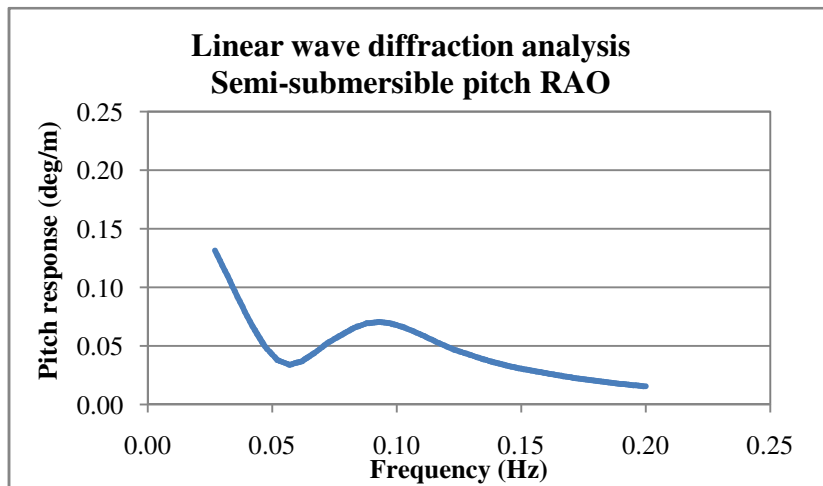


Figure 4. 27 Semi-submersible prototype pitch RAO by linear wave diffraction analysis

## 4.5    Comparison of results

The experimental model results were compared with the prototype analysis results using time domain analysis and diffraction analysis.  The frequency range used for model was from 0.4 Hz to 2 Hz.  For comparisons, these frequencies were converted to prototype frequencies given by $\frac{0.4}{6.3}$ to $\frac{2}{6.3}$ as 0.06 Hz to 0.32 Hz.

### 4.5.1  Spar platform results

A comparison of dynamic responses by model test, Morison equation, and diffraction theory discussed above were performed.  Figure 4.28 to Figure 4.30 show the comparison of the RAOs for spar prototype.

In comparison to Morison response, the surge RAO by diffraction theory showed better agreement to the test as illustrated in Figure 4.28.  Above the frequency 0.15 Hz, surge RAOs by Morison equation and diffraction theory agreed well with the response obtained by model test.

Large variation was observed between Morison RAO and the model test RAO at the frequency below 0.15 Hz.  The surge Morison RAO was found to be about 70% smaller than the model test results at 0.12 Hz.  At the same time, better agreement was found for diffraction theory, where the RAO was found to be about 20% greater than the model test RAO for this frequency region.

For frequency less than 0.15 Hz, the second order low frequency responses contributed greatly to the surge values.  This has not been taken care in the time domain analysis.  Also the wave diffraction effects are not taken into account.  That is the reason Morison surge RAO values are much below the other two values.
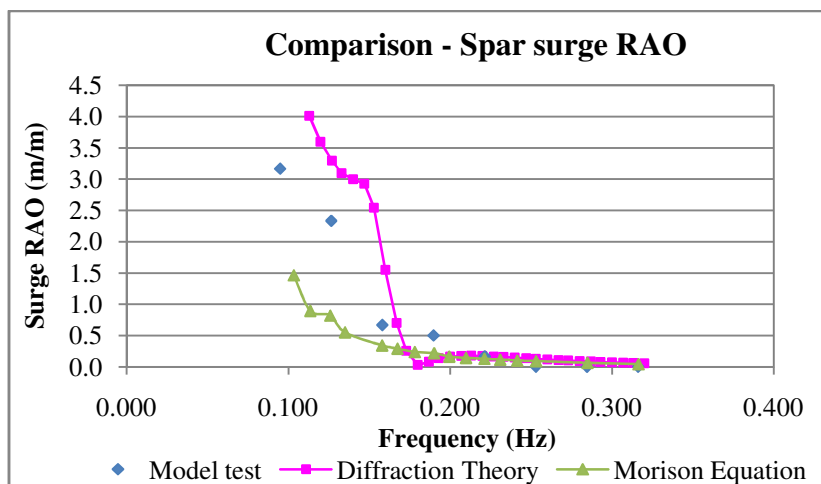


Figure 4. 28 Comparison of spar surge RAO by model test, Morison equation and diffraction theory

78

Figure 4.29 shows that the diffraction heave RAOs gave better agreement with the model RAOs, compared with Morison RAO. The trend shows very good resemblance and the values are about 15% less at the frequency 0.16 Hz. Large variation about 80 % less than the model RAO was found by Morison RAO at frequency 0.16 Hz. The maximum model test RAO was found to be 1 m/m and maximum diffraction RAO was found to be 0.9 m/m at frequency 0.16 Hz.

The Morison RAO values differ very much for the heave response at all frequencies mainly due to the wave diffraction effects play a very important part for the calculation of the wave force, wave damping and the responses for spar as discussed by Chakrabarti [32] has been neglected in the time domain integration method.
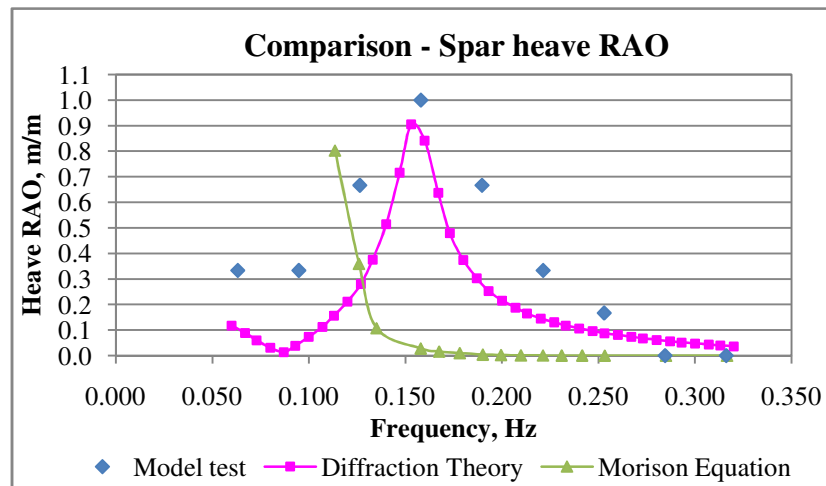


Figure 4. 29 Comparison of spar heave RAO by model test, Morison equation and diffraction theory

The pitch RAO by diffraction theory agreed well with the model test response as presented in Figure 4.30. The magnitude and trend of the pitch RAO was agreed well with the model test results. The maximum diffraction RAO was found to be 13.5 deg/m and the maximum model test RAO was 14.5 deg/m at frequency 0.16 Hz. The Morison RAO was found to be about 60% less than the model RAO at frequency 0.16 Hz, and the trend disagreed with the model test and diffraction theory response.

As discussed by Mirzaie and Ketabdari [9], the Morison RAO pitch values differ

very much to other values that might due to the dramatically change of velocity and acceleration field was not taken into account in the time domain integration method. In the case, these changes might significantly affect the pitch RAOs of the spar by Morison equation.
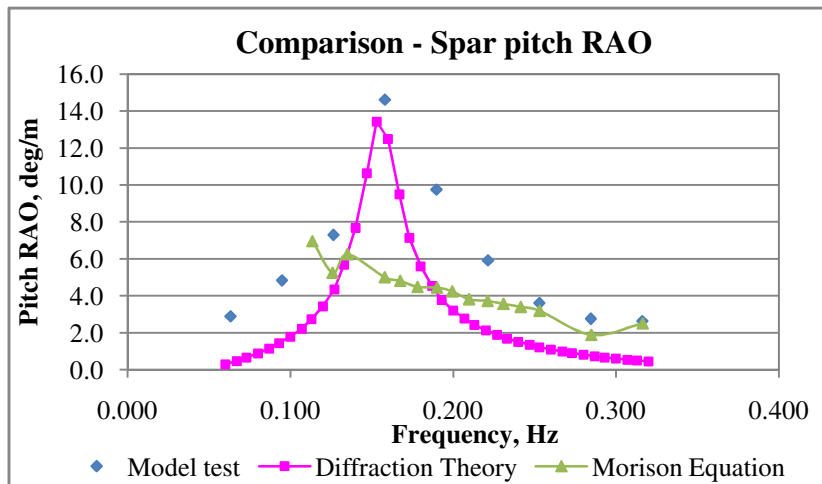


Figure 4. 30 Comparison of spar pitch RAO by model test, Morison equation and diffraction theory

The diffraction theory showed a better agreement in the responses of spar platforms in comparison to Morison results as presented. Morison equation might not be suitable for calculating wave force on a large body like spar, because the wave velocity and acceleration fields changed dramatically after hitting the members.

### 4.5.2   Semi-submersible results

Presented in Figure 4.31 to Figure 4.33 are the semi-submersible prototype comparison of RAOs for model test, Morison equation and diffraction theory.

Surge RAOs by diffraction theory gave better agreement with the model test responses in comparison to the Morison RAOs as shown in Figure 4.31. The Morison surge RAOs were found agreed well with the model test RAO only after frequency 0.2 Hz. However, the RAO by diffraction theory agreed well with the model test

response for all the frequencies. The diffraction RAO was found to be about 35% smaller than the model test RAO, but large variation about 80% smaller for the Morison RAO was found at frequency 0.126 Hz.

The maximum model RAO was observed to be 2.172 m/m at frequency 0.126 Hz. The maximum diffraction RAO and Morison RAO were found to be 2.676 m/m and 1 m/m at frequency 0.102 Hz and 0.06 Hz respectively.
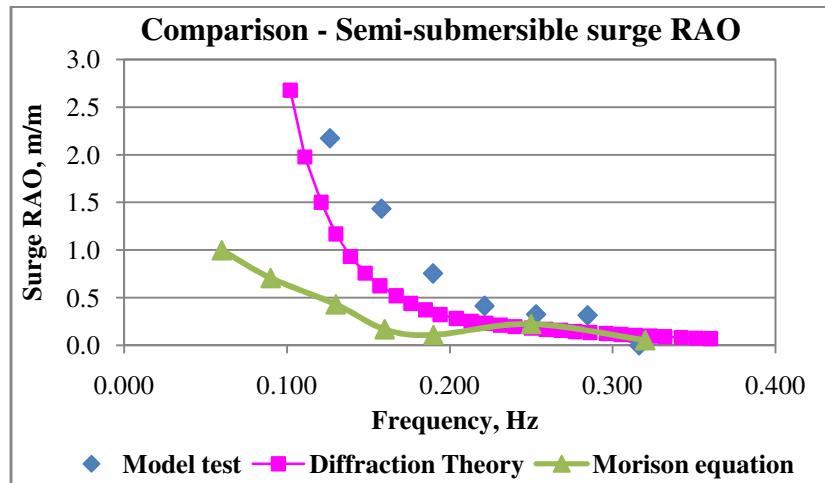


Figure 4. 31 Comparison of semi-submersible surge RAO by model test, Morison equation and diffraction theory

Figure 4.32 shows the comparison of the heave responses obtained by model tests, Morison equation and diffraction theory. The heave RAOs by diffraction theory agreed well with the model test RAO for semi-submersible prototype. The trend of the model test RAOs was found to be decreasing from 1.7 m/m at frequency 0.06 Hz to 1.0 m/m at frequency 0.1 Hz. It then increased to 1.05 m/m at frequency 0.126 Hz and reduced to almost nil at frequency 0.3 Hz. Similar trend for heave response by diffraction analysis was found. The diffraction RAO was found decreased from the maximum value of 1.5 m/m at frequency 0.04 Hz to almost nil at frequency 0.3 Hz. The heave RAOs by Morison equation was found almost nil after 0.2 Hz. The maximum Morison RAO was found to be 0.2 m/m at frequency 0.06 Hz.
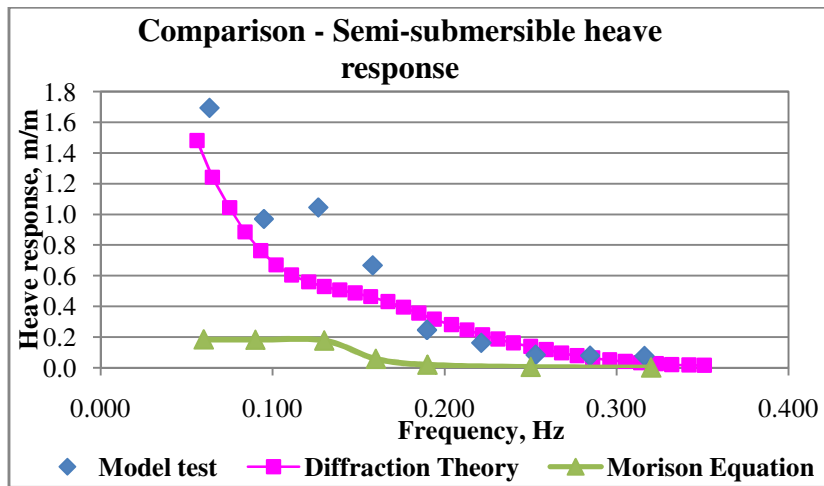
Figure 4. 32 Comparison of semi-submersible heave RAO by model test, Morison equation and diffraction theory

Better agreement was found between diffraction theory and model test response for semi-submersible prototype in comparison to the Morison response. Maximum RAO by diffraction theory and model test were found to be 0.9 deg/m at the 0.063 Hz. The response was found gradually reduced with the increment of frequencies, from the maximum RAOs by both approaches that found to be about 0.9 deg/m at 0.06 Hz to almost nil at frequency 0.2 Hz. The maximum response by Morison equation was observed to be 0.7 deg/m at frequency of 0.06 Hz. The trend was found slightly disagreed with the model test RAO at frequency 0.13 Hz. The Morison RAO increased up to 0.15 deg/m, and then decreased up almost nil at frequency 0.16 Hz. The RAO then increased and reaching a maximum value of 0.09 deg/m at frequency 0.25 Hz. Figure 4.33 illustrates the comparisons of all the approaches for the pitch response.
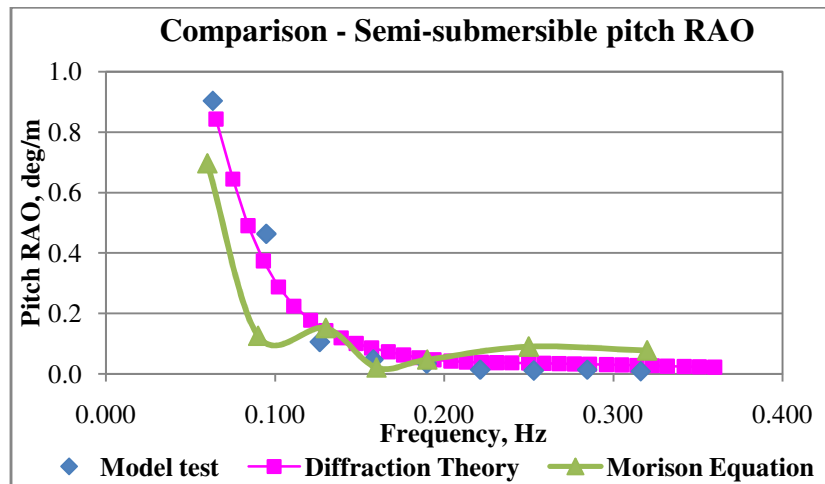
Figure 4. 33 Comparison of semi-submersible pitch RAO by model test, Morison equation and diffraction theory

The Morison RAO in surge, heave and pitch motions were found much below the other two values for the semi-submersible platform. In this case, the second order low frequency responses might significantly contribute to all the three degree of freedom for the frequencies less than 0.2 Hz. However, it was not been taken into consideration in the time domain analysis. Also the neglecting of the dramatically change of velocity and acceleration field due to the existence of the prototype and the wave diffraction effects might also contribute greatly to the surge, heave and pitch values.

## 4.6 Nonlinear multiple regression curves

From the above validation, it is possible to say that diffraction theory is the appropriate method for the wave force estimation for spar and semi-submersible platforms in comparison to the Morison equation. Therefore, the responses of diffraction theory were used for the determination of nonlinear multiple regression curves.

Diffraction theory for wave force calculation and for determining the damping characteristics is usually a very complicated process that needs costly software. The main intention for this recommendation is to provide a simpler approach for

83

researchers to obtain the response by diffraction theory. The following sub-chapters present and discuss on the nonlinear multiple regression curves suggested for both semi-submersible and spar platforms.

## 4.6.1   Spar platform

A regression analysis was performed on a large number of spar platforms, the nonlinear multiple regression curves were suggested for spar platform in surge, heave and pitch motions. The formulae require the wave frequency, spar diameter and draft length as input to obtain at the response of spar in surge, heave and pitch motions. In order to have a more accurate solution, the curves suggested were based upon, the frequency range and the draft length range.

As shown in Table 4.2 are the formulae for the nonlinear regression curve for draft length 150m to 160m, based on eight ranges of wave frequency between 0.027 Hz to 0.2 Hz for the surge response. Formulae suggested were compared with the diffraction response in surge response and present in Figure 4.34. From the figure, the nonlinear multiple regression curves seem to have high similarities to the diffraction response curve.

There are slightly different for draft length i.e. 160m to 170m, 170m to 180m, 180m to 190m and 190m to 200m. As illustrated in Table 4.3 to Table 4.6 are the formulae for the wave force estimation suggested for spar with draft length mentioned above. Wave frequencies were divided into seven ranges from 0.027 Hz to 0.2 Hz. Comparisons on both methods are shown in Figure 4.35 to Figure 4.38. It is probable to say that the nonlinear multiple regression curves suggested are agreed very well to the diffraction response curve, in terms of the trend and magnitude.

Table 4. 3 Formulae of nonlinear multiple regression curve in surge motion for spar platform (150m to 160m draft length)

| Frequency range | Formula for regression curve |
|---|---|
| $0.20 - 0.10$ | $R = 0.0124f^{-0.627}D^{-2.474}H^{-0.812}$ |
| $0.10 - f_1 = 5.314D^{0.379}H^{-1.117}$ | $R = 1.515f^{-3.134}D^{-1.891}H^{-0.658}$ |
| $f_1 = 5.314D^{0.379}H^{-1.117} - f_2 = 1.873D^{0.328}H^{-0.899}$ | $R = 1.951E\text{-}11f^{-0.647}D^{-1.811}H^{4.983}$ |
| $f_2 = 1.873D^{0.328}H^{-0.899} - f_3 = 0.314D^{0.222}H^{-0.480}$ | $R = 2.204f^{-10.018}D^{1.379}H^{-6.946}$ |
| $f_3 = 0.314D^{0.222}H^{-0.480} - f_4 = 0.394D^{0.138}H^{-0.480}$ | $R = 0.0002f^{-10.485}D^{2.103}H^{-5.707}$ |
| $f_4 = 0.394D^{0.138}H^{-0.480} - f_5 = 11.763D^{0.236}H^{-1.253}$ | $R = 21.365f^{-1.270}D^{-0.756}H^{-0.6442}$ |
| $f_5 = 11.763D^{0.236}H^{-1.253} - 0.037$ | $R = 0.9337f^{-1.706}D^{-0.831}H^{-0.245}$ |
| $0.037 - 0.027$ | $R = 0.1413f^{-2.363}D^{-0.791}H^{-0.321}$ |

Table 4. 4 Formulae of nonlinear multiple regression curve in surge motion for spar platform (160m to 170m draft length)

| Frequency range | Formula for regression curve |
|---|---|
| $0.20 - 0.10$ | $R = 2.259f^{-6.766}D^{-1.871}H^{-2.312}$ |
| $0.10 - f_1 = 1.138D^{0.274}H^{-0.739}$ | $R = 2.836f^{-2.735}D^{-1.191}H^{-1.074}$ |
| $f_1 = 1.138D^{0.274}H^{-0.739} - f_2 = 1.414D^{0.262}H^{-0.796}$ | $R = 613.71f^{5.801}D^{-3.002}H^{3.547}$ |
| $f_2 = 1.414D^{0.262}H^{-0.796} - f_3 = 3.584D^{0.091}H^{-0.876}$ | $R = 888999.6f^{-20.211}D^{2.319}H^{-15.68}$ |
| $f_3 = 3.584D^{0.091}H^{-0.876} - f_4 = 0.240D^{0.045}H^{-0.332}$ | $R = 3.328f^{-6.382}D^{-0.266}H^{-3.559}$ |
| $f_4 = 0.240D^{0.045}H^{-0.332} - f_5 = 0.257D^{0.05}H^{-0.369}$ | $R = 0.007f^{0.461}D^{-1.447}H^{2.456}$ |
| $f_5 = 0.257D^{0.05}H^{-0.369} - 0.027$ | $R = 0.1535f^{-2.124}D^{-0.870}H^{-0.120}$ |

Table 4. 5 Formulae of nonlinear multiple regression curve in surge motion for spar platform (170m to 180m draft length)

| Frequency range | Formula for regression curve |
|---|---|
| $0.20 - 0.10$ | $R = 0.0373f^{-6.854}D^{-2.202}H^{-1.350}$ |
| $0.10 - f_1 = 0.382D^{0.207}H^{-0.472}$ | $R = 0.0285f^{-2.895}D^{-1.076}H^{-0.369}$ |
| $f_1 = 0.382D^{0.207}H^{-0.472} - f_2 = 0.136D^{0.19}H^{-0.285}$ | $R = 0.0797f^{3.056}D^{-2.666}H^{3.521}$ |
| $f_2 = 0.136D^{0.19}H^{-0.285} - f_3 = 0.0516D^{0.0025}H^{0.0086}$ | $R = 2.89E\text{-}17f^{-17.905}D^{1.473}H^{-3.679}$ |
| $f_3 = 0.0516D^{0.0025}H^{0.0086} - f_4 = 0.031D^{0.142}H^{0.003}$ | $R = 0.0016f^{-4.211}D^{-0.521}H^{-0.617}$ |
| $f_4 = 0.031D^{0.142}H^{0.003} - f_5 = 0.5648D^{-0.158}H^{-0.392}$ | $R = 701.60f^{0.316}D^{-1.547}H^{0.201}$ |
| $f_5 = 0.5648D^{-0.158}H^{-0.392} - 0.027$ | $R = 0.471f^{-2.132}D^{-1.06}H^{-0.214}$ |

Table 4. 6 Formulae of nonlinear multiple regression curve in surge motion for spar platform (180m to 190m draft length)

| Frequency range | Formula for regression curve |
|---|---|
| 0.20 – 0.10 | $R = 0.627f^{-6.838}D^{-2.303}H^{-1.788}$ |
| $0.10 - f_1 = 0.373D^{0.361}H^{-0.579}$ | $R = 3.207f^{-2.975}D^{-1.577}H^{-0.943}$ |
| $f_1 = 0.373D^{0.361}H^{-0.579} - f_2 = 2.487D^{0.322}H^{-0.941}$ | $R = 56.219f^{2.747}D^{-3.10}H^{2.469}$ |
| $f_2 = 2.487D^{0.322}H^{-0.941} - f_3 = 2.009D^{0.105}H^{-0.769}$ | $R = 0.0074f^{-21.24}D^{2.913}H^{-12.952}$ |
| $f_3 = 2.009D^{0.105}H^{-0.769} - f_4 = 12.727D^{0.088}H^{-1.131}$ | $R = 158.47f^{-3.323}D^{-0.399}H^{-2.428}$ |
| $f_4 = 12.727D^{0.088}H^{-1.131} - f_5 = 21.429D^{0.098}H^{-1.258}$ | $R = 0.1913f^{0.136}D^{-1.232}H^{1.464}$ |
| $f_5 = 21.429D^{0.098}H^{-1.258} - 0.027$ | $R = 0.5585f^{-2.066}D^{-0.796}H^{-0.383}$ |

Table 4. 7 Formulae of nonlinear multiple regression curve in surge motion for spar platform (190m to 200m draft length)

| Frequency range | Formula for regression curve |
|---|---|
| 0.20 – 0.10 | $R = 9.832E{+}10f^{-6.928}D^{-2.085}H^{-6.87}$ |
| $0.10 - f_1 = 0.0014D^{0.19}H^{0.592}$ | $R = 1.42E{+}11f^{-3.118}D^{-1.167}H^{-5.949}$ |
| $f_1 = 0.0014D^{0.19}H^{0.592} - f_2 = 0.0029D^{0.369}H^{0.316}$ | $R = 7.931E{+}20f^{1.908}D^{-1.902}H^{-7.182}$ |
| $f_2 = 0.0029D^{0.369}H^{0.316} - f_3 = 0.1672D^{0.116}H^{-0.297}$ | $R = 6.72E{-}24f^{-20.418}D^{1.659}H^{-2.43}$ |
| $f_3 = 0.1672D^{0.116}H^{-0.297} - 0.047$ | $R = 1.087E{-}12f^{-10.174}D^{-0.301}H^{-2.212}$ |
| $0.047 - 0.042$ | $R = 0.0022f^{1.276}D^{-1.27}H^{3.01}$ |
| $0.042 - 0.027$ | $R = 0.0293f^{-2.044}D^{-0.873}H^{0.246}$ |
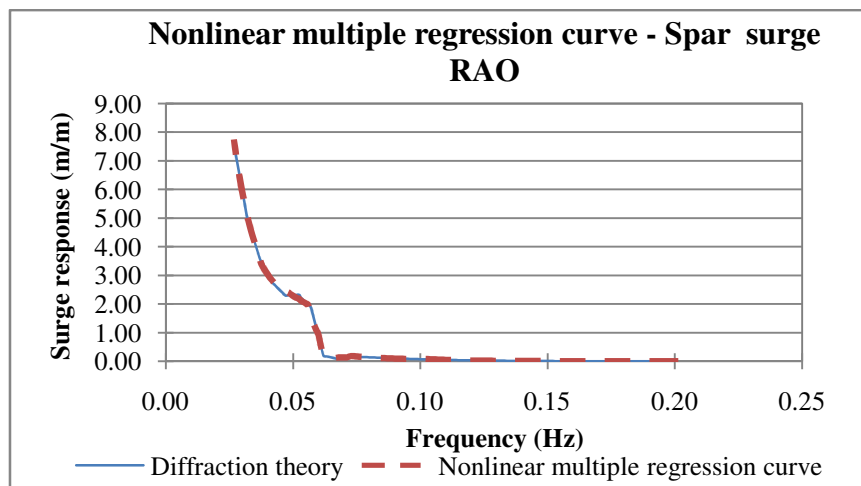


Figure 4. 34 Surge response of spar platform by diffraction theory and nonlinear multiple regression curves (150m to 160m draft length)
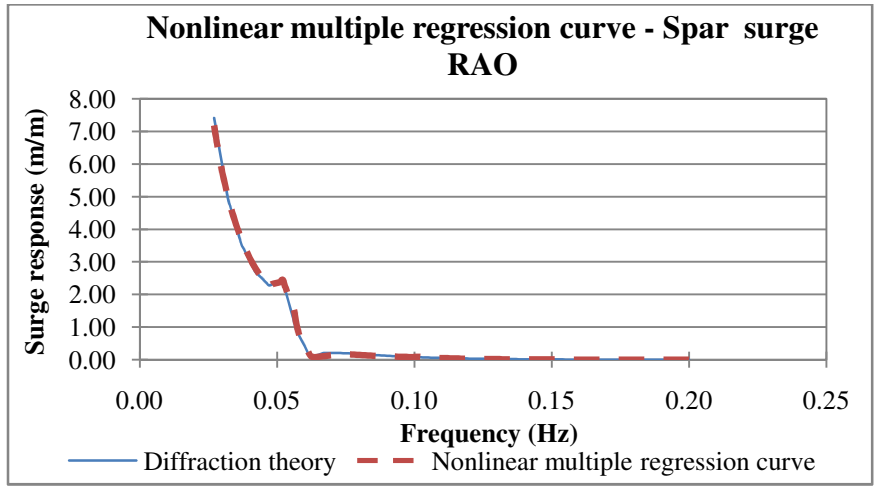
Figure 4. 35 Surge response of spar platform by diffraction theory and nonlinear multiple regression curves (160m to 170m draft length)



Figure 4. 36 Surge response of spar platform by diffraction theory and nonlinear multiple regression curves (170m to 180m draft length)

Figure 4. 37 Surge response of spar platform by diffraction theory and nonlinear multiple regression curves (180m to 190m draft length)



Figure 4. 38 Surge response of spar platform by diffraction theory and nonlinear multiple regression curves (190m to 200m draft length)

Six frequency ranges were suggested for the spar heave response by nonlinear multiple regression curves from 0.001 Hz to 0.2 Hz. As shown in Table 4.7 to Table 4.11 are the formulae for the nonlinear multiple regression curve based upon the frequency ranges. Comparison on both methods by input the wave frequency; spar diameter and draft length are shown in Figure 4.39 to Figure 4.43. Variations were found from 0.056 Hz to 0.06 Hz in Figure 4.39, which might have caused by the too wide range of frequency for that section. With that, the frequency range at this

section shall be narrowed to provide a better result; further studies are required to provide a result with higher reliability. However, Figure 4.40 to Figure 4.44 indicates good agreement on the heave response by both approaches.

Table 4. 8 Formulae of nonlinear multiple regression curve in heave motion for spar platform (150m to 160m draft length)

| Frequency range | Formula for regression curve |
|---|---|
| 0.20 – 0.10 | $R = 0.0128f^{-6.016}D^{-0.644}H^{-2.027}$ |
| 0.10 – 0.065 | $R = 0.0652f^{-4.266}D^{0.557}H^{-2.464}$ |
| 0.065 – $f = 0.127D^{0.176}H^{-0.286}$ | $R = 0.00002f^{-7.444}D^{1.282}H^{-3.052}$ |
| $f = 0.127D^{0.176}H^{-0.286}$– 0.047 | $R = 42.96f^{7.252}D^{-1.495}H^{4.396}$ |
| 0.047 – 0.032 | $R = 714.27f^{6.289}D^{-0.689}H^{2.665}$ |
| 0.032 – 0.001 | $R = 0.86f^{-0.577}D^{-0.097}H^{-0.832}$ |

Table 4. 9 Formulae of nonlinear multiple regression curve in heave motion for spar platform (160m to 170m draft length)

| Frequency range | Formula for regression curve |
|---|---|
| 0.20 – 0.10 | $R = 0.0227f^{-5.887}D^{-0.573}H^{-2.141}$ |
| 0.10 – 0.065 | $R = 0.5382f^{-3.940}D^{0.618}H^{-2.763}$ |
| 0.065 – $f = 12.244D^{0.214}H^{-1.211}$ | $R = 367.77f^{-7.519}D^{1.256}H^{-6.374}$ |
| $f = 12.244D^{0.214}H^{-1.211}$– 0.047 | $R = 0.0001f^{6.842}D^{-1.786}H^{7.009}$ |
| 0.047 – 0.032 | $R = 0.018f^{7.009}D^{-0.640}H^{5.182}$ |
| 0.032 – 0.001 | $R = 1.339f^{-0.619}D^{-0.463}H^{-0.693}$ |

Table 4. 10 Formulae of nonlinear multiple regression curve in heave motion for spar platform (170m to 180m draft length)

| Frequency range | Formula for regression curve |
|---|---|
| 0.20 – 0.10 | $R = 0.0001f^{-5.847}D^{-1.030}H^{-0.822}$ |
| 0.10 – 0.065 | $R = 0.0021f^{-3.787}D^{0.105}H^{-1.243}$ |
| 0.065 – $f = 0.077D^{-0.082}H^{-0.003}$ | $R = 1.365E - 08f^{-7.732}D^{0.486}H^{-1.2664}$ |
| $f = 0.077D^{-0.082}H^{-0.003}$– 0.047 | $R = 1938.63f^{6.661}D^{-1.982}H^{3.663}$ |
| 0.047 – 0.032 | $R = 184783.4f^{7.310}D^{-1.066}H^{2.524}$ |
| 0.032 – 0.001 | $R = 0.0159f^{-0.667}D^{-0.166}H^{-0.084}$ |

Table 4. 11 Formulae of nonlinear multiple regression curve in heave motion for spar platform (180m to 190m draft length)

| Frequency range | Formula for regression curve |
|---|---|
| 0.20 – 0.10 | $R = 0.0029f^{-5.627}D^{-0.504}H^{-1.678}$ |
| 0.10 – 0.065 | $R = 0.0202f^{-3.601}D^{0.521}H^{-1.885}$ |
| 0.065 – $f = 0.077D^{-0.082}H^{-0.003}$ | $R = 0.0099f^{-7.524}D^{1.465}H^{-4.445}$ |
| $f = 0.077D^{-0.082}H^{-0.003}$ – 0.047 | $R = 5475.11f^{7.444}D^{-1.216}H^{3.400}$ |
| 0.047 – 0.032 | $R = 4.474f^{8.306}D^{-0.120}H^{4.564}$ |
| 0.032 – 0.001 | $R = 0.1009f^{-0.673}D^{-0.426}H^{-8.262}$ |

Table 4. 12 Formulae of nonlinear multiple regression curve in heave motion for spar platform (190m to 200m draft length)

| Frequency range | Formula for regression curve |
|---|---|
| 0.20 – 0.10 | $R = 0.0001f^{-5.539}D^{-0.645}H^{-0.842}$ |
| 0.10 – 0.065 | $R = 0.0009f^{-3.496}D^{0.319}H^{-1.093}$ |
| 0.065 – $f = 7.969D^{0.326}H^{-1.184}$ | $R = 0.0003f^{-6.977}D^{0.926}H^{-3.105}$ |
| $f = 7.969D^{0.326}H^{-1.184}$ – 0.040 | $R = 0.930f^{6.763}D^{-1.646}H^{4.945}$ |
| 0.040 – 0.030 | $R = 1.016f^{6.855}D^{-0.256}H^{4.029}$ |
| 0.030 – 0.001 | $R = 0.852f^{-0.621}D^{-0.366}H^{-0.658}$ |
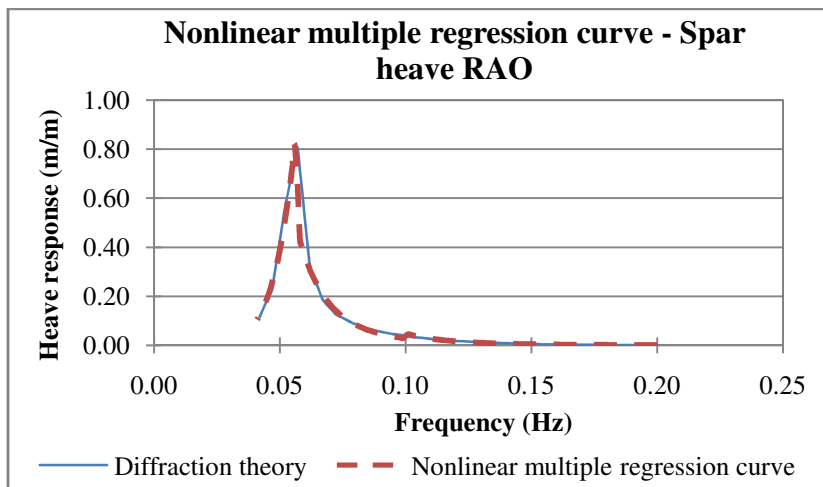


Figure 4. 39 Heave response of spar platform by diffraction theory and nonlinear multiple regression curves (150m to 160m draft length)
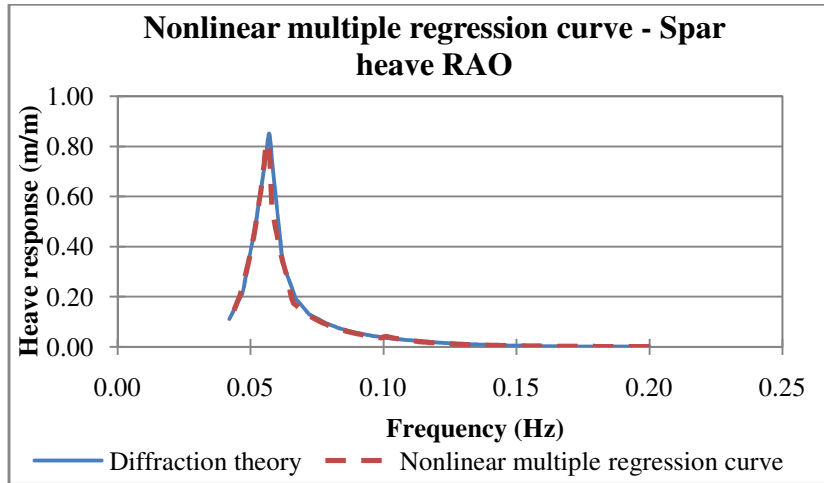
Figure 4. 40 Heave response of spar platform by diffraction theory and nonlinear

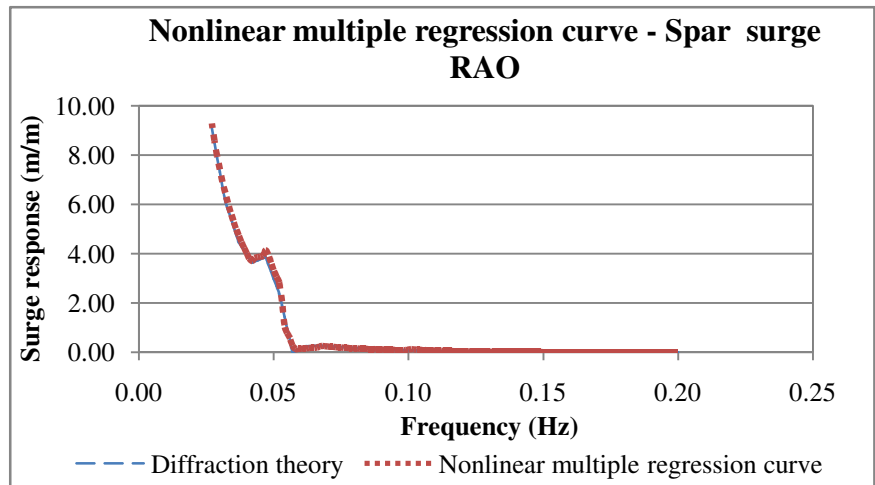multiple regression curves (150m to 160m draft length)



Figure 4. 41 Heave response of spar platform by diffraction theory and nonlinear

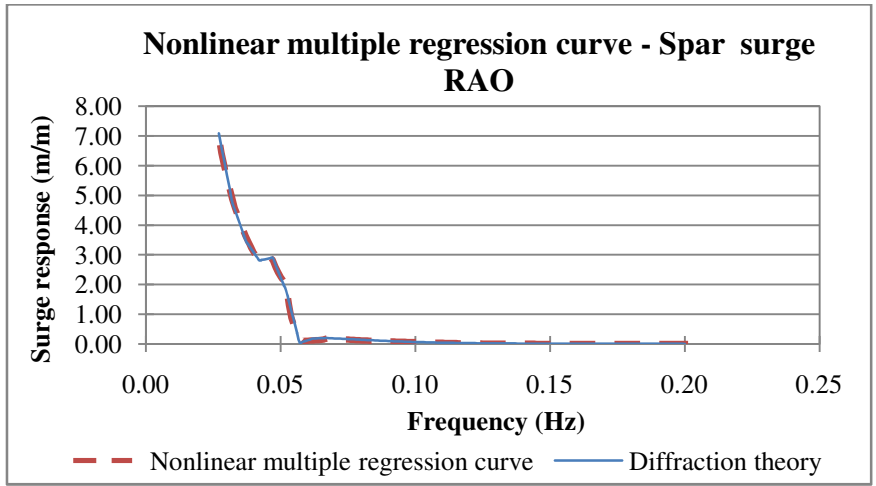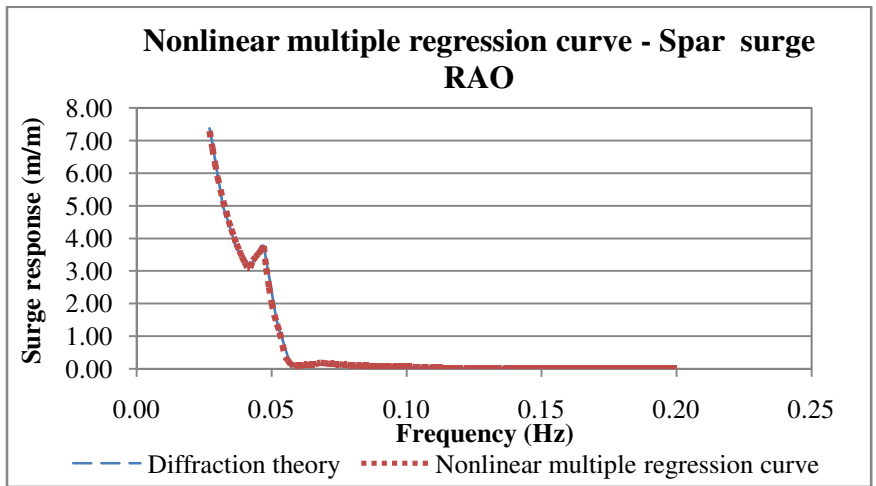multiple regression curves (170m to 180m draft length)

Figure 4. 42 Heave response of spar platform by diffraction theory and nonlinear
multiple regression curves (180m to 190m draft length)



Figure 4. 43 Heave response of spar platform by diffraction theory and nonlinear
multiple regression curves (190m to 200m draft length)

Nonlinear multiple regression curves for pitch motion responses were shown in Table 4.20 to Table 4.24 for draft length ranges i.e. 150m to 200m with 10m interval respectively. In additional, six frequency ranges were suggested for pitch regression curves. Figure 4.44 to Figure 4.48 below illustrate the comparison of nonlinear multiple regression curves and diffraction theory in pitch response for each of the draft lengths mentioned above. From the Figure 4.44, the regression response in frequency 0.060Hz to 0.066Hz was found to be around 20% smaller than the

diffraction response.  However, the regression curves showed good agreement as presented in Figure 4.45 to Figure 4.48.

Table 4. 13 Formulae of nonlinear multiple regression curve in pitch motion for spar platform (150m to 160m draft length)

| Frequency range | Formula for regression curve |
| --- | --- |
| 0.20 – 0.10 | $R = 53.118f^{-6.783}D^{-1.888}H^{-2.893}$ |
| 0.10 – 0.060 | $R = 12.876f^{-4.510}D^{-0.338}H^{-2.766}$ |
| $0.060 - f = 0.127D^{0.176}H^{-0.286}$ | $R = 0.0005f^{-4.141}D^{-0.094}H^{-0.619}$ |
| $f = 0.127D^{0.176}H^{-0.286} - 0.047$ | $R = 5791.53f^{7.147}D^{-2.492}H^{4.273}$ |
| 0.047 – 0.021 | $R = 27.456f^{3.535}D^{-1.281}H^{2.257}$ |
| 0.021 – 0.001 | $R = 0.792f^{-0.322}D^{-1.357}H^{-0.064}$ |

Table 4. 14 Formulae of nonlinear multiple regression curve in pitch motion for spar platform (160m to 170m draft length)

| Frequency range | Formula for regression curve |
| --- | --- |
| 0.20 – 0.10 | $R = 1211.35f^{-6.916}D^{-1.902}H^{-3.548}$ |
| 0.10 – 0.060 | $R = 1640.09f^{-4.170}D^{-0.399}H^{-3.506}$ |
| $0.060 - f = 12.244D^{0.214}H^{-1.211}$ | $R = 2.447E + 08f^{-6.013}D^{-0.117}H^{-6.982}$ |
| $f = 12.244D^{0.214}H^{-1.211} - 0.047$ | $R = 0.012f^{6.741}D^{-2.918}H^{6.910}$ |
| 0.047 – 0.016 | $R = 0.096f^{3.973}D^{-1.517}H^{3.823}$ |
| 0.016 – 0.001 | $R = 0.0038f^{-0.391}D^{-0.830}H^{0.537}$ |

Table 4. 15 Formulae of nonlinear multiple regression curve in pitch motion for spar platform (170m to 180m draft length)

| Frequency range | Formula for regression curve |
| --- | --- |
| 0.20 – 0.10 | $R = 0.3115f^{-7.0621}D^{2.493}H^{-1.585}$ |
| 0.10 – 0.065 | $R = 0.2473f^{-3.735}D^{-0.834}H^{-1.278}$ |
| $0.065 - f = 0.039D^{0.082}H^{0.003}$ | $R = 0.0002f^{-6.219}D^{-0.523}H^{-1.420}$ |
| $f = 0.039D^{0.082}H^{0.003} - 0.047$ | $R = 155780f^{6.379}D^{-3.029}H^{3.561}$ |
| 0.047 – 0.032 | $R = 207068f^{4.544}D^{-2.040}H^{1.688}$ |
| 0.032 – 0.001 | $R = 0.001f^{0.463}D^{-1.115}H^{1.858}$ |

Table 4. 16 Formulae of nonlinear multiple regression curve in pitch motion for spar platform (180m to 190m draft length)

| Frequency range | Formula for regression curve |
|---|---|
| 0.20 – 0.10 | $R = 11.692f^{-7.033}D^{-2.033}H^{-2.587}$ |
| 0.10 – 0.075 | $R = 27.14f^{-3.93}D^{-0.511}H^{-2.500}$ |
| 0.075 – $f = 0.158D^{0.239}H^{-0.379}$ | $R = 456.99f^{-7.292}D^{0.501}H^{-5.506}$ |
| $f = 0.158D^{0.239}H^{-0.379}$– 0.047 | $R = 987741f^{6.971}D^{-2.424}H^{3.149}$ |
| 0.047 – 0.016 | $R = 9.436f^{3.818}D^{-1.154}H^{2.557}$ |
| 0.016 – 0.001 | $R = 105.50f^{-0.400}D^{-1.108}H^{-1.247}$ |

Table 4. 17 Formulae of nonlinear multiple regression curve in pitch motion for spar platform (190m to 200m draft length)

| Frequency range | Formula for regression curve |
|---|---|
| 0.20 – 0.10 | $R = 0.5678f^{-7.076}D^{-2.085}H^{-1.992}$ |
| 0.10 – 0.057 | $R = 1.1937f^{-3.682}D^{-0.649}H^{-1.692}$ |
| 0.057 – $f = 7.969D^{0.326}H^{-1.184}$ | $R = 12.146f^{-6.961}D^{-0.102}H^{-4.227}$ |
| $f = 7.969D^{0.326}H^{-1.184}$– 0.042 | $R = 22.595f^{6.014}D^{-2.815}H^{4.886}$ |
| 0.042 – 0.016 | $R = 0.214f^{3.714}D^{-1.290}H^{3.297}$ |
| 0.016 – 0.001 | $R = 2192792f^{-0.254}D^{-0.713}H^{-3.257}$ |
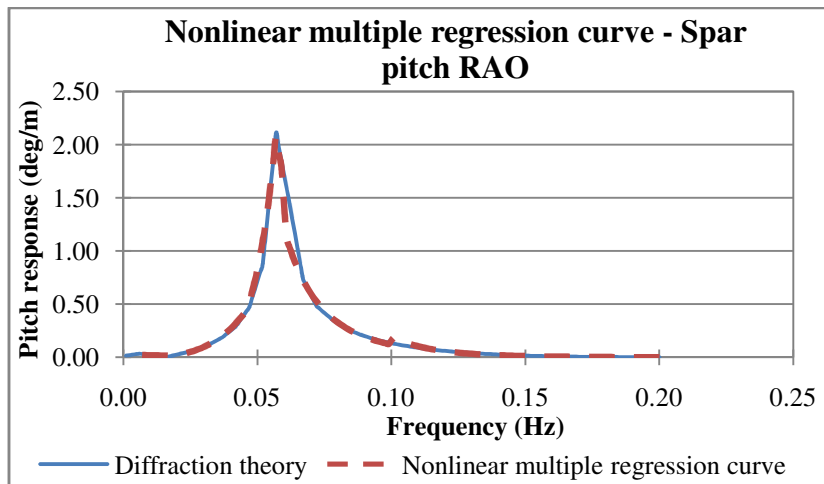


Figure 4. 44 Pitch response of spar platform by diffraction theory and nonlinear multiple regression curves (150m to 160m draft length)
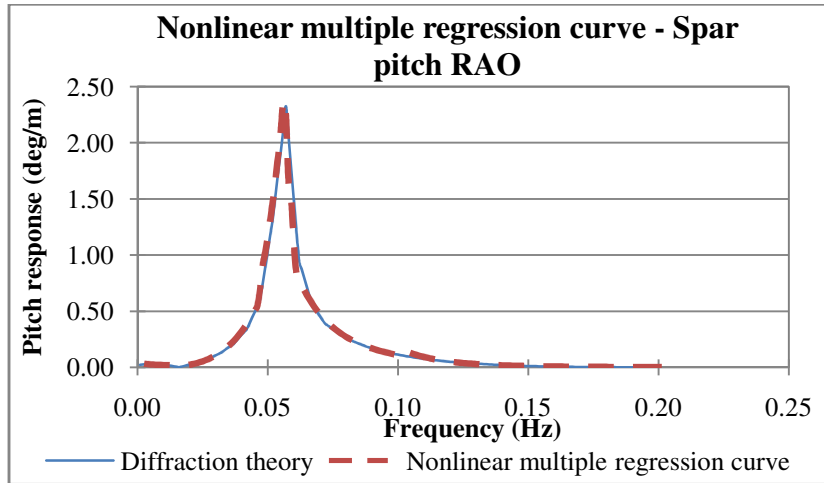
Figure 4. 45 Pitch response of spar platform by diffraction theory and nonlinear
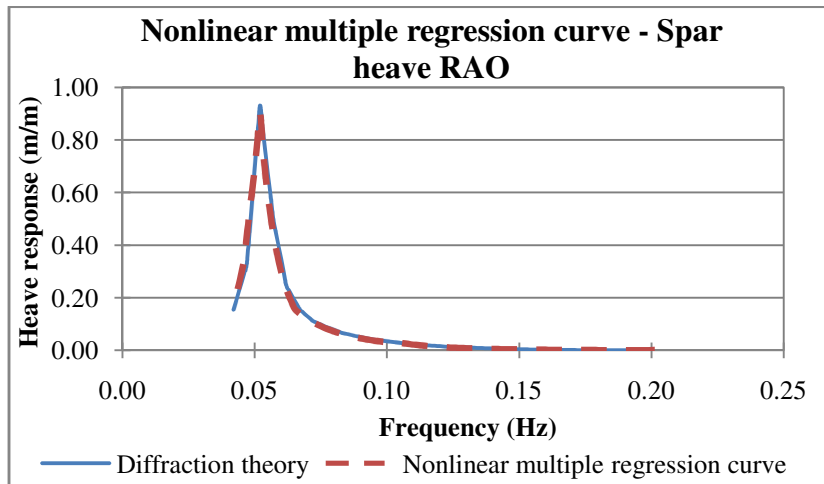multiple regression curves (160m to 170m draft length)
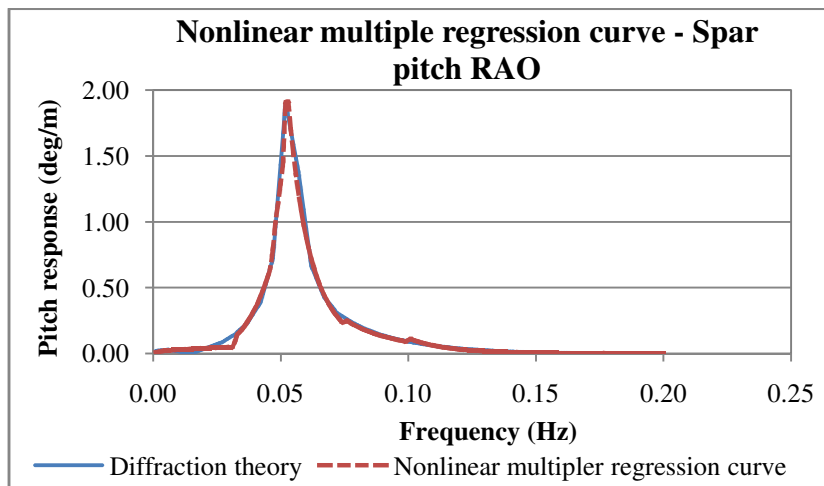


Figure 4. 46 Pitch response of spar platform by diffraction theory and nonlinear
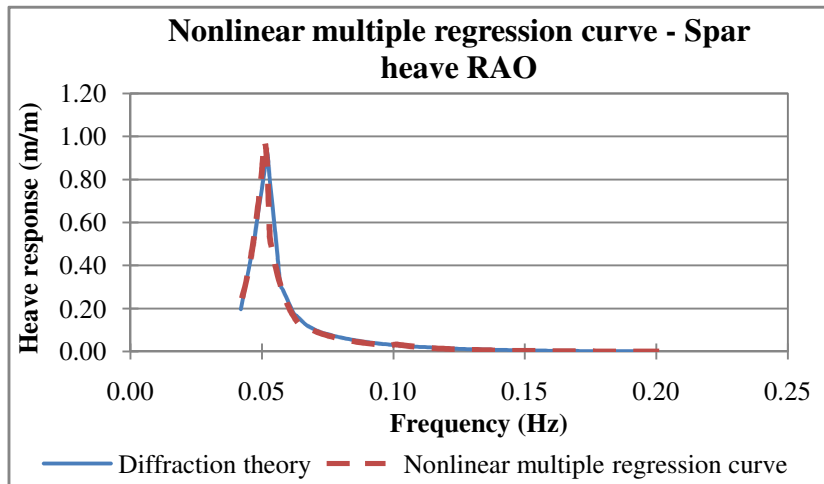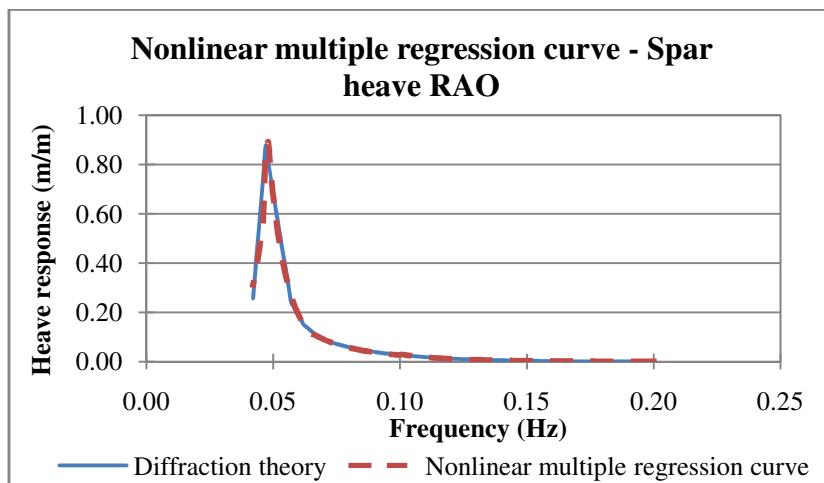multiple regression curves (170m to 180m draft length)

95
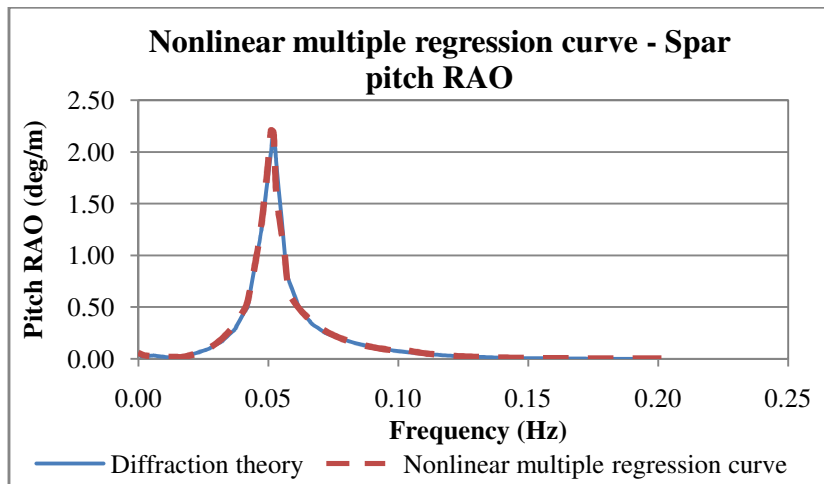
Figure 4. 47 Pitch response of spar platform by diffraction theory and nonlinear multiple regression curves (180m to 190m draft length)
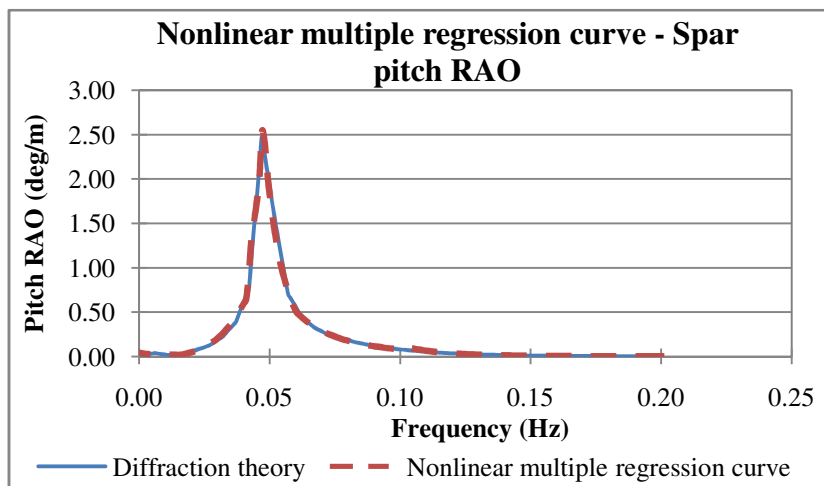


Figure 4. 48 Pitch response of spar platform by diffraction theory and nonlinear multiple regression curves (190m to 200m draft length)

### 4.6.2 Semi-submersible platform

Eight-columned semi-submersible platforms were considered in this study, with consideration of the platform columns diameter, draft, and wave frequency the nonlinear multiple regression curves for semi-submersible platform were suggested. The following discussion present and explain the results found.

The formulae suggested for the surge response of semi-submersible were divided

96

into six frequency ranges. In Table 4.17, the regression formulae suggested were listed for each frequency range. In additional to show the applicability, Figure 4.49 shows the comparison of nonlinear multiple regression curves to the diffraction response in surge response for semi-submersible platforms. It could be noticed that the nonlinear multiple regression curves were agreed well to the diffraction response curve.

Following discussions present and elaborate the results on the formulation of nonlinear multiple regression curves for heave responses. It varies with surge responses, three sets of the formulae for heave responses were suggested that based upon diameter ranges, i.e. 8m to 10m, 10m to 12m and 12m to 14m. Each set of the formulae suggested were based on five frequency ranges. As shown in Table 4.18 to Table 4.20 were the formulae for nonlinear multiple regression curves of the diameter ranges respectively.

Figure 4.50 to Figure 4.52 show the heave response comparison of nonlinear multiple regression curves to the diffraction theory. The suggested nonlinear multiple regression curves were found agreed well with the diffraction response curves. However, smoothness of the curve in Figure 4.51 needs to be improved. It could be noticed that, the connectivity of the curves for each frequency not as smooth as the curves in Figure 4.52. The connectivity of the points for the response found at each frequency need to be further studied.

Table 4.18 Formulae of nonlinear multiple regression curve in surge motion for semi-submersible platform

| Frequency range | Formula for regression curve |
|---|---|
| $0.20 - 0.154$ | $R = 0.00004 f^{-2.78} D^{1.48} H^{-0.09}$ |
| $0.154 - f_1 = -1.54 H^{-0.11} D^{0.67}$ | $R = 0.00002 f^{-2.40} D^{1.78} H^{0.04}$ |
| $f_1 = -1.54 H^{-0.11} D^{0.67} - f_2 = -1.5 H^{-0.17} D^{0.6}$ | $R = 0.00060 f^{-1.98} D^{1.28} H^{-0.26}$ |
| $f_2 = -1.5 H^{-0.17} D^{0.6} - f_3 = 1.4 H^{-0.30} D^{0.45}$ | $R = 0.00050 f^{-2.46} D^{1.29} H^{-0.53}$ |
| $f_3 = 1.4 H^{-0.30} D^{0.45} - f_4 = -1.54 H^{-0.39} D^{0.58}$ | $R = 0.00110 f^{-2.61} D^{1.30} H^{-0.90}$ |
| $f_5 = -1.54 H^{-0.39} D^{0.58} - 0.027$ | $R = 0.00140 f^{2.54} D^{1.74} H^{-1.19}$ |

Where $f$ is the wave frequency, $H$ is the draft length, and $D$ is the member diameter.
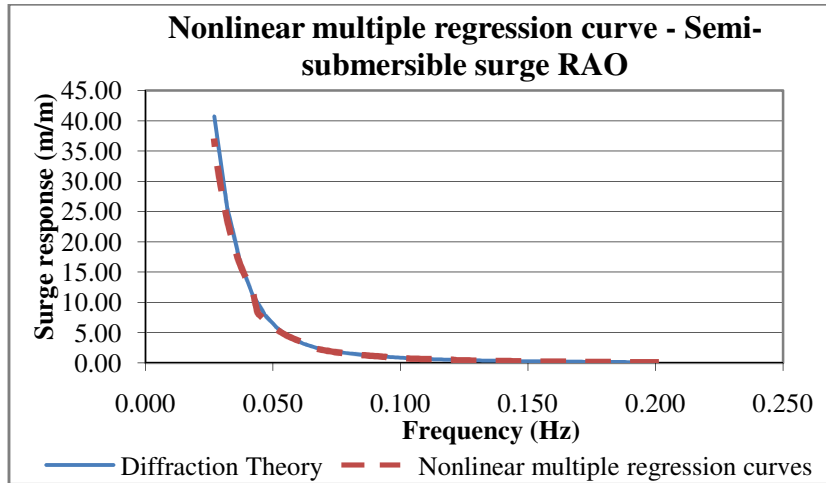
Figure 4.49 Surge response of semi-submersible platform by diffraction theory and nonlinear multiple regression curves

Table 4.19 Formulae of nonlinear multiple regression curve in heave motion for semi-submersible platform (8m to 10m column diameter)

| Frequency range | Formula for regression curve |
|---|---|
| $0.20 - f_1 = 0.8199D^{-0.098}H^{-0.445}$ | $R = 0.018f^{7.015}D^{-0.369}H^{-3.214}$ |
| $f_1 = 0.8199D^{-0.098}H^{-0.445} - f_2 = 0.7023D^{-0.104}H^{-0.44}$ | $R = 0.047f^{-3.969}D^{-0.393}H^{-1.751}$ |
| $f_2 = 0.7023D^{-0.104}H^{-0.44} - f_3 = 0.5575D^{-0.165}H^{-0.465}$ | $R = 0.124f^{-2.634}D^{-0.239}H^{-0.914}$ |
| $f_3 = 0.5575D^{-0.165}H^{-0.465} - f_4 = 0.2584D^{-0.096}H^{-0.489}$ | $R = 0.160f^{-1.029}D^{-0.116}H^{-0.346}$ |
| $f_4 = 0.2584D^{-0.096}H^{-0.489} - 0.027$ | $R = 0.808f^{-0.489}D^{-0.064}H^{-0.361}$ |

Table 4.20 Formulae of nonlinear multiple regression curve in heave motion for semi-submersible platform (10m to 12m column diameter)

| Frequency range | Formula for regression curve |
|---|---|
| $0.20 - f_1 = 0.981D^{-0.125}H^{-0.483}$ | $R = 0.098f^{-6.870}D^{-0.891}H^{-3.299}$ |
| $f_1 = 0.981D^{-0.125}H^{-0.483} - f_2 = 0.735D^{-0.131}H^{-0.435}$ | $R = 0.094f^{-4.382}D^{-0.610}H^{-2.060}$ |
| $f_2 = 0.735D^{-0.131}H^{-0.435} - f_3 = 1.257D^{-0.663}H^{-0.358}$ | $R = 0.274f^{-1.769}D^{-0.491}H^{-0.797}$ |
| $f_3 = 1.257D^{-0.663}H^{-0.358} - f_4 = 0.084D^{0.316}H^{-0.434}$ | $R = 0.164f^{-1.159}D^{-0.276}H^{-0.349}$ |
| $f_4 = 0.084D^{0.316}H^{-0.434} - 0.027$ | $R = 0.098f^{-0.669}D^{0.784}H^{-0.501}$ |

Table 4.21 Formulae of nonlinear multiple regression curve in heave motion for semi-submersible platform (12m to 14m column diameter)

| Frequency range | Formula for regression curve |
|---|---|
| $0.20 - f_1 = 1.278D^{-0.113}H^{-0.577}$ | $R = 0.065f^{-6.303}D^{-0.251}H^{-3.365}$ |
| $f_1 = 1.278D^{-0.113}H^{-0.577} - f_2 = 0.8182D^{-0.16}H^{-0.45}$ | $R = 0.1454f^{-4.212}D^{-0.522}H^{-2.168}$ |
| $f_2 = 0.8182D^{-0.16}H^{-0.45} - f_3 = 1.073D^{-0.901}H^{-0.117}$ | $R = 0.907f^{-1.305}D^{-0.785}H^{-0.614}$ |
| $f_3 = 1.073D^{-0.901}H^{-0.117} - f_4 = 0.0839D^{0.179}H^{-0.323}$ | $R = 0.060f^{-1.582}D^{-0.429}H^{-0.278}$ |
| $f_4 = 0.0839D^{0.179}H^{-0.323} - 0.027$ | $R = 0.0685f^{-0.945}D^{0.722}H^{-0.631}$ |
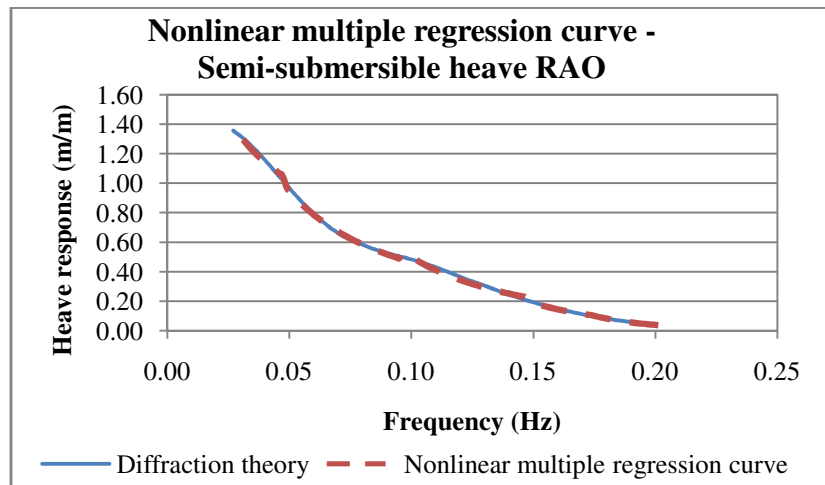


Figure 4. 50 Heave response of semi-submersible platform by diffraction theory and nonlinear multiple regression curves (8m to 10m column diameter)



Figure 4. 51 Heave response of semi-submersible platform by diffraction theory and nonlinear multiple regression curves (10m to 12m column diameter)

Figure 4. 52 Heave response of semi-submersible platform by diffraction theory and nonlinear multiple regression curves (12m to 14m column diameter)

The formulae suggested for the pitch response are presented. Table 4.21 to Table 4.23 show the formulae for nonlinear multiple regression curves for column diameter ranged i.e. 8m to 10m, 10m to 12m, and 12m to 14m respectively.

Figure 4.53 to Figure 4.55 show the comparison of nonlinear multiple regression curves and the diffraction theory for pitch responses for the diameter ranges as mentioned above. The regression curves suggested, was found agreed well with the diffraction response curve in pitch response. However, in Figure 4.58 the pitch response by nonlinear multiple regression curves was found to be about 10% less than the diffraction response at the frequency ranged from 0.10Hz to 0.17Hz.

Table 4. 22 Formulae of nonlinear multiple regression curve in pitch motion for semi-submersible platform (8m to 10m column diameter)

| Frequency range | Formula for regression curve |
|---|---|
| 0.20 – 0.164 | $R = 2.164E\text{-}07 f^{0.797} D^{1.374} H^{2.084}$ |
| 0.164 – 0.125 | $R = 2.668E\text{-}09 f^{0.231} D^{2.340} H^{3.410}$ |
| 0.125 – 0.100 | $R = 9.069E\text{-}10 f^{1.653} D^{2.292} H^{2.528}$ |
| 0.100 – 0.071 | $R = 0.0004 f^{-2.134} D^{0.523} H^{-0.737}$ |
| 0.071 – 0.027 | $R = 0.556 f^{-1.600} D^{-0.269} H^{-2.025}$ |

Table 4. 23 Formulae of nonlinear multiple regression curve in pitch motion for semi-submersible platform (10m to 12m column diameter)

| Frequency range | Formula for regression curve |
|---|---|
| $0.20 - f_1 = 0.61D^{-0.882}H^{0.283}$ | $R = 3.813E\text{-}07f^{-1.749}D^{1.39}H^{1.368}$ |
| $f_1 = 0.61D^{-0.882}H^{0.283} - f_2 = 3.598D^{-1.298}H^{-0.043}$ | $R = 1.954E\text{-}09f^{-0.99}D^{2.738}H^{2.453}$ |
| $f_2 = 3.598D^{-1.298}H^{-0.043} - f_3 = 16.217D^{-1.651}H^{-0.318}$ | $R = 2.728E\text{-}09f^{0.365}D^{3.817}H^{2.464}$ |
| $f_3 = 16.22D^{-1.651}H^{-0.318} - f_4 = 804.0D^{-3.177}H^{-0.464}$ | $R = 0.0018f^{-2.075}D^{-0.29}H^{-0.587}$ |
| $f_4 = 804.04D^{-3.177}H^{-0.464} - 0.027$ | $R = 0.051f^{-1.579}D^{0.888}H^{-2.092}$ |

Table 4. 24 Formulae of nonlinear multiple regression curve in pitch motion for semi-submersible platform (12m to 14m column diameter)

| Frequency range | Formula for regression curve |
|---|---|
| $0.20 - f_1 = 0.0066D^{0.706}H^{0.425}$ | $R = 4.972E\text{-}06f^{-1.842}D^{0.891}H^{0.895}$ |
| $f_1 = 0.0066D^{0.706}H^{0.425} - f_2 = 0.505D^{-0.417}H^{-0.182}$ | $R = 1.944E\text{-}07f^{-1.730}D^{2.321}H^{0.819}$ |
| $f_2 = 0.505D^{-0.417}H^{-0.182} - f_3 = 24.384D^{-1.465}H^{-0.679}$ | $R = 5.301E\text{-}07f^{1.460}D^{3.907}H^{1.552}$ |
| $f_3 = 24.384D^{-1.465}H^{-0.679} - f_4 = 6.343D^{-0.642}H^{-1.089}$ | $R = 0.757f^{-2.429}D^{-2.003}H^{-1.492}$ |
| $f_4 = 6.343D^{-0.642}H^{-1.089} - 0.027$ | $R = 2.468f^{-1.401}D^{-0.464}H^{-2.069}$ |
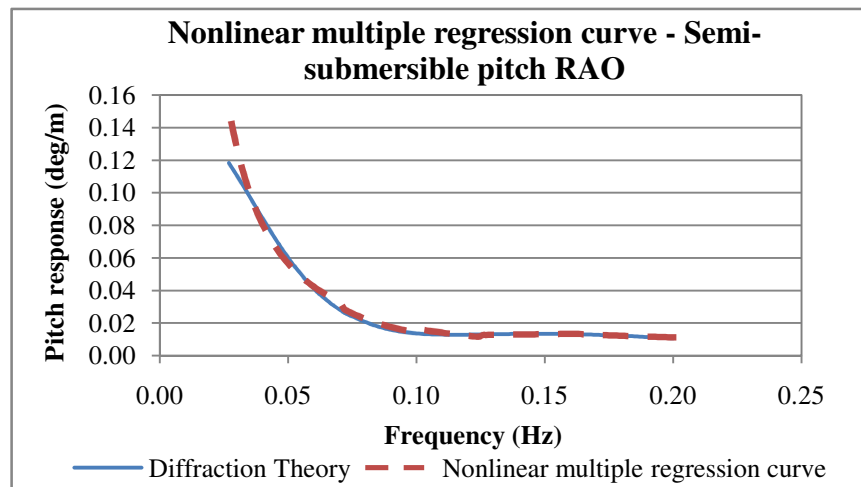


Figure 4. 53 Pitch response of semi-submersible platform by diffraction theory and nonlinear multiple regression curves (8m to 10m column diameter)
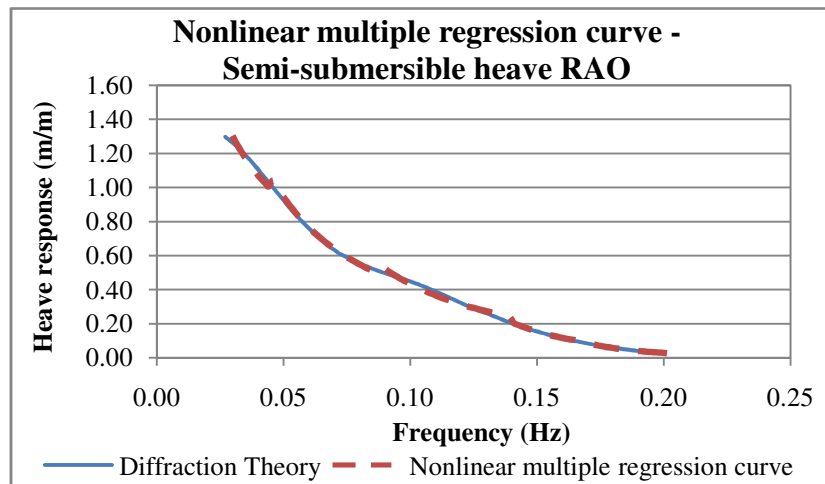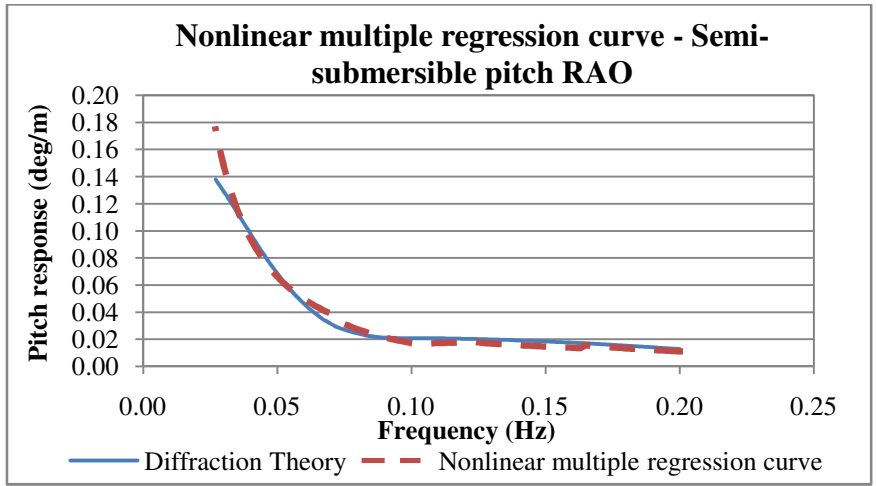
Figure 4. 54 Pitch response of semi-submersible platform by diffraction theory and nonlinear multiple regression curves (10m to 12m column diameter)
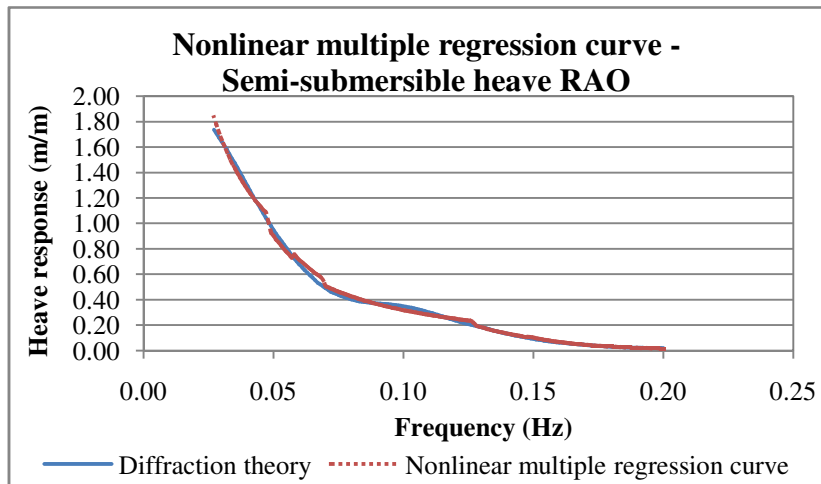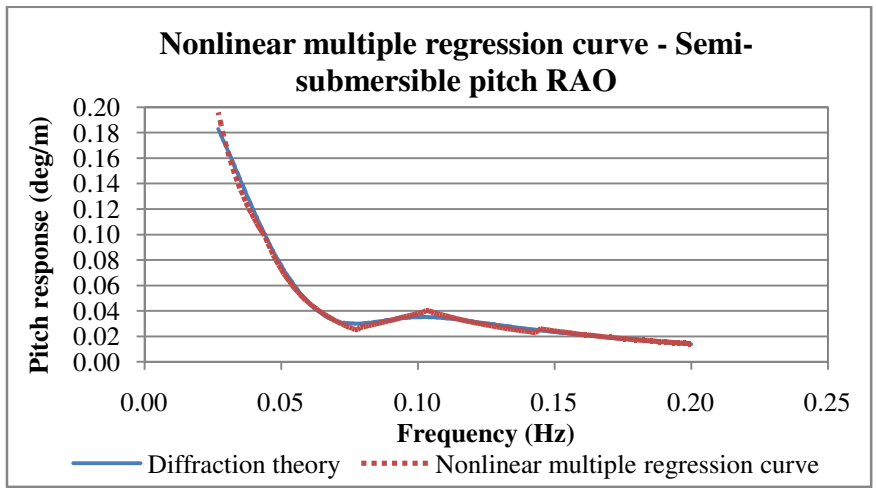


Figure 4. 55 Pitch response of semi-submersible platform by diffraction theory and nonlinear multiple regression curves (12m to 14m column diameter)

## 4.7 Chapter summary

In this chapter, the dynamic responses obtained by the wave tank test, time domain analysis, linear wave diffraction, and the comparisons were presented. The nonlinear multiple regression curves were recommended and compared.

From the comparison, it might be expressed that diffraction theory is the proper method for wave force estimation of offshore structure with large-sized hull. Hence the nonlinear multiple regression curves based upon diffraction theory was suggested, to provide a simpler approach for dynamic analysis based upon the diffraction theory. The curves were in comparison to the diffraction response to prove the applicability, and good agreement was found.

# CHAPTER FIVE

## CONCLUSION

### 5.1    Conclusions

1.  The dynamic responses of typical models of spar and semi-submersible subjected to regular wave determined by wave tank tests.  The tests were conducted to determine the responses of these models in 1 m water depth.  Four taut mooring lines were attached at each corner of the model to the wave tank base for station keeping.  The models were subjected to regular wave of frequency varying from 0.4 Hz to 2 Hz with 0.2 Hz incremental intervals.  The responses were recorded and measured.  The maximum surge RAO for spar model was observed to be 4 m/m at 0.4 Hz, the maximum heave RAO was 1 m/m at 1 Hz and the maximum pitch RAO was 13 deg/m at 1 Hz.  While, the maximum RAOs for semi-submersible model were found to be 2.4 m/m for surge RAO at 0.6 Hz, the maximum heave RAO and pitch RAO were 1.78 m/m and 0.53 deg/m at 0.4 Hz correspondingly.

2. The dynamic responses of the corresponding prototype of the spar and semi-submersible platforms were obtained by using a time domain integration method. A MATLAB program was developed using the time domain Newmark-beta integration method to solve the equations of motion for these prototypes. Linear wave theory and Morison equation were used for the determination of wave kinematics and wave force. The maximum surge RAO was found to be 0.042 m/m at 0.155 Hz, the maximum heave RAO was 0.10 m/m at 0.042 Hz and the maximum pitch RAO was 0.052 deg/m at 0.158 Hz by time domain analysis for spar prototype. The maximum RAO semi-submersible prototype was found to be 1 m/m, 0.185 m/m and 0.7 deg/m for surge, heave and pitch respectively at frequency 0.06 Hz. The responses obtained were compared with the model test results.

3. The dynamic responses of the corresponding prototype were obtained by using linear diffraction analysis software. A commercial code was used for the analysis, with similar inputs of the prototypes for time domain analysis. The maximum surge RAO was observed to be 7.1 m/m at 0.03 Hz, the maximum heave RAO was 0.81 m/m at 0.05 Hz and the maximum pitch RAO was 2.02 deg/m at 0.5 Hz for spar prototype. The maximum RAO by linear wave diffraction analysis for surge, heave and pitch was observed to be 29.23 m/m, 1.704 m/m and 0.127 deg/m respectively at frequency 0.3 Hz for semi-submersible prototype. The responses were compared with the model test and Morison results.

4. The diffraction RAOs for spar platform prototype showed better agreement to the model test RAOs. Surge response by both approaches showed the same trend and the magnitude of diffraction responses was found to be about 20% smaller at the low frequency range. Similar conclusion was drawn for the heave and pitch response by diffraction and model test RAOs. However, the Morison RAOs trend disagreed with the diffraction and model test RAOs. Large variations were found between Morison RAO and the model test RAOs, such as about 70 %, 80 % and 60% for surge, heave and pitch responses respectively for spar prototype.

5. The diffraction RAOs for semi-submersible platform showed good agreement with the model test RAOs. Diffraction responses were about 20 % to 30 % less than the model test responses for surge. The maximum variation was about 50% smaller than model test RAO at frequency 0.14 Hz. The heave and pitch responses showed good comparison, and about 90% of the diffraction responses agreed with the model test response in terms of the trend and magnitude. The Morison results varied largely with the model test results. The maximum variation between Morison RAOs and the model test RAOs were found to be about 80%, 90 % and 70% for surge, heave and pitch responses respectively.

6. As a simpler approach for the estimation of the dynamic responses, formulae based on nonlinear multiple regression analysis was suggested for both spar and semi-submersible platforms. Data such as the wave frequency, structure diameter, and structural draft length were required as the input data for the curves to obtain the dynamic responses. For spar platforms, five sets of formulae for draft varying from 150 m to 200 m with an increment of 10 m were recommended. Three sets of formulae for column diameter varying from 8 m to 10 m with 2 m interval were recommended for heave and pitch RAO of semi-submersible platforms. One set of formulae was suggested for its surge RAO. The RAOs obtained were compared with the diffraction responses, and very good agreement was found.

## 5.2   Further studies

Based on this study, the following suggestions are made for future study.

1. Model test :

    a. Mooring line - Typical mooring line tensions need to be concerned, so that the model's motion would not affected or restricted by the mooring lines.

    b. Scale – Scaling law shall be appropriate to fit the applicability of the wave maker and wave tank's condition.

    c. Wave condition – Based upon the capability of the wave makers, the best deepwater condition shall be simulated for deepwater structure's model test.

2. Diffraction analysis

    a. MATLAB code shall be developed

3. Nonlinear multiple regression analysis

    a. Mooring lines – Various types, conditions and number of mooring lines shall be taken into consideration.

    b. Wave direction – Could be considered in the formula suggested

    c. Environmental conditions - The wind force, current force etc, could be incorporated in the response curves suggested.

    d. Different offshore structures with large-sized hull - Truss spar, cell spar and tension leg platforms shall be considered

## REFERENCE

[1] M. S. Ayob, "Managing Structural Integrity of Offshore Platforms" presented in *Short course on 'Offshore Platform for Petroleum Exploration'* by Civil Engineering Department of Universiti Teknologi PETRONAS. Tronoh, Malaysia, Feb 24th - 26th, 2009.

[2] *Kikeh Floating Production, Storage and Offloading Development, Malaysia* from *http://www.offshore-technology.com/projects/kikeh/* Retrieved May 17, 2009

[3] S. K Chakrabarti (1994), "Introduction to Offshore Structures" In *Hydrodynamic of Offshore* Structures. Southampton: WIT Press, pp. 17-18.

[4] L. Wilhoit, & C. Supan, "2009 Worldwide survey of Spar, DDCV and MinDOC vessels", Houstan, Texas: Mustang Engineering, 2008.

[5] L. Wilhoit, & C. Supan, "2008 Worldwide survey of semi-FPSs and FPU", Houstan, Texas: Mustang Engineering, 2008.

[6] S. K Chakrabarti (1994), " Wave Force on Small Structures " In *Hydrodynamic of Offshore Structures.* Southampton: WIT Press, pp. 168-169.

[7] J. R. Morison, M. P. O'Brien, J. W. Johnson, & S. A. Schaaf, "The force exerted by surface waves on piles," *Petroleum Transaction, AIME ,* vol. 189, pp. 149-154, 1950.

[8] N. Mizutani & K. Iwata, "Diffraction Force on a Spherical Structure and Wave Diffraction. " *International Journal of Offshore and Polar Engineering ,* vol.3, no.1, pp. 7-16, 1993.

[9] S. S. Mirzaie & M. J. Ketabdari, "Estimation of Wave Forces on Large Compliant Platforms. " *J. Ocean Univ. China (Oceanic and Coastal Sea Research) ,* vol. 8, no.3, pp. 121-126, 2009.

[10] J. Pike, (n.d.). *Spars: GlobalSecurity.org*., from http://www.globalsecurity.org/military/systems/ship/platform-spar-comp.htm, Retrieved March 17, 2009

[11] F. Zhang, J. M. Yang, R. P. Li, & G. Chen, "Numerical Investigation on The Hydrodynamic Performance of A New Spar Concept. " *Journal of Hydrodynamics, Ser B. ,* vol. 19, no.4, pp. 473-481, 2007.

[12] F. Zhang, J. M. Yang, R. P. Li, & G. Chen, "Coupling Effects for Cell-Truss Spar Platform: Comparison of Frequency- and Time-Domain analysis with Model Test. " *Journal of Hydrodynamics ,* vol. 20, no. 4, pp. 424-432, 2008.

[13] Y. Wang, J. M. Yang, Z. Q. Hu, & L. F. Xiao, "Theoritical Research on Hydrodynamics of a Geometric Spar in Frequency- and Time-Domains. " *Journal of Hydrodynamics ,* vol.20, no. 1, pp. 30-38, 2008.

[14] E. F. H. Lim, & B. F. Ronalds, "Evolution of the Production Semisubmersible" presented in 2000 SPE Annual Technical Conference and Exhibition, Dallas, Texas, October 1st - 4th, *2000.*

[15] B. Collipp, J. Goldman, A. J. Laborde, B. Martinovich, F. Olsen, & A. R. Grange (Eds.). (2010, Febuary 02)., Aker Mek Verksted, Earl & Wright (A Sedco Company, Transocean Inc.), Fried & Goldman (Friede Goldman Halter), Neptune (Transocean Inc.), ODECO (Diamond Offshore Drilling), Shell , *First & Second Generation Semi Submersible Drilling Rigs*, Retrieved Febuary 20, 2010, from
http://www.oceanstaroec.com/fame/2000/semisubmersible.htm

[16] J. Pike, (n.d.). *Drilling Semi-submersible*. Retrieved Sept 17, 2009, from Globalsecurity.org:

http://www.globalsecurity.org/military/systems/ship/offshore-drillrig.htm

[17] *Marine Talk*. (2005, September 8). Retrieved August 2, 2009, from World's Biggest Semi-Submersible Rig:

http://www.marinetalk.com/articles-marine-companies/art/Worlds-Biggest-

Semi-Submersible-Rig-DET009103411IN.html

[18] N. Haritos, "Introduction to the Analysis and Design of Offshore Structures - An Overview." *EJSE Special Issue: Loading on Structures,* pp. 55-65, 2007.

[19] A.S. Chitrapu & R.C. Ertekin, "Time domain simulation of large amplitude responses of floating platforms." *Ocean Engng.,*vol. 22, No. 4, pp 367-385, 1995.

[20] Y. M Low, & R. S. Langley, "Time and Frequency Domain Coupled Analysis of Deepwater Floating Production Systems." *Applied Ocean Research , vol. 28*, pp. 371-385, 2006.

[21] R.C.T. Rainey, "A new equation for calculating wave loads on offshore structure." *J. Fluid Mech.*, vol. 204, pp 295-324, 1989.

[22] S.M. Han & H. Benaraya, "Comparison of linear and nonlinear responses of a compliant tower to random wave forces." *Chaos, Solitons and Fractals.,* vol. 14, pp 269-291, 2002.

[23] B. Teng & Y. C. Li, "Estimation of wave-current force coefficient on inclined cylinder in random waves." *Proc. Instn. Civ. Engrs. Wat., Marit. & Engergy ,* vol. 96, pp. 1-7, 1992.

[24] M. Isaacson & J. Baldwin, "Numerical Simulation of Morison Coefficient Estimation." *International Journal of Offshore and Polar Engineering ,*vol. 1, no. 2, 1991.

[25] M. Isaacson, K. Subbiah, & J. Baldwin, "Force Coefficient Estimation from Random Wave Data." *International Journal of Offshore and Polar Engineering ,* vol. 1, no. 4, 1991.

[26] S. K. Chakrabarti, "Hydrodynamic Coefficients and Depth Parameter." *Journal of Waterway, Port, Coastal and Ocean Engineering ,* pp. 123-127, 1985.

[27] M. Lake, H. P. He, A. W. Troech, M. Perlin & K. P. Thiagarajan, " Hydrodynamic Coefficient Estimation for TLP amd Spar Structures." *Journal*

*of Offshore Mechanics and Arctic Engineering* ,vol. 122, pp. 118-124, May 2000.

[28]     R. Burrow, R. G. Tickell, D. Hames & G. Najafian, "Morison wave force coefficients for application to random seas." *Applied Ocean Research* ,vol. 19, pp. 183-199, 1997.

[29]     S. K. Chakrabarti & D. C. Cotter, "Hydrodynamic Coefficients of a Moored Semisubmersible in Waves." *Journal of Offshore Mechanics and Arctic Engineering* , vol. 114, pp. 9-15, 1992.

[30]     I. Anam, "Evalutation of the dynamic reponse of spar platform." Ph.D. Dissertation, Texas A&M University, Civil Engineering, Texas, August 2000.

[31]     I. Anam, & J. M. Roesset, "Effect of Nonlinear Wave Kinematics on Dynamic Response of Spar." *Journal of Engineering Mechanics* , vol 128, no. 9, pp. 925-934, 2002.

[32]     S. K Chakrabarti (1994), "Wave Force on Large Structures " In *Hydrodynamic of Offshore Structures.* Southampton: WIT Press, pp. 244-322.

[33]     B. B. Mekha, C. P. Johnson, & J. M. Roesset, "Nonlinear Response of a Spar in Deep Water: Different Hydrodynamic and Structural Models." *Proceedings of the Fifth (1995) International Offshore and Polar Engineering Conference* , pp. 462-469, 1995.

[34]     B. B. Mekha, D. C. Weggel, C. P. Johnson, & J. M. Roesset, "Effects of Second Order Diffraction Forces on the Global Response of Spars." *Proceedings of the Sixth (1996) International Offshore and Polar Engineering Conference* , pp. 273-280, 1996.

[35]     I. Prislin, J. Halkyard, J. F. Debord Jr, J. I. Collins, & J. M. Lewis, " Full-Scale Measurements of the Oryx Neptune Production Spar Platform Performance. " presented in Offshore Technology Conference. Houston, Texas, May 3rd-6th, 1999.

[36]     Q. W. Ma, & M. H. Patel, "On the non-linear forces acting on a floating spar platform in ocean waves". *Applied Ocean Research* , pp. 29-40, 2001.

[37]     A. K. Agawal, & A. K. Jain,"Dynamic behavior of offshore spar platforms under regular sea waves." *Ocean Engineering* , vol. 30, pp. 487-516, 2003.

[38]     P. D. Spanos, R. Ghosh, L. D. Finn, & J. Halkyard, "Coulped Analysis of a Spar Structure: Monte Carlo and Statistical Linearization Solutions." *Journal of Offshore Mechanics and Arctis Engineering* , vol. 127, pp. 11-16, 2005.

[39]     K. V. John, B. S. Wong, & O. A. A Montasir, "Frequency Domain Analysis of Truss Spar Platform" presented in ICCBT 2008, Kuala Lumpur, June 16th - 20th, 2008.

[40]     O.A.A. Montasir, K.V. John, S.P. Narayanan, & M.A.W. Mubarak, "Dynamic Response of Spar Platforms Subjected to Waves and Current" presented in ICCBT 2008, Kuala Lumpur, June 16th - 20th, 2008.

[41] A. Steen, M. H. Kim, & M. Irani, "Prediction of Spar Responses: Model Test vs. Analysis. " presented in Offshore Technology Conference. Houston, Texas, May 3$^{rd}$ - 6$^{th}$, 2004.

[42] K. Sadeghi, A. Incecik, & M. J. Downie, "Response analysis of a truss spar in the frequency domain". *Journal of Marine Science and Technoloogy* , pp. 126-137, 2004

[43] A.K., Jha, P. R Jong, & S. R. Winterstein, "Motions of a Spar Buoy in Random Seas: Comparing Predictions and Model Test Results". *Proceedings of BOSS-97*, pp. 333-347, 1997.

[44] N. H. Kim, M. S. Park, & S. B. Yang, "Wave Force Analysis of the Vertical Circular Cylinder by Boundary Element Method". *KSCE Journal of Civil Engineering* , pp. 31-35, January 2007

[45] N. H. Kim, & T. N. Cao, "Wave Force Analysis of the Two Vertical Cylinders by Boundary Element Method". *KSCE Journal of Civil Engineering* , pp. 359 – 366, 2008.

[46] O. Yilmaz & A. Incecik, "Extreme Motion Response Analysis of Moored Semi-submersible. *Ocean Engineering*",vol. 23, no. 6,pp. 497-517, 1996.

[47] M. Soylemez, & A. Incecik, "Identification of Nonlinear Effects in Predicting the Motion Response of an Offshore Platform". *Ocean Engineering* ,vol. 24, no. 8, pp. 695-720, 1997.

[48] G. F. Clauss, C. E. Schmittner, & K. Stutz, "Freak Wave Impact on Semi-submersibles - Time-Domain Analysis of Motions and Forces" presented in *The Thirtenth (2003) International Journal of Offshore and Polar Engineering Conference,* May 25$^{th}$ -30$^{th}$ , 2003.

[49] S. K. Chakrabarti, J. Barnett, H. Kanchi, A. Mehta, & J. Yim, "Desgin analysis of a truss pontoon semi-submersible concpet in deep water". *Ocean Engineering* , vol. 34, pp. 621-629, 2007.

[50] H. Q. Zhang, & J. C. Li, "Effects of Volumetric Allocation on Heave Response of Semi-submersible in Deep Sea". *Science in China Series E-Technological Series* ,vol. 52, no. 3, pp. 651-657, 2009.

[51] A. S. Chitrapu, S. Saha and V. Y. Salpekar, "Time-Domain Simulation of Spar Platform Response in Random Waves and Current", *17$^{th}$ International Conference on Offshore Mechanics and Arctic Engineering*, pp. 1-8, 1998

[52] M. E. A. Yassir & V. J. Kurian, "Time domain hydrodynamic analysis of semi-submersible platform" presented in ICET 2009, Kuala Lumpur, December 8$^{th}$-10$^{th}$, 2009.

**BIBLIOGRAPHY**

[1]     R. G. Tickell, R. Burrows & P. Holmes, "Long-term wave loading on offshore structures". *Proc. Inst. Civ. Engrs.* Part 2, vol. 61, pp. 145-162, 1976.

[2]     C. J. Garrison & R. Stacey, "Wave loads on North Sea gravity platforms: A comparison of theory and experiment". *Offshore Technology Conference*, pp. 513-517, 1977.

[3]     N. Hogben, B. L. Miller, J. W. Searle & G. Ward, "Estimation of fluid loading on offshore structures". *Proceedings of Instn. Civ. Engrs.*, pp. 515-562, 1977.

[4]     R. Burrows, "The choice of period when estimating loading on cylinders from regular waves". *Proc. Instn. Civ. Engrs.* Part 2, vol. 67, pp. 501-507, 1979.

[5]     R. B. Campbell & J. K. Vandiver, "The estimation of natural frequency and damping ratios of offshore structures" presented in 12th Annual Offshore Technology Conference 1980 in Houston, Texas, May 5-8, 1980.

[6]     J. A. Pinkster, "Mean- and low-frequency wave forces on semi-submersibles" presented in 13th Annual Offshore Technology Conference 1981 in Houston, Texas, May 4-7, 1981.

[7]     M. F. Cook & J. K. Vandiver, "Measured and predicted dynamic response of a single pile platform to random wave excitation" presented in 14th Annual Offshore Technology Conference in Houston, Texas, May 3-6, 1982

[8]     M. Rahman & D. S. Chehil, "Second-order wave force on a large cylinder". *Acta Mechanica* , pp. 127-136, 1982.

[9]     M. Isaacson, "Solitary wave diffraction around large cylinder". *Journal of Waterway, Port, Coastal and Ocean Engineering* , vol. 109, no. 1, pp. 121-127, 1983.

[10]    D. C. Cotter, & S. K. Chakrabarti, "Wave force tests on vertical and linclined cylinders". *Journal of Waterway, Port, Coastal and Ocean Engineering* , vol. 110 , no. 1, pp. 1-14, 1984.

[11]    S. K. Chakrabarti, "Hydrodynamic coefficients and depth parameter". *Journal of Waterway, Port, Coastal and Ocean Engineering* , pp. 123-127, 1985.

[12]    J. R. Chaplin, "Morison inertia coefficients in orbital flow". *Journal of Waterway, Port, Coastal and Ocean Engineering*, vol. 111, no. 2. pp. 201-215, 1985.

112

[13]   M. Isaacson, & S. Sinha, "Directional wave effects on large offshore structures". *Journal of Waterway, Port, Coastal and Ocean Enginnering* , vol. 112, no. 4, pp. 482-497, 1986.

[14]   M. Rahman & L. Debnath, "Nonlinear Diffraction of Water Waves by Offshore Structures". *International Journal of Math. & Math. Sci.* , pp. 625-652, 1986.

[15]   S. K. Chakrabarti, & S. F. Armbrust, "Total Force Coefficients for Inclined Cylinders". *Journal of Waterway, Port, Coastal and Ocean Engineering* , vol 113, no. 4, pp. 421-425, 1987.

[16]   S. L. Hu, & L. D. Lutes, "Non-normal descriptions of Morison-type wave forces". *Journal of Engineering Mechanics* , vol. 113 no. 2, pp. 196-209, 1987.

[17]   A. G. Abul-Azm & A. N. Williams, "Second-order diffraction loads on truncated cylinders". *Journal of Waterway, Port, Coastal and Ocean Engineering* , vol. 114, no. 4, pp. 436-454, 1988.

[18]   S. K. Chakrabarti, "Forces on vertical cylinder due to random waves". *Journal of Waterway, Port, Coastal and Ocean Engineering* , vol. 114, no. 3, pp. 267-280, 1988.

[19]   R. T. Hudspeth, J. H. Nath, & P. Khare, "Wave phase amplitude effects on force coefficients". *Journal of Waterway, Port, Coastal and Ocean Engineering* , vol. 114, no. 1, pp. 34-49, 1988.

[20]   P. Justesen, "Hydrodynamic forces on large cylinders in oscillatory flow". *Journal of Waterway, Port, Coastal and Ocean Engineering* , vol. 115, no. 4, pp. 497-514, 1989.

[21]   M. Isaacson, & K. F. Cheung, "Time-Domain Solution for Second-Order Wave Diffraction". *Journal of Waterway, Port, Coastal and Ocean Engineering* ,pp. 191-210, 1990.

[22]   K. F.Cheung, & M. Isaacson, "On two alternative field solutions for second order wave diffraction". *Journal of Offshore Mechanics and Arctic Engineering* , vol. 113, pp. 185-192, 1991.

[23]   M. Isaacson, & J. Baldwin, "Numerical Simulation of Morison Coefficient Estimation". *International Journal of Offshore and Polar Engineering* , vol. 1, no. 2, 1991.

[24]   M. Isaacson, & T. Mathai, "Hydrodynamic coefficients of vertical cylinders of arbitrary section". *Journal of Offshore Mechanics and Arctic Engineering* , vol. 113, pp. 109-116, 1991.

[25] M. Isaacson, K. Subbiah, & J. Baldwin, "Force Coefficient Estimation from Random Wave Data". *International Journal of Offshore and Polar Engineering* , vol. 1, no. 4, 1991.

[26] J. N. Newman, "Wave effects on deformable bodies". *Applied Ocean Research*, vol. 16, pp. 47-59, 1994.

[27] A. S. Chitrapu, & R. C. Ertekin, "Time-domain simulation of large-amplitude response of floating platforms". *Ocean Engineering* , vol. 22 no. 4, pp. 367-385, 1995.

[28] M. Soylemez, "Motion tests of a twin-hulled semi-submersible". *Ocean Engineering* , pp. 643-660, 1995.

[29] D. K. Sunil, & M. Mukhopadhyay, "Free Vibration of Semisubmersible: A Parametric Study". *Ocean Engineering* , pp. 489-502, 1995.

[30] K. F. Cheung, M. Isaacson, & J. W. Lee, "Wave Diffraction Around Three Dimensional Bodies in a Current". *Journal of Offshore Mechanics and Arctic Engineering* , pp. 247-252, 1996.

[31] R. J. Pamos & J. Zhang, "Prediction of Low-Frequency Offshore Structure Response to Irregular Waves Using Linear and High-Order Wave Theories" presented in Petroleum Conference and Exhibition of Mexico, Villarhermosa, Mexico, March 5-7 1996

[32] J. Bowers, I. Morton, & G. Mould, "Multivariate Extreme Value Analysis of a Moored Semi-submersible". *Marine Structure* , pp. 443-463, 1997.

[33] R. Burrows, R. G. Tickell, D. Hames, & G. Najafian, "Morison wave force coefficients for application to random seas". *Applied Ocean Research* , vol. 19, pp. 183-199, 1997.

[34] J. B. Song, Y. H. Wu, & R. Collinson, "A new linearized equation of random wave forces". MODSIM 97 , pp. 111-114, 1997.

[35] J. R. Chaplin & K. Subbiah, "Large scale horizontal cylinder forces in waves and currents". *Applied Ocean Research*, vol. 19, pp. 211-223, 1997.

[36] A. Naess & A. A. Pisano, "Frequency domain analysis of dynamic response of drag dominated offshore structures", *Applied Ocean Research*, vol. 19, pp. 251-262, 1997

[37] S. Wu, J. J. Murray, & G. S. Virk, "The Motions ans Internal Forces of a Moored Semi-submersible in Regular Waves". *Ocean Engineering* , vol. 24, no.7, pp. 593-603, 1997.

[38] F. J. Fischer, & R. Gopalkrishnan, "Some Observations on the Heave Behavior of Spar Platforms". *Journal of Offshore Mechanics and Arctic Engineering* , pp. 221-225, 1998.

[39] A. Incecik, J. Bowers, G. Mould, & O. Yilmaz, "Response-based extreme value analysis of moored offshore structures due to wave, wind and current". *Journal of Marine Science and Technology* , vol. 3, pp. 145-150, 1998.

[40] D. L. Kriebel, "Nonlinear wave interaction with a vertical circular cylinder: Wave forces". *Ocean Engineering*, vol. 25, no. 7, pp. 597-605, 1998.

[41] M. Rahman, "Nonlinear Hydrodynamic Loading on Offshore Structures". *Theoritical and Computational Fluid Dynamics* , vol. 10, pp. 323-347, 1998.

[42] M. Soylemez, "Motion response simulation of a twin-hulled semi-submersible". *Ocean Engineering* , vol. 25, no. 4-5, pp. 359-383, 1998.

[43] J. Vasconsellos, "A decision support system for floating production design". *Ocean Engineering* , vol.26, 865-889, 1999.

[44] J. Wolfram, & M. Naghipour, "On the estimation of Morison force coefficients and their predictive accuracy for very rough circular cylinders". *Applied Ocean Research* ,vol. 21, pp. 311-328, 1999.

[45] G. Najafian, R. G. Tickell, R. Burrows and J. R. Bishop, "The UK Christchurch Bay Compliant Cylinder Project: Analysis and interpretation of Morison wave force and response data". *Applied Ocean Research* ,vol. 22, pp. 129-153, 2000.

[46] X. H. Chen, J. Zhang & W. Ma, "On dynamic coupling effects between a spar and its mooring lines". *Ocean Engineering*, pp. 863-887, 2001.

[47] I. Anam & J. M. Roesset, "Effect of Nonlinear Wave Kinematics on Dynamic Response of Spars". *Journal of Engnineering Mechanics* , vol. 128, no. 9, pp. 925-934, 2002.

[48] S. M. Han, & B. Benoraya, "Comparison of linear and nonlinear of a compliant tower to random wav forces". Chaos, Solitons and Fractals , pp. 269-291, 2002.

[49] J. B. Rho, & H. S. Choi, "Heave and Pitch Motions of a Spar Platform with Damping Plate". *Proceedings of The Twelfth (2002) International Offshore and Polar Engineering Conference*. Kitakyushu, Japan, 2002, pp. 198-201.

[50] E. V. Buldakov, R. E. Taylor, & P. H. Taylor, "Diffraction of a directionally spread wave group by a cylinder". *Applied Ocean Research* , pp. 301--320, 2003.

[51] G. F. Clauss, C. E. Schmittner, & K. Stutz, "Freak Wave Impact on Semi-submersible - Time domain analysis of Motions and Forces". *Proceedings of Thirtheen (2003) International Offshore and Polar Engineering Conference* , pp. 1-8, 2003.

[52] P. Ferrant, D. L. Touze, & K. Pelletier, "Nonlinear time domain models for irregular wave diffraction about offshore structures". *International Journal for Numerical Methods in Fluids* , pp. 1257-1277, 2003.

[53] K. M. Kleefsman, & A. E. Veldman, "Numerical Simulation of Wave Loading on a Spar Platform". *Proceedings of IWWWFB03, 18th International Workshop on Water Waves and FLoating Bodies*, 2003.

[54] A. Nestgard, M. Ronaess, G. Skeie, J. Dalheim, & T. Vada, "Numerical Models for SPAR Platform Dynamics". *Proceedings of the Thirteenth (2003) International Offshore and Polar Engineering Conference*. Honolulu, Hawaii. 2003, pp. 167-174.

[55] S. Chandrasekaran, A. K. Jain, & N. R. Chandak, "Influence of hydrodynamic coefficients in the response behavior of triangular TLPs in regular waves". *Ocean Engineering* , vol. 31, pp. 2319-2342, 2004.

[56] S. A. Mavrakos, "Hydrodynamic coefficients in heave of two concentric surface-piercing truncated circular cylinders". *Applied Ocean Research* , pp. 84-97, 2004.

[57] W. Qiu, J. M. Chuang, & C. C. Hsiung, "Numerical Solution of WAve Diffraction Problem in the Time Domain WIth the Panel-Free Method". *Journal of Offshore Mechanics and Arctic Engineering* , pp. 1-8, 2004.

[58] L. B. Tao, & S. Q. Cai, "Heave motion suppression of a spar with a heave plate". *Ocean Engineering* , pp. 669-692, 2004.

[59] L. Tao, K. Y. Lim, & K. Thiagarajan, "Heave Response of Classic Spar with Variable Geometry". *Journal of Offshore Mechanics and Arctic Engineering* , pp. 90-95, 2004.

[60] O. Yilmaz, "An iteraticve procedure for the diffraction of water waves by multiple cylinders". *Ocean Engineering* , pp. 1437-1446, 2004.

[61]    J. S. Kwon, I. Y. Paik, & S. P. Chang, "Nonlinear Frequency Domain Analysis of Flexible Offshore Structures Using Volterra Series". *KSCE Journal of Civil Engineering* , vol. 9, no. 5, pp. 391-401, 2005.

[62]    V. Sundar, R. Sundaravadivelu, & M. Kalyani, "Forces due to oblique waves on a submerged open moored cylinder in deep waters". *Ocean Engineering* , vol. 32, pp. 651-666, 2005.

[63]    O. Yilmaz, "Second order diffraction of water waves by a bottom mounted vertical circular cylinder and some related numerical problems". *Journal of Offshore Mechanics and Arctic Engineering* , pp. 68-70, 2005.

[64]    A. Naess, H. C. Karlsen, & P. S. Teigen, "Numerical methods for calculating the crossing rate of high and extreme response levels of compliant offshore structures subjected to random waves". *Applied Ocean Research* , vol. 28, pp. 1-8, 2006.

[65]    B. J. Wu, Y. H. Zheng, Y. G. You, D. S. Jie & Y. Chen, "On diffraction and radiation problem for two cylinders in water of finite depth". *Ocean Engineering* ,vol. 33, pp. 679-704, 2006.

[66]    O. Yilmaz, "Second order diffraction of water waves by a bottom mounted vertical circular cylinder and some related numerical problems". *Journal of Offshore and Arctic Engineering* , vol. 129, pp. 68-70, 2007.

[67]    P. Siddorn, & R. E. Taylor, "Diffraction and independent radiation by an array of floating cylinders". *Ocean engineering* , pp. 1289-1303, 2008.

[68]    S. K. Chang, D. Kim, & C. H. Chang, "Active response control of an offshore structure under wave loads using a modified probabilistic neural network". *Journal of Marine Science Technology* , vol. 14, pp. 240-247, 2009.

[69]    G. H. Dong, L. Sun, Z. Zong, Y. P. Zao, "Numerical analysis of the forces exerted on offshore structures by ship waves". *Ocean Engineering*, 2009.

[70]    T. J. Stallard, S. D. Weller, & P. K. Stansby, "Limiting heave response of a wave energy device by draft adjustment with upper surface immersion". *Applied Ocean Research* , pp. 1-8, 2009.

[71]    W. T. Bennett & A. J. Laborde, Patent No. US 6,190,089 B1. United States, 2001.

[72]    P. H. Kristensen, & E. Petterson, Patent No. US 2006/0260526 A1. United States, 2006.

[73]    E. V. Daalen, "Numerical and theoritical studies of water waves and floating bodies". Ph.D Dissertation, University of Twente, Netheland, 1993.

[74]     J. Klepsvik, "Nonlinear wave loads on offshore structures". M.S. Dissertation, Massachusetts Institute of Technology, Cambridge, 1995.

[75]     Z. H. Ran, "Coupled Dynamic Analysis of Floating Structure in Waves and Currents". Ph.D Dissertation, Texas A&M University, 2000.

[76]     R. Taghipour, "Efficient prediction of dynamic response for flexible and multibody marine structures". Ph.D Dissertation, Department of Marine Technology, Norwegian University of Science and Technology, Trondheim, Norway, 2008.

[77]     C. H. Lee, (1995). WAMIT Theory Manual. Cambridge: Massachusettes Institute of Technology, Department of Ocean Engineering.

[78]     A. Morandi, (2004). Assessment of performance of deepwater floating production facilities during Hurricane Lili. Global Maritime, Houston, Texas.

[79]     S. Haver, (2005) Design of offshore structures: Impact of the possible existence of freak waves. Hawaii, United States.

**PUBLICATION**

Published paper

1. **C. Y. Ng**, V. J. Kurian, M. A. W. Mohamed, "Diffraction method for spar platforms" presented in ICET 2009, Kuala Lumpur, December 2009.

2. V. J. Kurian, **C. Y. Ng**, M. A. W. Muhammad, "Response of Classic Spar by Morison Equation and Diffraction Theory" presented in Offshore Asia Conference & Exhibition 2010, Kuala Lumpur, March 2010.

3. **C. Y. Ng**, V. J. Kurian, O. A. A. Montasir, "Experimental and Analytical Investigation of Classic Spar Responses" presented in ESTCON 2010, Kuala Lumpur, June 2010

Paper under preparation

4. **C. Y. Ng**, V. J. Kurian, M. A. Yassir, "Response of Semi-Submersible PLATFORM by Morison Equation and Diffraction Theory", Full paper submitted, WEC 2010, Kuching, August 2010.

5. **C. Y. Ng**, V. J. Kurian, O. A. A. Montasir, "Response of Spar Platform by Morison Equation and Diffraction Theory", Under preparation, APOC 2010, Kuala Lumpur, December 2010.